



CLASS VI PERMIT

Application Narrative

Gulf Coast Sequestration, LLC (G1037)

Project Minerva, Cameron Parish
Minerva South CCS Well Nos. 001 and 002

EPA Project Id: R06-LA-0002

LDENR Appl Nos: 45031 & 45032

Date: November 2024



45031 & 45032

CERTIFICATION

Per LAC 43:VII §3603.H.1, the geoscientific aspects of the Narrative have been prepared by or under the supervision of a licensed Professional Geologist authorized to practice by and in good standing with the Louisiana Board of Professional Geoscientists. A separate certification page will be submitted with the Attachments to the Narrative that require certification.

Kaycee M. Garrett
LA License No. 1325

I, Kaycee M. Garrett, certify that I have personally examined and am familiar with the information submitted in this document and the attached documents, and that, based on my inquiry of those individuals immediately responsible for obtaining the information, I believe that the submitted information is true, accurate, and complete.



NARRATIVE SECTIONS (Including applicable Tables, Figures, and Appendices)

Section 1 Project Background

Section 2 Site Characterization

Per LAC 43:VII §3603.H.2, the engineering aspects of the Narrative have been prepared by or under the supervision of a licensed Professional Engineer (PE) authorized to practice by and in good standing with the Louisiana Board Professional Engineering and Land Surveying. Since the engineering aspects of the applications have been designed by a consulting PE, the required documents will be certified once the technical review is completed by LDENR. A separate certification page will be submitted with the attachments to the Narrative that require certification.



TABLE OF CONTENTS

1	PROJECT BACKGROUND AND GENERAL INFORMATION.....	1-1
1.1	Project Overview.....	1-1
1.2	Facility/Site Information	1-1
1.3	Ownership	1-2
1.4	CO ₂ Source	1-2
1.5	Proposed Injection Mass/Volume	1-2
1.6	Project Timeline	1-3
1.7	Permit Compliance	1-3
1.8	Associated Permits	1-3
1.9	Environmental Justice	1-3
1.10	Environmental Analysis	1-4
1.11	GSDT Submission	1-4
2	SITE CHARACTERIZATION	2-1
2.1	Geology and Hydrogeology.....	2-1
2.1.1	Regional Geology	2-1
2.1.2	Local Geology	2-16
2.2	Maps and Cross-Sections of the AoR	2-22
2.2.1	Subsurface Interpretation and Integration	2-23
2.2.2	Cross-Sections	2-36
2.2.3	Structure Maps	2-39
2.2.4	Isopach Maps	2-39
2.3	Faults and Fractures	2-40
2.3.1	Description of Faulting	2-40
2.3.2	Fault Transmissivity	2-41
2.3.3	Faulting within the AoR.....	2-44
2.4	Injection Zone and Confining Zone System Details	2-47
2.4.1	Geologic Summary.....	2-48
2.4.2	Description of the Injection Zone and Confining Zone System	2-48
2.5	Geomechanical and Petrophysical Information	2-55
2.5.1	Geomechanical Information	2-55
2.5.2	Petrophysical Information	2-58

2.6	Seismic History.....	2-62
2.6.1	Gulf Coast Basin Seismic History.....	2-62
2.6.2	Project Minerva's Seismic History	2-62
2.6.3	Project Minerva's Seismic Risk Analysis	2-63
2.6.4	Induced Seismicity.....	2-66
2.7	Hydrologic and Hydrogeologic Information.....	2-68
2.7.1	Data Sources	2-68
2.7.2	USDW within the AoR	2-69
2.8	Geochemistry	2-73
2.8.1	Sources of Data	2-73
2.8.2	Geochemical Modeling	2-75
2.9	Other Information	2-78
2.9.1	Magnetometer Survey	2-78
2.10	Site Suitability.....	2-79
2.10.1	Lithological Distribution	2-79
2.10.2	Confinement	2-80
2.10.3	CO ₂ Stream Compatibility	2-80
2.10.4	Storage Capacity	2-81
2.10.5	Modelling Approach and Simulation	2-82
3	AOR AND CORRECTIVE ACTION	3-85
3.1	Project Plan	3-85
3.2	GSDT Submission	3-85
4	FINANCIAL RESPONSIBILITY DEMONSTRATION	4-86
4.1	Financial Responsibility Demonstration Report	4-86
4.2	GSDT Submission	4-86
5	INJECTION WELL CONSTRUCTION.....	5-1
5.1	Well Construction Plans	5-1
5.2	Construction Requirements	5-2
5.2.1	Prevention of Vertical Fluid Migration	5-2
5.2.2	Drilling Practices and Contingencies.....	5-3
5.2.3	Testing and Monitoring Devices Within the Borehole and Annulus	5-4
5.3	CASING PROGRAM	5-4
5.3.1	Injection Zone Depth	5-4

5.3.2	Lithology of Injection and Confining Zones	5-4
5.3.3	Borehole and Casing Size and Grade.....	5-4
5.3.4	Downhole Temperature	5-6
5.4	Cementing Program	5-6
5.4.1	Circulation of Cement	5-6
5.4.2	Cement and Cement Additives	5-6
5.5	Tubing and Packer.....	5-6
5.6	Mechanical Integrity.....	5-7
5.6.1	Internal Integrity.....	5-8
5.6.2	External Integrity	5-8
6	PRE-OPERATIONAL LOGGING AND TESTING	6-9
6.1	Project Plan	6-9
6.2	GSDT Submission	6-9
7	WELL OPERATION.....	7-1
7.1	Operational Procedures	7-1
7.1.1	Injection Rate.....	7-1
7.1.2	Injection Pressure	7-1
7.1.3	Stimulation Program.....	7-2
7.1.4	CO ₂ Volume	7-2
7.1.5	CO ₂ Stream Characteristics.....	7-2
7.2	Proposed Carbon Dioxide Stream	7-2
8	TESTING AND MONITORING.....	8-1
8.1	Project Plan	8-1
8.2	GSDT Submission	8-1
9	INJECTION WELL PLUGGING PLAN.....	9-1
9.1	Project Plan	9-1
9.2	GSDT Submission	9-1
10	POST INJECTION SITE CARE AND SITE CLOSURE	10-1
10.1	Project Plan	10-1
10.2	GSDT Submission	10-1
11	EMERGENCY AND REMEDIAL RESPONSE PLAN	11-1
11.1	Project Plan	11-1
11.2	GSDT Submission	11-1



45031 & 45032

12 REFERENCECS 12-1

LIST OF TABLES, FIGURES, AND APPENDICES

TABLES

Table 1.1-1	Wells Used to Construct Maps
Table 1.8-1	Permits Associated with Project Minerva
Table 2.2.1-1	Regulatory Zones Correlated to the Geostatistical Model Formation Tops and Reservoir Simulation Model Layers
Table 2.4.2-1	Frio Formation Sidewall Core Samples
Table 2.4.2-2	Mineral Composition Percentages of Two Samples Taken from the Frio Formation
Table 2.4.2-3	Clay Mineral Composition Percentages Taken from the Frio Formation
Table 2.4.2-4	Anahuac Formation Sidewall Core Samples
Table 2.4.2-5	Analysis of Miocene Shale Permeabilities
Table 2.5.2-1	Samples Taken from Anahuac and Frio Formations Near Vinton Dome
Table 2.5.2-2	Minimum Effective Shale Porosity in Gulf Coast Environments
Table 2.6.2-1	Seismic Events within 115-mile Radius of Project Minerva
Table 2.7.1-1	Water Well Data within 2-mile radius of Project Minerva
Table 2.7.2-1	Archie's Formula for Different Lithology
Table 2.10.3-1	Composition CO ₂ Stream
Table 5.3.1-1	Regulatory Zones and Formation Depths
Table 5.3.3-1	Proposed Casings and Tubular for MS CCS 1 and MS CCS 2
Table 5.3.3-2	Casing Design Details for MS CCS 1 and MS CCS 2
Table 5.4-1	Cement Details for MS CCS 1 and MS CCS 2
Table 5.4.2-1	Cement Additives and Material Descriptions for MS CCS 1 and MS CCS 2
Table 5.5-1	Proposed Injection Summary for MS CCS 1 and MS CCS 2
Table 5.5-2	Proposed Injection Tubing for MS CCS 1 and MS CCS 2
Table 5.5-3	Proposed Packer of MS CCS 1 and MS CCS 2
Table 7-1	Operating Conditions for MS CCS 1 and MS CCS 2

FIGURES

Figure 1.1-1	Topographic Map of Project Minerva
--------------	------------------------------------

Figure 2.1.1-1 General Stratigraphic Column of Gulf of Mexico Coastal Plain

Figure 2.1.1-2 Evolutionary Stages of the Gulf of Mexico and East Texas Basin

Figure 2.1.1-3 Schematic Cross-Section of Cretaceous Shelf Margin, Growth Faults, and Fault Zones

Figure 2.1.1-4 Depositional Environments of the Northern Gulf of Mexico

Figure 2.1.1-5 Depositional Cycles of the Northern Gulf of Mexico

Figure 2.1.1-6 Lower Miocene Depositional Systems and Elements of the Gulf Coast

Figure 2.1.1-7 Cross-Section of Pliocene and Pleistocene Deposits

Figure 2.1.1-8 Regional North-South Geologic Cross-Section of Southwest Louisiana

Figure 2.1.1-9 Regional Salt Diaps

Figure 2.1.1-10 Salt Diaps Adjacent to Project Minerva

Figure 2.1.1-11 Stratigraphic Column of the Hydrogeologic Framework of Southwestern Louisiana

Figure 2.1.1-12 Regional Hydrostratigraphic Cross-Section for Southeastern Texas

Figure 2.1.1-13 Regional North-South Hydrogeologic Cross-Section of Southwestern Louisiana

Figure 2.1.1-14 Regional North-South Hydrogeologic Cross-Section of the Gulf Coast Aquifer -TWDB

Figure 2.1.1-15 Boundary Extent of Fresh Groundwater of the Chicot Aquifer System in Southwest Louisiana

Figure 2.1.1-16 Potentiometric Surface and Direction of Groundwater Flow of Chicot Aquifer System in Southwestern Louisiana

Figure 2.1.1-17 Regional Chicot Aquifer Cross-Section Across Calcasieu and Cameron Parishes Delineating Saltwater Encroachment

Figure 2.1.2-1 Basemap of Cross-Sections at Project Minerva

Figure 2.1.2-2 North-Southwest Geologic Cross-Section (B-B') at Project Minerva

Figure 2.1.2-3 West-East Geologic Cross-Section (A-A') at Project Minerva

Figure 2.1.2-4 Paleogeographic Reconstruction of Hackberry Depositional Environments

Figure 2.1.2-5 Generalized Depositional Environments of the Hackberry Trend in Southern Louisiana

Figure 2.1.2-6 Piper Diagram of Water Chemistry in Lake Charles Area

Figure 2.1.2-7 Chicot Aquifer System Cross-Sections Across Calcasieu and Cameron Parishes

Figure 2.2.1-1 Big Island 3D Survey Header for the PSTM

Figure 2.2.1-2 Black Bayou 3D Survey Header for the MIGNR Processed Data Set

Figure 2.2.1-3 Seismic Data Coverage Map

Figure 2.2.1-4 Detectable Fault Trough Variants in Seismic Data

Figure 2.2.1-5 Structural Geostatistical Model Cross-Section Showing Anahuac and Upper Frio Formations

Figure 2.2.1-6 Correlation of Geostatistical Model Formation Tops with Well Logs

Figure 2.2.1-7 Porosity-Permeability Relationship Analysis Chart

Figure 2.2.1-8 Reservoir Simulation (REVEAL) Grid Derived from Geostatistical Model

Figure 2.2.3-1 Top of Anahuac Formation (Upper Confining Zone) Structure Map

Figure 2.2.3-2 Top of Upper Frio Formation (Injection Zone) Structure Map

Figure 2.2.3-3 Top of Middle Frio Formation (Lower Confining Zone) Structure Map

Figure 2.2.4-1 Anahuac Formation (Upper Confining Zone) Isopach Map

Figure 2.2.4-2 Upper Frio Formation (Injection Zone) Isopach Map

Figure 2.2.4-3 Middle Frio (Lower Confining Zone) Isopach Map

Figure 2.3.1-1 Black Bayou 3D: InLine 1210

Figure 2.3.1-2 Black Bayou 3D: InLine 1230

Figure 2.3.1-3 Black Bayou 3D: InLine 1250

Figure 2.3.1-4 Black Bayou 3D: InLine 1270

Figure 2.3.1-5 Black Bayou 3D: InLine 1290

Figure 2.3.1-6 Black Bayou 3D: InLine 1310 through MS CCS 002

Figure 2.3.1-7 Black Bayou 3D: InLine 1330

Figure 2.3.1-8 Black Bayou 3D: InLine 1350

Figure 2.3.1-9 Black Bayou 3D: InLine 1370

Figure 2.3.1-10 Black Bayou 3D: Composite NE-SW Line through MS CCS 001 & 002

Figure 2.3.1-11 Black Bayou 3D: Composite NW-SE Line

Figure 2.3.1-12 Black Bayou 3D: XLine 1590

Figure 2.3.1-13 Black Bayou 3D: XLine 1610

Figure 2.3.1-14 Black Bayou 3D: XLine 1630

Figure 2.3.1-15 Black Bayou 3D: XLine 1650

Figure 2.3.1-16 Black Bayou 3D: XLine 1670 Through MS CCS 002

Figure 2.3.1-17 Black Bayou 3D: XLine 1690 Through MS CCS 001



45031 & 45032

Figure 2.3.1-18 Black Bayou 3D: XLine 1710

Figure 2.3.1-19 Black Bayou 3D: XLine 1730

Figure 2.3.2-1 Sealing and Non-Sealing Faults in Louisiana Gulf Coast

Figure 2.3.3-1 Faults Included in Fault Slip Potential Analysis

Figure 2.3.3-2 Fault F02 Divisions, 13 Segments Based on Similar Dip Azimuth Trends

Figure 2.3.3-3 Fault F13 Divisions, 3 Segments Based on Similar Dip Azimuth Trends

Figure 2.3.3-4 Fault F03 Divisions, 3 Segments Based on Similar Dip Azimuth Trends

Figure 2.3.3-5 Fault F19 Divisions, 3 Segments Based on Similar Dip Azimuth Trends

Figure 2.4.2-1 Regulatory Zones Type Section

Figure 2.4.2-2 Anahuac and Frio Core Samples Collected near Vinton Dome

Figure 2.5.1-1 Location of BEG Pilot and Ramos Studies

Figure 2.5.1-2 Determination of Direction of Maximum Horizontal Stress

Figure 2.5.1-3 Young's Modules and Poisson's Ratio Values

Figure 2.5.1-4 Definitions of Poro-elastic and Thermo-elastic Coefficients Used in Petroleum Experts' REVEAL Manual

Figure 2.6.2-1 USGS Earthquake Hazards Program's US Seismic Risk Map

Figure 2.6.2-2 Seismic Events Within 115-mile Radius of Project Minerva

Figure 2.6.3-1 FEMA Earthquake Hazards Map of the Eastern US

Figure 2.7.1-1 Water Well Data within a 2-mile Radius of Project Minerva

Figure 2.7.2-1 USDW Well Location and Structure Map

Figure 2.7.2-2 North-South USDW Cross-Section (B-B')

Figure 2.7.2-3 West-East USDW Cross-Section (A-A')

Figure 2.7.2-4 Graphic Solution of the Spontaneous Potential Equation

Figure 2.7.2-5 Resistivity Nomograph for NaCl Solutions

Figure 2.8.2-1 CO₂ Solubility Model—Partition Between REVEAL and PHREEQC

Figure 2.8.2-2 Comparison of CO₂ Solubility Data from Diamond, 2004 and Reveal—Zero Salinity

Figure 5-1 Proposed Wellbore Schematic for Minerva South CCS Well No. 001

Figure 5-2 Proposed Wellbore Schematic for Minerva South CCS Well No. 002

Figure 5-3 Proposed Injector Well Head System for MS CCS 1 and MS CCS 2

Figure 5.3.3-1 Triaxial Envelope for 20" Casing for MS CCS 1

- Figure 5.3.3-2 Triaxial Envelope for 20" Casing for MS CCS 2
- Figure 5.3.3-3 Triaxial Envelope for 13 5/8" Casing for MS CCS 1
- Figure 5.3.3-4 Triaxial Envelope for 13 5/8" Casing for MS CCS 2
- Figure 5.3.3-5 Triaxial Envelope for 9 5/8" Casing (Stage 2) for MS CCS 1
- Figure 5.3.3-6 Triaxial Envelope for 9 5/8" Casing (Stage 2) for MS CCS 2
- Figure 5.3.3-7 Triaxial Envelope for 9 5/8" Casing (Stage 1) for MS CCS 1
- Figure 5.3.3-8 Triaxial Envelope for 9 5/8" Casing (Stage 1) for MS CCS 2

APPENDICES

- Appendix I Environmental Justice Plan
- Appendix II Environmental Analysis- "IT" Response
- Appendix III Summary of Requirements
- Appendix IV Water-Use by Aquifer Summaries
- Appendix V Logs Used to Create Maps
- Appendix VI Fault Slip Potential Study
- Appendix VII Geochemistry
 - VII-1 CECOS, WDW No. 004 Completion Report
 - VII-2 GCS Phase 1 - Geochemical Modeling Report
- Appendix VIII Magnetometer Survey
 - VIII-1 Magnetometer Survey Strategy
 - VIII-2 Magnetometer Survey Results
- Appendix IX CO₂ Stream Compatibility
 - IX Nippon Steel Material Recommendation
 - IX -2 PermaSet Cement System
- Appendix X Drilling Plans
 - X-1 Drilling Plan for MS CCS 1
 - X-2 Drilling Plan for MS CCS 2
- Appendix XI Stimulation Plans
 - XI-1 Stimulation Plan for MS CCS 1
 - XI-2 Stimulation Plan for MS CCS 2



45031 & 45032

Appendix XII Operating Plans

XII-1 Operating Plan for MS CCS 1

XII-2 Operating Plan for MS CCS 2



45031 & 45032

LIST OF ATTACHMENTS

Attachment A	Area of Review (AoR) and Corrective Action Plan
Attachment B	Financial Assurance and Responsibility Demonstration
Attachment C	Pre-Operational Logging and Testing Program
Attachment D	Testing and Monitoring Plan
Attachment E	Injection Well Plugging Plan
Attachment F	Post-Injection Site Care (PISC) and Site Closure Plan
Attachment G	Emergency Remedial Response Plan (ERRP)



LIST OF ACRONYMS

2D	Two Dimensional	MS CCS 1	Minerva South CCS Well No. 001
3D	Three Dimensional	MS CCS 2	Minerva South CCS Well No. 002
AoR	Area of Review	MSL	Mean Sea Level
APSTM	AVO Pre-stack Time Migration	NAD	North American Datum
AVO	Amplitude Verses Offset	NEPA	National Environmental Policy Act
CCS	Carbon Capture Sequestration	NMR	Nuclear Magnetic Resonance
CDR	Carbon Dioxide Removal	NRC	Nuclear Regulatory Commission
CEO	Chief Executive Officer	OBE	Operating Basis Earthquake
CEQ	Council on Environmental Quality	P&A	Plugged and Abandoned
CFR	Code of Federal Regulations	PEF	Photoelectric Factor
DOE	Department of Energy	PHREEQC	PH (pH) RE (redox) EQ (equilibrium) C (program written in Q)
DSCA	Differential Strain Curve Analysis	PISC	Post-Injection Site Characterization
EJ	Environmental Justice	PSTM	Pre-Stack Time Migration
EOR	Enhanced Oil Recovery	RPSTM	Raw Pre-stack Time Migration
EPSTM	Enhanced Pre-stack Time Migrations	SDC	Seismic Design Category
FEMA	Federal Emergency Management Agency	SDRD	Submitted Drillers Reports Database
FLIGHT	Facility Level Information on Greenhouse Gases Tool	SDWA	Safe Drinking Water Act
FSP	Fault Slip Potential	SONRIS	Strategic Online Natural Resources Information System
GR	Gamma Ray	SP	Spontaneous Potential
GCS	Gulf Coast Sequestration, LLC	SWD	Saltwater Disposal
GSDT	Geologic Sequestration Data Tool	T&M	Testing and Monitoring
ICW	Intracoastal Waterway	TDS	Total Dissolved Solids
IMD	Injection and Mining Division	TRRC	Texas Railroad Commission
LAC	Louisiana Administrative Code	TVDSS	True Vertical Depth Sub Sea
LDENR	Louisiana Department of Energy and Natural Resources	TWDB	Texas Water Development Board
LDTOD	Louisiana Department of Transportation and Development	TWT	Two Way Time
LNG	liquid natural gas	UIC	Underground Injection Control
Max	Maximum	US	United States
Min	Minimum	USDW	Underground Sources of Drinking Water
MD	Measured Depth	USEPA	United States Environmental Protection Agency
MIGNR	Migration with Noise Reduction	USGS	United States Geological Survey
MMI	Modified Mercalli Intensity	UTC	Universal Time Coordinated
MMT	Million Metric Tons	VSP	Vertical Seismic Profile



45031 & 45032

CHEMICAL/COMPOUNDS

CO ₂	carbon dioxide
H ₂	hydrogen gas
H ₂ CO ₃	carbonic acid
H ₂ S	hydrogen sulfide
Hg	mercury
NaCl	sodium chloride
O ₂	oxygen
SO ₄ ²⁻	sulfate
NO ₂	nitrogen dioxide

UNITS

%	percent
μm	micrometer
cm	centimeters
ft	feet
g	grams
g/cm ³	grams per cubic centimeter
GPa	gigapascal
lb	pounds
km	kilometers
mi ²	square miles
Mblg	magnitude
mD	millidarcies
mg/L	milligrams per liter
Mgal/d	million gallons per day
MMT	million metric tons
Mpa	megapascal
ppm	parts per million
psi	pounds per square inch
psia	psi absolute



45031 & 45032

1 PROJECT BACKGROUND AND GENERAL INFORMATION

1.1 PROJECT OVERVIEW

Gulf Coast Sequestration, LLC (GCS) seeks to build and responsibly operate a safe, permanent carbon dioxide (CO₂) sequestration asset for the Louisiana Gulf Coast. Our initial Carbon Capture Sequestration (CCS) development is identified as Project Minerva, located in Calcasieu and Cameron Parishes in southwest Louisiana. The project will be developed incrementally and will initially include a CCS facility connected by pipeline to two Class VI CCS injection wells. Minerva Facility will be located in Calcasieu Parish at a site north of the Gulf Intracoastal Waterway and will be connected by approximately 3-mile pipeline to the Minerva South (MS) well pad located in Cameron Parish south of the waterway. The well pad will contain Minerva South CCS Well No. 001 (MS CCS 1) and Minerva South CCS Well No. 002 (MS CCS 2). The two Class VI injection wells were sited to maximize access to the available pore volume of the upper Frio Formation and to disperse and maximize the flow of CO₂ from the project area. A topographic map showing the property boundaries of the Minerva Facility, the location of the proposed injection wells, MS CCS 1 and MS CCS 2, and the delineated Area of Review (AoR) is provided at Figure 1.1-1. The map also identifies wells used to create maps and cross-sections with Map ID numbers, which are keyed to Table 1.1-1.

The Louisiana Department of Energy and Natural Resources (LDENR) has primary permit and enforcement authority (primacy) over Class VI Injection Wells through their Underground Injection Control (UIC) program. The UIC program is administered through the Office of Conservation's Injection and Mining Division (IMD). The primary rule and regulatory priority are to protect human health and the environment for the State of Louisiana, including the protection of potential USDWs, surface waters, and the land from endangerment by regulating the subsurface injection of wastes such as CO₂ sequestration.

This application is being submitted in compliance with LDENR regulations for Class VI Injection Wells, Louisiana Administrative Code (LAC), Title 43, Part XVII, Chapter 36 (LAC 43:XVII §3601-3633). In accordance with Title 40, Chapter I, Subchapter D, Part 146.91 of the Code of Federal Regulations (40 CFR 146.91) and LAC 43:XVII §3629.A.3, the complete application will be submitted to the United States Environmental Protection Agency (USEPA) via the Geologic Sequestration Data Tool (GSDT).

1.2 FACILITY/SITE INFORMATION

Facility Name: Minerva Facility

Injection Wells: Minerva South CCS Well No. 001 (MS CCS 1)
Minerva South CCS Well No. 002 (MS CCS 2)

Facility Contact: David Cook, CEO
5599 San Felipe Street, Suite 1450, Houston, Texas 77056
(713) 419-6808; dcook@gcscarbon.com

Well Locations: Sec 3, T12S, R13W, Cameron Parish, Louisiana



45031 & 45032

MS CCS 1 (North American Datum (NAD) 1927)
Surface: 30° 02' 34.10"W, -93° 40' 20.63"N
Bottom-Hole: 30° 02' 34.10"W, -93° 40' 20.63"N
MS CCS 2 (NAD 1927)
Surface: 30° 02' 33.84"W, -93° 40' 20.48"N
Bottom-Hole: 30° 02' 13.74"W, -93° 40' 42.07"N

1.3 OWNERSHIP

GCS (LDENR Operator Code: G1037) was established in 2019 with the single purpose of building and operating a world-scale carbon sequestration solution for companies who operate in the southwest Louisiana industrial corridor. The company will partner with industrial customers to capture CO₂ and safely contain it underground to help them reduce carbon emissions and achieve their long-term sustainability goals. GCS is comprised of an exceptional management team with more than 15 decades of experience across the core disciplines of energy, finance, operations and subsurface technical that are required to successfully execute one of the first sequestration projects in Louisiana.

GCS has leased land from a multi-generational single-family (Stream) office, based in Lake Charles, Louisiana, for this project. In addition to other investments, the Stream family are long-term landowners in southwestern Louisiana, owning and operating land assets for well over a century within the community. An affiliated business, Stream Wetland Services, has protected and restored tens of thousands of acres of wetlands and sustainably managed thousands of acres of timber assets.

1.4 CO₂ SOURCE

Project Minerva envisions sourcing CO₂ volumes from multiple sources of CO₂ from industrial facilities in Lake Charles industrial corridor in southwestern Louisiana and Beaumont industrial corridor in southeastern Texas. According to USEPA's Facility Level Information on Greenhouse Gases Tool (FLIGHT), the total CO₂ emissions from the four counties/parishes adjacent to Project Minerva - Orange County, Beaumont County, Calcasieu Parish, and Cameron Parish - emitted nearly 57 MMT of CO₂ in 2018 (EPA, 2023).

The emissions that are anticipated for Project Minerva in the near term are likely to be higher purity CO₂ that is economically capturable from natural gas processing and other natural gas derived processes including blue Hydrogen (H₂) and Liquified Natural Gas (LNG). The Gulf Coast region of Southeast Texas and Southwest Louisiana have a variety of currently operating or planned facilities for natural gas processing. Such applications can meet the CO₂ specification that GCS has proposed. Further, such specification of CO₂ is consistent with the existing CO₂ pipeline infrastructure in the region.

1.5 PROPOSED INJECTION MASS/VOLUME

Project Minerva is designed to operate for 30 years as a CO₂ sequestration facility, operating each injection well, MS CCS 1 and MS CCS 2, at a maximum daily injection rate of 0.002 million metric tons (MMT) per day (MMT/day) and an annual average injection rate of 0.674



45031 & 45032

MMT/year from combined CO₂ sources. The total injection mass, over the life of each well, is anticipated to be at least 10.1 MMT. The total injection mass for the project is anticipated to be at least 20.2 MMT.

1.6 PROJECT TIMELINE

The total project timeline for Project Minerva is approximately 89 years. This timeline includes a pre-injection timeframe of approximately 4 years, and an injection and post-injection timeline of approximately 85 years.

The pre-injection timeline includes approximately 2 years for permitting and 2 years for construction. Once injection commences, GCS proposes to operate the project for 30 years. During that time, GCS will conduct testing and monitoring (T&M) of the project until the injection wells are plugged and abandoned (P&A), at which time the 50-year Post-Injection Site Care (PISC) period will begin. The CO₂ plume stabilizes and the pressure front disappears within the PISC period (45 years post-injection). Once the PISC period concludes, GCS will initiate site closure activities and submit the proper demonstrations to LDENR, which may take as long as 5 years.

1.7 PERMIT COMPLIANCE

The objective of this permit application is to comply with all conditions of a permit set forth under in the requirements of LAC 43:XVII §3609.D. GCS understands appropriate actions are required to prevent the movement of fluids into or between Underground Sources of Drinking Waters (USDWs) or into any unauthorized zones consistent with the requirements of LAC 43:XVII §3617.1.a. For purposes of enforcement, compliance with this permit application during its term constitutes compliance with Part C of the Safe Drinking Water Act (SDWA).

In the case GCS is unable to maintain compliance with any conditions of this permit or mitigate any adverse impacts of USDW contamination, GCS understands this constitutes an act of noncompliance and if the LDENR Commissioner of Conservation (Commissioner) determines that such noncompliance endangers USDWs can enforce action such as permit termination, revocation and reissuance, or modification, or for denial of a permit renewal application.

1.8 ASSOCIATED PERMITS

Per LAC 43:XVII §3607.B.9, a list of all permits or construction approvals that have been received or applied for that may affect our legal or technical ability to undertake Project Minerva is provided in Table 1.8-1. The table lists the federal, tribal, state and local permits applicable to Project Minerva; those permits specified in LAC 43:XVII §3607.B.9 are bolded.

1.9 ENVIRONMENTAL JUSTICE

GCS has prepared an Environmental Justice (EJ) Plan to ensure potentially adverse environmental effects associated with Project Minerva will be minimized and/or mitigated, as applicable, and to prevent a disproportionate share of environmental or socioeconomic



45031 & 45032

impacts on any racial, ethnic, or socioeconomic group. The EJ Plan is provided as Appendix I and has been prepared in accordance with the Council of Environmental Quality's (CEQ) environmental justice guidance under National Environmental Policy Act (NEPA) and USEPA's *Promising Practices for EJ Methodologies in NEPA Reviews*.

1.10 ENVIRONMENTAL ANALYSIS

Louisiana Constitutional Article IX, § 1, of the Louisiana Constitution imposes a duty of environmental protection on all State agencies and officials and requires a balancing process in which environmental costs and benefits must be given careful consideration along with economic, social and other factors.

So that LDENR-Office of Conservation can implement a balancing process in their review of Class VI permit applications, they have requested applicants to prepare responses to the following questions:

1. Have the potential and real adverse environmental effects of the proposed project been avoided to the maximum extent possible?
2. Does a cost benefit analyses of the environmental impact costs versus the social and economic benefits of the proposed project demonstrate that the latter outweighs the former?
3. Are there alternative projects which would offer more protection to the environment than the proposed project without unduly curtailing non-environmental benefits?
4. Are there alternative sites which would offer more protection to the environment than the proposed site without unduly curtailing non-environmental benefits?
5. Are there mitigating measures which would offer more protection to the environment than the proposed project without unduly curtailing non-environmental benefits?

GCS has prepared responses to these questions in adequate detail, together with sufficient justification and supporting data, to allow LDENR to fulfill their constitutional obligation to perform an environmental analysis for Project Minerva. The Environmental Analysis will be provided to the Commissioner as Appendix II of this Narrative at least 30 days prior to preparation of a Draft Permit for this project.

1.11 GSDT SUBMISSION

The Class VI Permit Application Narrative for Project Minerva has been submitted via the *Project Information Tracking* module in GSDT. The Application Narrative and supporting materials (tables, figures, appendices, and references) were uploaded in the *Class VI Permit Application Narrative* field of the *Updated Information* tab of the module. The Form UIC-60 CCS Class VI Well Permit Application, location plats, and property owner table with associated map were uploaded in the *Information to Support Permit Application* field of the same tab. The remaining tabs that required input data or file uploads were completed and submitted via the GSDT.

A Summary of Requirements is provided as Appendix III, which includes tables of all of the



45031 & 45032

inputs provided in the GSDT required fields, as well as, information pertinent to the operating conditions, reporting requirements, shutdown procedures, and emergency notification of Project Minerva.

2 SITE CHARACTERIZATION

2.1 GEOLOGY AND HYDROGEOLOGY

2.1.1 Regional Geology

The Gulf of Mexico is a relatively small ocean basin covering an area of more than 579,000 square miles (mi^2) (1.5 million kilometers (km^2)) (National Ocean and Atmospheric Administration, 1985). It began to form via rifting during the Triassic and Jurassic Periods. Sediment input has been particularly voluminous since the start of the Paleogene Period and is responsible for extensive deformation of underlying salt and the resulting abundance of prolific hydrocarbon systems along the Gulf Coast of Texas and Louisiana (Foote, 1984). Project Minerva is comprised of more than 8,000 feet (ft) of regionally extensive clastic strata. A regional geologic stratigraphic column is provided in Figure 2.1.1-1.

The earliest record of sedimentation in the Gulf of Mexico Basin occurred during the Late Triassic to Early Jurassic period, between 160 and 140 million years ago. Repeated cycles of seawater flooding and evaporation resulted in the formation of extensive salt accumulations ranging locally from 10,000 ft to 15,000 ft thick. Subsequently, buoyancy-driven flow created the salt diapirs, pillows and massifs which contribute to the characterization of the Gulf Coast structure present day (Foote, 1984).

The early phases of continental rifting resulted in the deposition of non-marine red bed and deltaic sediments including shales, siltstones, sandstones, and conglomerates of the Eagle Mills Formation in a series of restricted, graben fault-block basins (Figure 2.1.1-2). Following the Eagle Mills Formation, the deposition of thick sequences of anhydrite and salt beds, known as the Werner Anhydrite and Louann Salt, occurred within the major structural basins (Kreitler, et al., 1981). Overlying the Louann Salt, the Norphlet Formation marked the end of the deposition of evaporites with clastic, non-fossiliferous sandstones and conglomerates (Figure 2.1.1-1) (Mancini, Mink, Bearden, & Wilkerson, 1985; Todd & Mitchum, 1977).

Broad carbonate banks composed of limestones, dolomites, and interbedded anhydrites developed along the edges of the Gulf of Mexico Basin, with fine carbonate-muds deposited in deeper water areas. Reef construction and sedimentation kept pace with regional subsidence, which allowed thick carbonate sequences to accumulate (Foote, 1984). These shallow-water carbonates and clastic rocks make up the Smackover, Buckner, Haynesville formations, and the Cotton Valley Group, non-skeletal, carbonate sands and muds in which accumulated on a ramp-type shelf with reef buildups developed on subtle basin highs (Baria, Stoudt, Harris, & Crevello, 1982).

During the Upper Cretaceous, a large tectonic uplift formed the Rocky Mountains, while the Gulf of Mexico basin subsided. Large volumes of clastic sediments from the uplift were deposited as wedges into the basin. This effectively shuts off the production of carbonates, except in the Florida and Yucatan regions. Since the Cretaceous, the rate of terrigenous sediment influx has been greater than the rate of basin subsidence, resulting in significant progradation of the continental shelf margin (Figure 2.1.1-3).

Sediment supplies during Cenozoic time overwhelmed the general rate of subsidence,

Commented [KG1]: @McKenzie Morrison Add Swanson, Karlsen & Valentine Reference to text

causing the margins to prograde up to 240 miles from the edges of Cretaceous carbonate banks to the current position of the continental slopes off Texas and Louisiana (Foote, 1984). The geometry of Cenozoic deposition in the Gulf Coast Basin was primarily controlled by the interaction of the following factors:

- Changes in the location and rates of sediment input, significantly shifting the areas of maximum sedimentation,
- Changes in the relative position of sea level, developing a series of large-scale depositional cycles throughout Cenozoic time,
- Diapiric intrusion of salt and shale in response to sediment loading, and
- Flexures and growth faults due to sediment loading and gravitational instability.

Early Tertiary sediments are thickest in the Rio Grande Embayment of southern Texas, reflecting the role of the ancestral Rio Grande and Nueces Rivers as sediment sources to the Gulf of Mexico basin (Figure 2.1.1-4). By the Oligocene, deposition had increased to the northeast, suggesting that the ancestral Colorado, Brazos, Sabine, and Mississippi Rivers were increasing in importance. Miocene time is marked by an abrupt decrease in the amount of sediment entering the Rio Grande Embayment, with a coincidence increase in the rate of sediment supply in southeast Texas, Louisiana, and Mississippi. Throughout the Pliocene and Pleistocene Epochs, the maximum depocenters of sedimentation were controlled by the Mississippi River and are located offshore of Louisiana and Texas.

Tertiary sediments accumulated to great thickness where the continental platform began to build toward the Gulf of Mexico, beyond the underlying Mesozoic shelf margin and onto transitional oceanic crust. Rapid loading of sand on water-saturated prodelta and continental slope muds resulted in contemporaneous growth faulting (Loucks, Dodge, & Galloway, 1986). The effect of this syndepositional faulting was a significant expansion of the sedimentary section on the downthrown side of the faults. Sediment loading also led to salt diapirism, with its associated faulting and formation of large salt withdrawal basins (Galloway, Hobday, & Magara, 1982).

Sediments of the Tertiary progradational wedges were deposited in continental, marginal marine, nearshore marine, shelf, and basinal environments and present a complex depositional system along the Texas Gulf Coast.

Overlying the Tertiary progradational wedges along the Texas Gulf Coast are the Pleistocene and Holocene sediments of the Quaternary Period. The voluminous infilling of the Gulf basin during Tertiary time was followed by sediment influx of similar proportions due to the profound effects of continental Pleistocene glaciation (Foote, 1984). Pleistocene sedimentation occurred during a period of complex glacial activity and corresponding sea level changes. As the glaciers made their final retreat, Holocene sediments were deposited under the influence of a fluctuating, but overall rising, sea level. Quaternary sedimentation along the Louisiana Gulf Coast occurred in fluvial, marginal and marine environments.

The formations of interest at Project Minerva are both Oligocene and Miocene stratigraphy. During these periods of time, four sediment-dispersal axes dominated the Gulf margin

including (1) the Norma delta, (2) the Norias delta (Rio Grande Embayment), (3) the Houston delta (Houston Embayment), and (4) the central Mississippi delta (Figure 2.1.1-4). The Houston Embayment and central Mississippi delta provided a source of coarse-grained sediment for southeast Texas and southwest Louisiana (Swanson & Karlsen, 2009). This coarse-grained sediment consisted of Oligocene and Miocene deposits and were deposited as major progradational wedges along the margin of the Gulf Coast Tertiary basin, a basin comprised of the Houston Embayment and South Louisiana Salt Basin sub-basins (Swanson, Karlsen, & J, 2013).

Major progradational wedges are typically characterized by an up-dip section of interbedded continental and marginal marine sediments underlain by a thick marine section composed of under compacted slope and basin claystone. The instability caused by the direct and rapid loading of water saturated, unconsolidated sediments resulted in the development of large scale, syndepositional, down-to-the-basin faults and intraformational deformation (Galloway, Hobday, & Magara, 1982).

Three major progradational delta complexes, designated the Central Mississippi, Houston and Norias delta systems, identified by (Galloway, Henry, & Smith, 1982), were centered in the South Louisiana Salt Basin, Houston Embayment and Rio Grande Embayment, respectively (Figure 2.1.1-4). Three fluvial systems, the ancestral Mississippi, Chita/Corrigan, the Gueydan, supplied sediment to the delta complexes. The Houston delta system of Texas and southwestern Louisiana is centered in southern Harris County, Texas. The system is composed of several minor, laterally coalescent, and frequently shifting delta lobes. The Chita/Corrigan fluvial systems supplied sediment. Up-dip deltas exhibited wave-dominated, arcuate geometries, while lobate delta geometries characterized episodes of maximum progradation or an area where high subsidence rates were associated with salt withdrawal basins. Due to constant switching of delta lobes, the rate of coastal progradation was slow for the Houston delta system (Galloway, Henry, & Smith, 1982).

A major global sea level rise occurred during the late Cretaceous, creating the Mississippi Embayment and allowing the farthest inland transgression of a shallow epicontinental sea (Vail, Mitchum, & Thompson III, 1977). This embayment is part of the Mississippi Alluvial plain and supplied sediment to the southwestern portion of Louisiana. By the Oligocene, deposition had increased from the northeast, suggesting that the ancestral Colorado, Brazos, Sabine, and Mississippi Rivers were increasing in importance

2.1.1.1 Regional Stratigraphy

The Gulf Coastal Plain is characterized by rapid subsidence in areas of high sediment loading through multiple cyclic depositional episodes (Figure 2.1.1-5). These cycles represented various transgressive and regressive stages driven by variations in sediment supply and subsidence. Oligocene and Miocene deposits are subdivided according to depositional cycles and paleontological zones (Foote, 1984; Swanson, Karlsen, & J, 2013). These subdivisions are listed below in ascending order:

- Vicksburg Group (early Oligocene). Represents a transgressive phase (mainly shale and some sandstone lenses),

- Frio Formation (middle Oligocene). Represents a dominantly regressive phase. (Mixture of marginal marine and deltaic sandstones and shales, with localized deep marine shales and turbidite sandstones) Downdip equivalent of the continental Catahoula Formation (Swanson, Karlsen, & J, 2013),
- Anahuac Formation (late Oligocene). Represents transgression (marine shales and thin sandstones), and
- Fleming Formation (Miocene). Represents a very high number of alternating regressive and transgressive phases (progradational sandstones and retrogradational shales).

Vicksburg Formation

The Vicksburg Formation lies within the Tertiary depositional wedge of the Gulf Coastal Plain and is regionally extensive across the Gulf Coast of Texas and Louisiana (Coleman & Galloway, 1990). The Vicksburg Formation consists of fluvial-deltaic sandstones, silts, and clays (Swanson, Karlsen, & J, 2013; Delaney, 1963). The Vicksburg sediments were deposited by delta flanks and associated shorezone, strand plain, and barrier systems (Coleman & Galloway, 1990).

In southeast Texas and southwestern Louisiana, the Vicksburg Formation is comprised of interbedded deltaic, outer-shelf and slope deposits, massive bedded shales, and medium bedded sandstones (Gregory, 1966; Coleman & Galloway, 1990; Swanson, Karlsen, & J, 2013). In the Houston Embayment and the westernmost portion of the South Louisiana Salt Basin of the Gulf Coast Salt Basin, the Vicksburg formation was deposited in a series of stacked delta environments (Figure 2.1.1-3) (Coleman & Galloway, 1990; Swanson, Karlsen, & J, 2013).

During major deltaic progradation in the early Oligocene, the Vicksburg Fault Zone was created in south Texas and northern Mexico, which is a narrow fault zone characterized by vertical displacement of the underlying Frio Formation. The Vicksburg Fault Zone, or flexure, forms the updip limit of significant structural deformation of the Frio Formation. In south Texas, thickening and displacement of Frio sediments are significantly greater in the Frio Fault Zone, downdip of the Vicksburg Fault Zone, than in the Vicksburg Fault Zone. In Louisiana, thickening and displacement of Frio sediments thin spanning across Louisiana from west to east (Swanson & Karlsen, 2009).

Frio Formation

The Frio Formation was deposited during the middle Oligocene and is composed of a thick sequence of mainly regressive sediments that were deposited rapidly in alluvial, lagoonal, marginal marine and deep marine environments, forming a major progradational wedge along the Gulf. The Frio Formation thickness and depth increases southwards, with localized variations occurring around salt diapirs and major faults. Non-marine sands were deposited in constantly shifting deltas and are interbedded with marine shales were deposited during periods of local transgression. In areas between major delta systems such as the central Mississippi delta, shoreface and shallow marine environments deposited

broad sandstone units interbedded with marine silts and shales during transgressive periods. The progradational Frio wedge was initiated by a major global fall in sea level, with subsequent Frio sediments deposited under the influence of a slowly rising sea (Galloway, Henry, & Smith, 1982).

The Norias delta system of south Texas constitutes the Frio Formation depocenter in the South Texas Coastal Plain. Typical sand content ranges from 25 percent (%) to 40% for a total Frio Formation section that can be more than 12,000 ft thick. The lateral boundaries of the Norias delta system remained fixed through time, centering on Kennedy County, Texas. Deposition of the system prograded the continental margin more than 60 miles basin ward, primarily during deposition of the lower and middle Frio Formation sections. This major off lapping episode was terminated by the shale-rich Anahuac Formation transgression (Galloway, Henry, & Smith, 1982).

Regionally, the Frio Formation and Catahoula Formation (up-dip equivalent) can be divided into a number of distinct depositional systems. Within Louisiana, the upper Frio Formation transitions into fine-grained, mix-load dominated fluvial sediments up-dip, north of Beauregard Parish, ultimately pinching out in central Louisiana. To the south (offshore Gulf of Mexico) the downdip limit of the upper Frio Formation is defined by large-scale fault-related juxtaposition against thick, fine-grained formations in the overlying Neogene (Swanson, Karlsen, & J, 2013). Local structural highs are the result of salt diapirism, and associated faulting, in combination with the regional structural fabric of major faults dipping dominantly southwards, parallel with the Gulf coastline.

Anahuac Formation

As sea level continued to rise during the late Oligocene, the underlying Frio Formation progradational platform flooded. Wave reworking of sediment along the encroaching shoreline produced thick, time transgressive blanket sands at the top of the Frio Formation and base of the Anahuac Formation section. The transgressive marine shale-rich Anahuac Formation deposited conformably on top of the blanket sands throughout the Texas and Louisiana coastal region. The Anahuac Formation was deposited in an inner-shelf, shallow marine, proximal deltaic, distal deltaic, and slope environments (Swanson, Karlsen, & J, 2013). It is typically composed of calcareous, marine shales with localized, lenticular, micritic limestone units. In western and central parts of Louisiana, including Project Minerva, the interval mostly comprises shales with lesser sandstones. Limestones and calcareous clastics dominate in eastern Louisiana and the eastern Gulf of Mexico, where clastic influx was minimal (Swanson, Karlsen, & J, 2013).

The Anahuac Formation dips towards the Gulf of Mexico and thickens regionally from its inshore margin to nearly 2,000 ft offshore (Galloway, Henry, & Smith, 1982). In southwestern Louisiana, the Anahuac Formation reaches a thickness of more than 1,300 ft. An erosional unconformity marks the top of the Anahuac Formation, and the start of a regressive period in the basal Miocene interval. Local variations in gross thickness are likely the result of this unconformity combined with variable fault movement along regional faults, and around salt diapirs.

Fleming Group

The thick, Miocene strata of the Fleming Group is comprised of more transgressive-regressive cycles than any other epoch. (Rainwater, 1968) has interpreted the middle Miocene as a major delta-forming interval comparable to the present-day Mississippi Delta system. The middle Miocene is representative of much of the entire Miocene interval, with only the site of deposition changing in response to various transgressions and regressions. The result is a complex of interbedded shallow neritic clays; restricted marine clays, silts, sands; and deltaic deposits of sands, silts, and clays. If a composite were made of the thickest Miocene intervals around the Gulf Basin, more than 40,000 ft of accumulated sediment would be obtained, of which about 20,000 ft were deposited in southern Louisiana (Rainwater, 1968).

The two formations in which form the major units of the Fleming Group, in ascending order: (1) the Oakville Formation, and (2) the Lagarto Formation. These formations were deposited in relatively shallow water across a broad, submerged, shelf platform constructed during Frio Formation and Anahuac Formation deposition throughout the Gulf Coast region and are equivalent to the Oakville and Lagarto Formations of East Texas, as well as the Catahoula, Hattiesburg, and Pascagoula Formations of Mississippi (Swanson & Karlsen, 2009). Three major depositional regimes characterize the Fleming Group. Figure 2.1.1-6 shows the distribution of the lower Miocene depositional systems across the Texas Coastal Plain.

Goliad Sand

Conformably overlying the Fleming Group is the Goliad Sand. Similar like the Catahoula Tuff or Sandstone, Willis Sand, and Beaumont Clay, the Goliad Sand is often interchangeably referred to in literature as a formation. The Goliad Sand is comprised of coarse-grained sediments, including localized cobbles, clay balls, and wood fragments at the base of the formation. The Goliad Sand can be distinguished into an upper and lower formation differentiating by sand content (Figure 2.1.1-7). The boundary between the upper and lower Goliad sand class identifies the discrepancy between the base of the Chicot aquifer and the top of the Evangeline aquifer considering the Chicot aquifer is regionally composed of a sandier sedimentary setting (Young, et al., 2006; Chowdhury & Turco, 2006).

The Goliad Sand was deposited during Pliocene time and is similar in character to underlying late Miocene stratigraphic units reflecting a regional depositional transition from fluvial channel and intervening floodplain facies (updip) to a mixture of deltaic and marginal marine environments (downdip) (Young, et al., 2006). The width of the Goliad Sand gradually increases southeastward in Texas toward the Rio Grande Embayment from coastal counties (Baker Jr, 1978). Along the coastal county of Jim Wells, Texas, the Goliad Sand is approximately 400 ft to 600 ft in thickness and yields moderate quantities of fresh to slightly saline water-bearing sands southeastward (Mason, 1963).

Willis Sand

Conformably overlying the Goliad Sands are the Willis Sands. The Willis Sand was deposited in a fluvial-deltaic depositional environment and are comprised of coarsening-upward

sequence, commonly indicative of delta-front facies (Young, et al., 2006). In southeast Texas, the Willis Sand deposits consist of fossiliferous sand and gravelly sand beds and are complexly faulted along the coastal counties. The Willis Sands are locally extensive and grade conformably into the overlying Holocene depositional units consisting of the Lissie Formation and Beaumont Clay (Chowdhury & Turco, 2006). The Willis Sand ranges in thickness up to 80 ft in southeast Texas (Houser & Ryan, 1983).

The Willis Sands were deposited during Pleistocene time under the influence of the complex fluctuations of sea level changes. The changes in sea level influenced the sand and clay content of the Chicot aquifer, which contains the Willis Sand, Bentley Formation, Montgomery Formation, and Beaumont Clay of Pleistocene age and any overlying undifferentiated Holocene alluvium. The Willis Sand comprises the lower part of the Chicot Aquifer yielding the high sand content and yields good quantities of fresh groundwater where the lower part of the Chicot aquifer contains slightly saline groundwater (Baker Jr, 1978; Young, et al., 2006).

[Lissie Formation, Beaumont Clay, and Holocene Series](#)

The Lissie Formation and Beaumont Clay are the two dominant subdivisions of the Pleistocene system whereas the Willis Sand represents only a part of the Pleistocene system. The Lissie Formation is unconformably contained between the Goliad Sand and the overlying Beaumont Clay and is comprised of, in ascending order, the Bentley Formation and the Montgomery Formation (Chowdhury & Turco, 2006; Baker Jr, 1978). The Lissie Formation consists of continental deposits laid down on flood plains and partly as delta sands, silts, and mud at the mouth of rivers (Figure 2.1.1-7). Although the Goliad Sand grades into the Lissie Formation and Beaumont Clay, the Lissie contains relative less conglomerates than the underlying Goliad Sand and is often identified by caliche beds marked at the base of the formation (Chowdhury & Turco, 2006).

The Beaumont Clay is contained between the underlying Lissie Formation and overlying Holocene series. The Beaumont Clay is made up of poorly bedded, marly clay and forms a thin mantle extending eastward. The Beaumont Clay was deposited largely by rivers in the form of natural levees and deltas that coalesced as river mouths shifted along the coast and, to a lesser extent, by marine and lagoonal water in the bays and embayments between stream ridges and delta banks (Figure 2.1.1-7) (Chowdhury & Turco, 2006).

The Holocene series consists of undifferentiated river alluvium and coastal deposits. The Holocene series was deposited in floodplains and point bars with grain sizes ranging from clay to gravel. The Holocene series is the largest surficial outcrop along the Texas and Louisiana Gulf Coast. The Holocene series provides a direct hydraulic connection between the surface water and groundwater systems (Chowdhury & Turco, 2006).

2.1.1.2 Regional Structure

The Gulf of Mexico continental margins and deep ocean basin regions are relatively stable areas (Foote, 1984). The Gulf of Mexico region is characterized by structural dip towards the Gulf Coast, with normal- and growth faults of Miocene/Oligocene age parallel to the

contemporaneous shelf edge (Figure 2.1.1-3 and Figure 2.1.1-8) (Jones, Turcan Jr, & Skibitzke, 1954) Tectonism driven in large part by sediment loading and gravity played a key role in contemporaneous and post-depositional deformation of Tertiary strata (Foote, 1984). Deeper fault zones are present at basement level, mirroring the trend of the shallower Oligocene-level faults, but do not appear to be directly linked (Figure 2.1.1-3).

Salt mobilization led to extensive diapirism across the Texas and Louisiana Gulf Coast. The remobilized salt, originating from the deep Louann Salt Formation, may be present in a number of geometrical forms, including diapirs and pillows. In the area of Project Minerva, salt features typically occur as diapirs, or “salt domes” (Figure 2.1.1-9). Such diapirs buoyantly moved upwards through many thousands of feet of younger strata concurrently with sedimentation during the Oligocene and Miocene. Regional salt features can be rooted deeply in the subsurface, extending vertically several thousand feet deep, where in other cases salt features may have been severed from deeper sources (Swanson, Karlsen, & J, 2013).

Two examples of salt domes are Vinton Salt Dome (Vinton Dome) and Black Bayou Salt Dome (Black Bayou Dome). The Vinton Dome is located in Calcasieu Parish, Louisiana, approximately 7 miles from the bottom-hole location of MS CCS 1 and approximately 7.7 miles from the bottom-hole location of MS CCS 2. Black Bayou Dome is located in Cameron Parish, Louisiana, approximately 2.4 miles east of the bottom-hole location of MS CCS 1 and approximately 2.7 miles east of the bottom-hole location of MS CCS 2 (Figure 2.1.1-10).

Associated faulting is caused either in response to local salt mobilization or evacuation, and on a larger scale where significant volumes of strata have been transported on listric fault surfaces which likely detach along deeper shales and/or salt intervals. Faulting induced by salt evacuation commonly causes an expanded sedimentary section on the downthrown side of the fault (growth fault), usually either down-to-the-coast or down-to-the-basin. Faulting associated with salt movement in the area of Project Minerva includes local radial faulting emanating from Black Bayou Dome.

A second cause of faulting common to the Texas and Louisiana Gulf Coast is the cause-and-effect relationship between rapid progradation of sediments and slope failure in the vicinity of the shelf edge or outer platform margin. Sediment accumulated in a series of wedges that thicken and dip gulfward. As a result of rapid progradation and sediment loading, large growth-fault systems formed near the downdip edge of each sediment wedge within the area of maximum deposition. Faulting typically aligned parallel with the contemporary shelf edges in the Gulf Coast region. The greatest displacement of faults and thickest accumulations of Oligocene and Miocene sediments occurred in an area known as the Frio Expanded Zone (Figure 2.1.1-3).

The regional structural trends of the Frio and Anahuac formations are demonstrated on Figure 2.1.1-8 (Jones, Turcan Jr, & Skibitzke, 1954). Depth increases significantly from north to south and is linked to frequent normal and growth faults striking perpendicular to dip, detaching along deep shale or salt intervals. Such faults are only resolvable with three dimensional (3D) seismic data and appear as noise in lower resolution structural maps generated from regional well data. Localized structural highs are associated with salt

diapirism in the regional area of Project Minerva. Synclines within the broad structural regime result from the interplay of major regional faults with salt domes and the associated counter-regional faulting.

Figure 2.1.1-3 and Figure 2.1.1-8 demonstrate the significant increase in Oligocene strata thickness observed as the “Frio Stable Shelf Fault Zone” (north Orange County and Central Calcasieu Parish, Louisiana) trends southeastwards into the “Frio Expanded Fault Zone” (Figures 2.1.1-3) (Swanson, Karlsen, & J, 2013). While no major growth faulting is observed in the Project Minerva 3D seismic dataset, it is believed that regionally, Oligocene sediments greatly expanded and filled vast amounts of accommodation space created by movement along growth faults within the “Frio Expanded Fault Zone” (Swanson, Karlsen, & J, 2013).

The shallower Oligocene through Holocene section thickens basinward, periodically interrupted by low-relief, broad salt domes and anticlines. Some minor fault displacement occurs as well, particularly where the system overlies deep-seated Eocene or Oligocene growth-fault trends (Galloway, Henry, & Smith, 1982). Structural modification is greatest where the Cenozoic sedimentary section is warped upwards along the margins of salt diapers (Figure 2.1.1-8).

2.1.1.3 Regional Hydrogeology

The USDW is defined by LAC 43:XVII §3601 as an aquifer or its portion which supplies any public water system or contains a sufficient quantity of ground water to supply a public water system and currently supplies drinking water for human consumption or contains fewer than 10,000 milligrams per liter (mg/L) total dissolved solids (TDS) and which is not an exempted aquifer. The following sections detail regional and local hydrogeology and hydrostratigraphy in the area and are located at Project Minerva.

The regional aquifer system is called the Gulf Coast Aquifer System and stretches from Texas, across Louisiana, Mississippi, and Alabama, and includes the westernmost portion of Florida. Miocene and younger formations contain usable quality water (<3,000 mg/L TDS) and potentially usable quality water (<10,000 mg/L TDS), which is defined as the base of lowermost USDW within this system. These aquifer systems regionally crop out in bands parallel to the coast and consist of units that dip and thicken towards the southeast. (Baker Jr, 1978) describes four major hydrogeologic units that comprise the Gulf Coast Aquifer System in the Texas and Louisiana region. In ascending order, the four units are:

- Jasper aquifer
- Burkeville confining system
- Evangeline aquifer
- Chicot aquifer

The Burkeville confining system hydrologically separates the Evangeline aquifer from the underlying Jasper aquifer. However, the Chicot and Evangeline aquifers are thought to be hydrologically connected. A hydrogeologic stratigraphic column for southwestern Louisiana is provided as Figure 2.1.1-11. The following sections provide details on the regional expanse

and parameters pertaining to the hydrostratigraphy for the defined systems from deepest to shallowest intervals. A regional stratigraphic cross-section (A-A') parallel to dip from (Baker Jr, 1978) depicting the aquifers in the regional area of southeast Texas is provided as Figure 2.1.1-12 and a local stratigraphic cross-section (A-A') parallel to dip from (Lindaman, 2023) depicting the aquifers in the local area of southwest Louisiana is provided as Figure 2.1.1-13.

Regional Hydrostratigraphy

Jasper Aquifer

The Jasper aquifer is a hydrostratigraphic unit contained within the Miocene sands in the southwestern portion of Louisiana and Texas. The base of the aquifer coincides with the stratigraphic lower boundary of the Fleming Formation. In parts of Texas, this also includes the Oakville Sandstone. However, in the area of Project Minerva, this geological interval is not present. The Jasper aquifer is separated from the deeper saline formation waters of the upper Frio Formation by the shale-rich Anahuac Formation and is a confined system overlain by the Burkeville confining unit (Figure 2.1.1-12). The system is laterally extensive throughout the southern portion of Louisiana and along Texas and Louisiana Gulf Coast of Texas. Regionally, the Jasper aquifer system dips southwards and becomes deeper increasing in salinity towards the Gulf of Mexico.

In Louisiana, the Jasper Aquifer System is only used as a freshwater source north of Project Minerva in Vernon, Beauregard, Rapides and Allen Parishes. In the area of Project Minerva, the Jasper aquifer contains saline waters, ranges in thickness from 50 ft to 2,400 ft thick regionally and is comprised of medium- to fine-grained sands. It is geologically isolated from other aquifers by laterally extensive overlying and underlying clay strata with recharge to the system northward (up-dip) of Project Minerva.

Burkeville Confining System

The Burkeville confining system separates the Jasper and Evangeline aquifers and retards the interchange of water between the two aquifers. The Burkeville confining system is comprised of compacted clays and fine-grained silts, with occasional lenses of sands. This system is shown to be an effective confining unit due to the differing hydrostatic pressures within the underlying Jasper aquifer and overlying Evangeline aquifer. The thickness of the Burkeville confining system is 300 ft along the Gulf Coast of Texas (Baker Jr, 1978). However, the unit thickness can vary from 100 ft to 1,000 ft within the Gulf Coast region. The Burkeville confining system's clay fraction varies across the Gulf Coast, from greater than 0.8 in southwest Texas to less than 0.3 in southeast Texas and southwestern Louisiana. The areas of low clay fraction is indicated by an increase in sand layers, containing fresh to slightly saline water, but because of the unit's relatively large percentage of silt and clay, the when compared to the Jasper aquifer and Evangeline aquifer, the Burkeville confining system functions strictly as a confining unit (Intera, 2020).

Figure 2.1.1-12 identifies and depicts the confining system dipping down toward the Gulf Coast of Texas, and although the geological units of the Gulf Coast Aquifer System are

stratigraphically correlated across the Texas-Louisiana border, the stratigraphic charts of Louisiana (Figure 2.1.1-11) do not identify the confining unit as the “Burkeville confining unit,” but instead inferred as the “Castor Creek confining unit” (Louisiana Geological Survey, 2000). Figure 2.1.1-14 is a hydrogeologic cross-section (Section -1) from the Texas Water Development Board (TWDB) study of the Gulf Coast Aquifer; the study extended from southeast Texas to southwest Louisiana (Young, Ewing, Hamlin, Baker, & Lupton, 2012). Both Figure 2.1.1-12 and Figure 2.1.1-14 demonstrate a confining clay separating the Jasper aquifer and Evangeline aquifer, and although assigned a different name in the Louisiana stratigraphic nomenclature (Castor Creek confining unit), this confining unit can be traced across neighboring state lines and are hydrogeologically the same.

Evangeline Aquifer

The Evangeline aquifer consists of Pliocene and late Miocene deposits ranging from loosely consolidated sands to gravels, with interbeds of silts and clays. The sands of the Evangeline aquifer are moderately well- to well-sorted and fine- to medium-grained with interbedded coarse sand, silt, and clay. The Evangeline aquifer includes the Goliad Sand and the upper unit of the Lagarto Formation, a member of the Miocene Fleming Group (DEQ of Louisiana, 2009). In southwest Louisiana, the Evangeline aquifer includes, in ascending order, the Castor Creek confining unit, Blounts Creek Member, and the lower units of the Pliocene Upland Allogroup (Lindaman, 2023).

The Evangeline aquifer underlies the Chicot aquifer and is separated from the Jasper aquifer by a Castor Creek confining unit. The upper portion of the Evangeline aquifer is separated from the Chicot aquifer by thin clay beds, although in some areas, the confining beds do not exist, and the upper sands of the Evangeline aquifer are in direct contact with the basal sands of the Chicot aquifer (DEQ of Louisiana, 2009).

In southwest Louisiana, recharge to the Evangeline aquifer occurs via rainfall inland from the Gulf of Mexico, and minimally, by leakage downwards from other shallow aquifers. The hydraulic conductivity of the Evangeline aquifer varies between 20 ft to 100 ft/day. The maximum depths of the Evangeline aquifer fresh water range from 150 ft ASL to 2,250 ft BSL, and the freshwater interval thickness ranges from 50 ft to 1,900 ft deep (DEQ of Louisiana, 2009).

Chicot Aquifer System

The Chicot aquifer system consists of Pleistocene and Holocene deposits ranging from unconsolidated to loosely consolidated gravels and coarse graded sands. The Chicot aquifer system includes the Pleistocene Willis Sand, Lissie Formation, and Beaumont Formation, as well as the Holocene undifferentiated alluvial sediments (Lindaman, 2023).

The Chicot aquifer system and the Evangeline aquifer have similar hydraulic frameworks, but the Chicot aquifer system is largely comprised of one major undifferentiated sand whereas the Evangeline aquifer contains interbedded silts and clays. In central and western Calcasieu and Cameron Parishes, the Chicot aquifer system includes the “200-,” “500-,” and “700-foot” sands (White & Griffith, 2020; Nyman, 1984). These sands are discussed in detail in Section 2.1.2.3 (Local Hydrogeology). The uppermost sand of the Chicot aquifer

system contains freshwater underlain by saltwater in Cameron Parish (Nyman, 1984), except along the southeastern coast where no freshwater is present (Smoot, 1988). Freshwater to saline water interface is driven northwards from the coast by water production for public supply, rice irrigation, and aquaculture. The southern limit of freshwater in the upper aquifer occurs near the coastline (Nyman, 1984). The Chicot aquifer system is the main regional aquifer system that provides usable groundwater for southwestern Louisiana (White & Griffith, 2020).

In southwestern Louisiana, the recharge to the Chicot aquifer system occurs where the Chicot outcrops in southern Rapides and Vernon Parishes, and in northern Allen, Beauregard, and Evangeline Parishes. There is also minimal recharge to the aquifer system via vertical leakage from the shallow overlying alluvial deposits. The aquifer system thickens and deepens to the south at a rate of about 30 ft/mile (Nyman, 1984).

Regional Groundwater Usage

The most recent Louisiana groundwater withdrawals from aquifers are reported by (Collier & Sargent, 2018) and summarize water withdrawals by 13 aquifer or aquifer system in on Appendix IV – Water-use by Aquifer Summaries. The Chicot aquifer system, Chicot equivalent aquifer system (southeastern Louisiana), Evangeline aquifer, Evangeline equivalent aquifer system (southeastern Louisiana), Jasper aquifer system, Jasper equivalent aquifer system (southeastern Louisiana) are all represented in Appendix IV – Water-use by Aquifer Summaries for the period 1980 – 2015.

The United States Geological Survey (USGS), in partnership with the Louisiana Department of Transportation and Development (LDOTD), has conducted a water-withdrawal and water-use inventory on a five-year basis since 1960. In *Water Use in Louisiana, 2015*, is to date the most recent Louisiana water use inventory report (Collier & Sargent, 2018; Purpera, 2020).

According to *Water Use in Louisiana, 2015*, the Jasper aquifer system is not a major source for regional freshwater use along the Louisiana Gulf Coast, except in Beauregard, Rapides and Vernon Parishes (Collier & Sargent, 2018). The Jasper aquifer contains freshwater for varying distances downdip regionally toward the gulf coast beyond which the aquifer contains saltwater. The increase in salinity is less commercially ideal to produce in comparison to the overlying Chicot and Evangeline aquifers as both are prolific water-yielding groundwater reservoirs in southern Louisiana. Precipitation on the outcrop of the Jasper aquifer is the source of recharge to the aquifer (Baker Jr, 1986). The aquifer's primary uses are for public water supply and industry with groundwater withdrawals in Louisiana at 47.95 million gallons per day (Mgal/d) (Collier & Sargent, 2018).

According to *Water Use in Louisiana, 2015*, groundwater withdrawal from the Evangeline aquifer in Louisiana is 28.56 Mgal/d, approximately half of that from the Jasper aquifer system. The Evangeline aquifer is used primarily in Evangeline, Allen, Avoyelles, and Beauregard Parishes for public supply and industry (Collier & Sargent, 2018).

The Chicot aquifer system yields the highest amount of groundwater withdrawals in Louisiana at 849.90 Mgal/d. The Chicot aquifer system is used primarily in Acadia,

Calcasieu, Cameron, and Jefferson Davis Parishes (Collier & Sargent, 2018). Although prolific aquifers, because of both the Chicot and Evangeline aquifers shallower positions and downdip edge of the aquifer's outcrop toward the coast, only the upper portion of the aquifer is used as a source of groundwater (Baker Jr, 1986). The largest contributor for withdrawal is rice irrigation and aquaculture, specifically water used for crawfish ponds. According to the *Water Use in Louisiana, 2015*, in southwestern Louisiana, the Chicot aquifer system is the major source of groundwater, providing 95.60 Mgal/day of groundwater used for public supply (Collier & Sargent, 2018).

According to *Water Use in Louisiana, 2015*, from 1980 to 2015 (i.e., the most recent reported Louisiana groundwater withdrawals from aquifers), total groundwater withdrawals decreased by 1.8% (Collier & Sargent, 2018). Unregulated groundwater withdrawals from aquifers can cause groundwater levels to decline especially if the water is withdrawn from the ground at a faster rate than it is replenished, resulting in seawater intrusion, land subsidence, streamflow depletion, and wells running dry. As groundwater is withdrawn, it lowers the water level near any proximity well and can result in a "cone of depression" around the well. Therefore, with a decrease in groundwater withdrawal, the less influence there is on water level in the aquifer, the less risk there is associated with the South Site injection wells or injection operations. GCS will monitor and measure groundwater levels at Project Minerva to ensure the injection well and injection operations are **stable** and safe, as well as provide protection to the USDW.

[Regional Groundwater Flow](#)

Groundwater moves through aquifer systems from areas of high hydraulic head to areas of lower hydraulic head (Woessner & Poeter, 2020). In some areas, contributors of withdrawal, such as industry and the public water system usage, can alter flow directions of groundwater in aquifers (Lovelace, Fontenot, & Frederick, 2004).

The Chicot aquifer system is the primary source of fresh groundwater in southwestern Louisiana. Project Minerva and Lake Charles are located within the boundary of fresh groundwater of the Chicot aquifer system (Figure 2.1.1-15). Rice irrigation and aquaculture are the largest contributors of withdrawal for the Chicot aquifer system; therefore, seasonal pumping of these water uses have altered flow directions and induced lateral or upward movement of saltwater (Lovelace, Fontenot, & Frederick, 2004). Figure 2.1.1-16 shows the potentiometric surface and the direction of groundwater flow of the Chicot aquifer system in southwestern Louisiana.

As pumping continues, wells in southwestern Louisiana could draw an increase proportion of water from lower, more saline parts of the aquifer. This occurrence is known as saltwater coning, or more formerly, "upconing." To reduce the potential for upconing saltwater in wells, decreasing the rate or duration of pumping and screening high-capacity wells as far above the base of freshwater could substantially recover the declining seasonal water levels and stop saltwater encroachment in agricultural activities (Lovelace, Fontenot, & Frederick, 2004). Figure 2.1.1-17 shows saltwater encroachment of the Chicot aquifer system on two local cross-sections extending across Calcasieu and Cameron Parishes in southwestern

Louisiana. Project Minerva is located in the divot, south- to southwest in the boundary of fresh groundwater of the Chicot aquifer system, and less than the interpreted 20 ft potentiometric contour where water-level declines occur due to seasonal ground-water withdrawals (Lovelace, Fontenot, & Frederick, 2004; White & Griffith, 2020). This indicates that Project Minerva is less impacted by the increase in groundwater withdrawals and saltwater encroachment.

2.1.1.4 Regional Groundwater Flow in the Injection Zone

Project Minerva is located in northwestern Cameron Parish, Louisiana in the Coastal Lowlands Aquifer System of the Gulf Coast Aquifer System in the Texas and Louisiana region (Lindaman, 2023; Baker Jr, 1978). This physiographic area is composed of Oligocene deposits and younger sediments of heterogenous unconsolidated to semi-consolidated sediments deposited in a range of shifting nonmarine, transitional, and marine environments (Lindaman, 2023).

The four major hydrogeologic units that comprise the Gulf Coast Aquifer System in the Texas and Louisiana regions, in ascending order, include:

- Jasper aquifer,
- Burkeville confining system,
- Evangeline aquifer, and
- Chicot aquifer.

A hydrogeologic stratigraphic column for southwestern Louisiana is provided as Figure 2.1.1-11. The two major aquifers of the Gulf Coast Aquifer System and Coastal lowlands aquifer system are the Chicot and Evangeline aquifers (Teeple, Becher, Walton-Day, Humberson, & Gallegos, 2022). The geologic units that make up these two hydrogeologic units, in ascending order, include:

- Fleming Formation / Lagarto Clay¹ (Miocene)
- Goliad Sand (Pliocene),
- Willis Sand (Pleistocene),
- Lissie Formation (subdivided into the Montgomery and Bentley formations) (Pleistocene),
- Beaumont Formation (Pleistocene), and
- Holocene alluvial sediments.

The Injection Zone lies within the deeper saline sands of the Frio Formation (middle Oligocene) that contains the Catahoula aquifer, below the Jasper aquifer (Miocene). The top

¹ The Fleming Formation and Lagarto Clay are considered equivalent throughout the region.

of the Catahoula aquifer is Anahuac Formation (late Oligocene), a regionally extensive transgressive marine shale unit. The Frio Formation is the downdip equivalent of the continental Catahoula Formation (up-dip equivalent). The Frio Formations is comprised of a mixture of marginal marine and deltaic sandstones and shales, with localized deep marine shales and turbidite sandstones (Teeple, Becher, Walton-Day, Humberson, & Gallegos, 2022; Griffith, 2003). The Catahoula aquifer is known to contain only saltwater due to its greater depths compared to other shallower hydrogeologic units. Aquifers underlying the Catahoula aquifer are known to contain only saltwater in southern Louisiana. The saline waters in the Injection Zone flow downdip toward the modern coastline (Griffith, 2003).

Overlying the Catahoula aquifer where the Injection Zone is located is the Jasper aquifer immediately overlain by the Fleming Formation / Lagarto Clay. This geologic unit is included as a hydrogeologic unit that contains part of the Evangeline aquifer (Pliocene and late Miocene) due to its relatively large sand content. Lower Fleming Formation is the deepest geologic unit of the hydrogeologic units and consists of progradational fluvial-delta mudstones and sandstones (Teeple, Becher, Walton-Day, Humberson, & Gallegos, 2022).

The Goliad Sand and the Fleming Formation / Lagarto Clay are the two geologic units that contain the Evangeline aquifer. The Goliad Sand is composed of predominately fluvial-deltaic sands, marginal marine sands, and occasional conglomerates, and reaches approximately 730 ft near the modern coastline (Teeple, Becher, Walton-Day, Humberson, & Gallegos, 2022).

The Willis Sand, Lissie Formation, and Beaumont Formation are the Pleistocene geologic units that contain the Chicot aquifer. The Willis Sand and Beaumont Formation contain fluvial-deltaic sands, whereas the overlying Lissie Formation is primarily a fluvial system. The combined thickness of the Pleistocene formations is approximately 1,200 ft, which coincides with the base of the USDW (the deepest occurrence of groundwater having less than 10,000 mg/l total dissolved solids).

Holocene alluvial sediments, where present and saturated are also included in the Chicot aquifer. At Project Minerva, Holocene alluvial sediments are composed of basal coarse-grained sand and gravel, which grade upward into finer-grained sandstones, siltstones, and clays with a total thickness of approximately 50 ft.

A detailed discussion on regional and local hydrogeology is contained in Sections 2.1.1.3 (Regional Hydrogeology) and 2.1.2.3 (Local Hydrogeology), respectively.

2.1.1.5 Frio Formation Fluid Background Velocity

Many of the studies for flow rates in deep saline aquifers come from the search for nuclear waste isolation sites. These studies show sluggish circulation to nearly static conditions in the deep subsurface (Bethke, Altaner, Harrison, & Upson, 1988). Flow rates in the deep saline aquifers (Clark, 1981), were found generally to be in the order of inches per year. A south-southeastern (down-dip) direction of regional flow established for the upper Frio Formation is consistent with the theory of deep basin flows and the physical mechanisms

(topographic relief near outcrops and deep basin compaction) identified as contributing to natural formation drift (Bethke, Altaner, Harrison, & Upson, 1988; Kreitler, et al., 1981).

Gulf Coast Sequestration has provided “Groundwater Flow in Deep Saline Aquifers (Clark, 1988)” in the bibliography reference materials, showing that background velocities in the deep subsurface, in general, and in the Frio in particular, are generally less than 1.0 ft/year.

Site specific data on regional fluid flow in the upper Frio Formation (Injection Zone) will be collected via the injection wells and in-zone monitoring wells once completed.

According to (Williamson, Grubb, & Weiss, 1990), the density of saline water in the deeper parts of an aquifer system probably has a substantial effect on regional groundwater flow. Variables in water density resulting from variations in salinity and temperature can be a significant driving force that moves saline water from salt formations in multiple directions at great distances, including updip (Williamson, Grubb, & Weiss, 1990). According to (Clark, 1981), the natural horizontal groundwater flow rates in deep saline aquifers are less than those for shallower freshwater aquifers. In general, groundwater flow in the deeper saline aquifers, such as the Middle Frio Formation that contains the Catahoula aquifer, is a function of lower permeability of the sand units rather than hydraulic gradients. Studies conducted by the federal government in search of suitable sites to isolate nuclear waste indicate that deeper units have less porosity and permeability and have higher salinity content. These studies suggest the groundwater is static and the slow circulation further demonstrates that geologic confinement is effective on both a local and regional scale (Clark, 1981).

The Gulf Coast is a well-known example of an overpressured basin, but the simulation indicates that widespread geopressures developed only in the past 2 million years. From the Eocene to the Pliocene, a band of overpressures developed beneath the active depocenters. Geopressures develop because the impermeable sediments cannot expel fluids quickly enough to compact fully during burial.

The Gulf Coast basin contains two principal hydrologic regimes: a meteoric system in which ground waters are driven basinward by the topographic relief of the coastal plain, and a deeper system in which saline brines migrate upward and landward in response to sediment compaction.

The effect of compaction on permeability still shows brine areas with significant flow rates and velocities

The Middle Frio Formation has an average downdip velocity flow rate is approximately 9 inches per year for the Frio Formation at a depth of 6800 feet near Harris County, Texas.

2.1.2 Local Geology

The structural geology and stratigraphy beneath Project Minerva were developed from a series of structure maps, stratigraphic maps, and cross sections prepared from the publicly available well-control data / information locally. Figure 2.1.2-1 is a basemap showing an entire view of both Figure 2.1.2-2 (N-SW cross-section) and Figure 2.1.2-3 (W-E cross-

section). Figure 2.1.2-2 and Figure 2.1.2-3 are detailed cross-sections across Project Minerva. Data logs used in the cross-sectional figures are provided in Appendix V.

The analysis of regional and local geology near Project Minerva demonstrates that the subsurface is geologically ideal for injection. The middle Oligocene massive sandstones of the upper Frio Formation serve as effective injection reservoirs for the Injection Zone, in terms of their lateral extent, mineralogical composition, and petrophysical characteristics.

Initial studies show that the Injection Zone has effective permeability, porosity, thickness, and lateral continuity to accept and contain waste. Shales of the overlying late Oligocene Anahuac Formation possess the necessary criteria to serve as the Upper Confining Zone and provide effective barriers to upward movement. Effective Secondary Confining Zone is provided by a shale-rich Undifferentiated Miocene interval. Significant separation exists between the Upper Confining Zone and the base of the lowermost USDW (Figure 2.1.2-2 and Figure 2.1.2-3).

The following sections provide a detailed assessment of the local geology as it pertains to Project Minerva.

2.1.2.1 Local Stratigraphy

At Project Minerva, the stratigraphic units of interest, in descending order, include:

- Quaternary interval (i.e., glacial sediments and regional potable water aquifers) - Base of the Lowermost USDW
- Undifferentiated Miocene Strata - Secondary Confining Zone
- Late Oligocene, Anahuac Formation - Upper Confining Zone
- Middle Oligocene, upper Frio Formation - Injection Zone
- Middle Oligocene, middle Frio Formation - Lower Confining Zone

The stratigraphic units of interest have been correlated across Project Minerva by constructing north-south and west-east cross-section lines, centered on the proposed injection well locations and extending at least two miles beyond the extent of the proposed AoR (Figure 2.1.2-1). Figure 2.1.2-2 shows the north-southwest oriented cross-section line (B-B') that is approximately parallel to strike, and Figure 2.1.2-3 shows the west-east oriented cross-section line (A-A') that is approximately parallel to dip.

Hackberry Trend

In the project area, the only stratigraphic difference from the regional stratigraphy (Section 2.1.1.1) is the presence of the “Hackberry Trend” within the middle Frio Formation. The “Hackberry Trend” is a transgressive, deep-water shale and sandstone unit that occurs in the middle to lower Frio Formation and is local to east Texas and southwestern Louisiana (Figure 2.1.1-4 and Figure 2.1.1-5). Shales and sandstones of the Hackberry Trend pinch out to the north along the “Hartburg” flexure and formed a southward-thickening wedge

(Swanson, Karlsen, & J, 2013). The “Hartburg” flexure represents a zone deposited during the Oligocene as growth faulting which likely generated an area of deep marine environment (Figure 2.1.2-4).

In up-dip areas north of Project Minerva, submarine canyons up to 800 ft deep were incised through pre-Hackberry sediments (Figure 2.1.2-5). Here, the Hackberry Trend is characterized by thick shales punctuated by sand-rich channel-fill facies deposited in submarine canyons.

Further downdip across Project Minerva and southward basin floor turbidite fan systems and isolated slope channel-fill sandstones typically appear encased in thick shale sequences (Swanson, Karlsen, & J, 2013).

2.1.2.2 Local Structure

The local structure at Project Minerva is the result of subsidence along deep-seated northeast-southwest faults in combination with salt diapir movement at Black Bayou Dome to the east. The two proposed Class VI injection wells, MS CCS 1 and MS CCS 2, are strategically located so that drainage is dominantly up-dip to the west (Figure 2.1.2-3) and southwest (Figure 2.1.2-2).

The structure of the project area is presented in Section 2.2.3 (Structure Maps) and structural interpretation is discussed in Section 2.4.2 (Description of the Injection Zone and Confining Zone System). The following subsections discuss the influence of salt dome development and faulting on the local structure.

Local Salt Dome

Project Minerva is located westward from the Black Bayou Salt Dome (Black Bayou Dome) in Cameron Parish, Louisiana, approximately 2.5-miles east of the bottom-hole locations of MS CCS 1 and MS CCS 2 (Figure 2.1.1-10). Black Bayou Dome is a southwestern Louisiana salt dome where the salt is relatively near the surface. The Louisiana Gulf Coast is approximately 19-miles south of the dome and the Intracoastal Waterway (ICW) is 2-miles north. Black Bayou Dome underlies a marsh that is crisscrossed by a canal and bayou network. Black Bayou, which crosses over the center of the dome, is a large bayou extending from Sabine Lake, and is connected to the ICW by the Black Bayou Cutoff Canal.

Black Bayou Dome has a shallow piercement structure with steep, nearly vertical sides, circular horizontal cross-section, and generally flat top. The approximate depth to caprock is 881 ft to a maximum of 1,369 ft, and the approximate depth to the shallowest salt is 1,035 ft BSL and the deepest salt is 8,553 ft BSL on the northeast periphery of the dome. The caprock is composed of 76.3 ft of calcite, 66 ft of gypsum, and 800 ft of anhydrite (DOE, 1978).

The base of freshwater in the area of Black Bayou Dome is approximately 500 ft below MSL. Slightly saline groundwater occurs in the approximate depth interval of 500 ft to 900 ft below MSL (DOE, 1978).

The Black Bayou Dome is a productive salt dome producing petroleum from the cap rock of the reservoir. Drilling for sizable deposits of Sulphur have been produced as a result of drilling for oil (Beckman & Williamson, 1990).

[Local Faulting](#)

In the area of Project Minerva, the direction of majority faulting is parallel to the edge of the Louisiana Gulf Coast. Local faulting connected to the growth and presence of numerous salt features originating from Black Bayou Dome to the southeast of Project Minerva adds complexity to structural architecture. Faults located further from Black Bayou Dome tend strike between 70° and 90°, although, radial faults originating from Black Bayou Dome have a wide variation in strike due to the complex structural regime associated with diapiric salt structures regionally. Section 2.3.3 (Faulting within the AoR) details the local faulting and structures at Project Minerva.

2.1.2.3 Local Hydrogeology

As previously discussed in Section 2.1.1.3 (Regional Hydrogeology), the four major hydrogeologic units that comprise the Gulf Coast Aquifer System in the Texas and Louisiana region include, in ascending order, the Jasper aquifer, the Burkeville confining system, the Evangeline aquifer, and the Chicot aquifer.

In the area of Project Minerva, the top of the Jasper aquifer strikes (east to west) at approximately 4,080 ft MSL and dips (north to south) at approximately 5,080 ft MSL toward the Gulf Coast of Louisiana. The approximate average thickness of the Jasper aquifer ranges from 1,601 ft to 2,400 ft thick (Intera, Frontera-Exploration, Hamlin, & Baker, 2012).

Locally, the Burkeville confining system, recognized by the stratigraphic charts of Louisiana as the “Castor Creek confining unit,” separates the underlying Jasper aquifer and the overlying Evangeline aquifer (Louisiana Geological Survey, 2000). In the area of Project Minerva, the confining unit is located in the middle of the Lagarto Formation of early Miocene time with the top of confining unit at a strike (east to west) of approximately 4,020 ft MSL and a dip (north to south) of approximately 5,010 ft MSL toward the Gulf Coast of Louisiana. The approximate average thickness of the confining unit ranges from 201 ft to 400 ft thick (Intera, Frontera-Exploration, Hamlin, & Baker, 2012).

In the area of Project Minerva, the top of the Evangeline aquifer strikes (east to west) at approximately 1,040 ft MSL and dips (north to south) at approximately 1,070 ft MSL toward the Gulf Coast of Louisiana. The approximate average thickness of the Evangeline aquifer ranges from 2,401 ft to 3,200 ft thick (Intera, Frontera-Exploration, Hamlin, & Baker, 2012).

In the Project Minerva area, the Chicot aquifer’s approximate average thickness ranges up to 1,070 ft thick (Intera, Frontera-Exploration, Hamlin, & Baker, 2012). Project Minerva is located in Cameron Parish, Louisiana within the boundary of fresh groundwater of the Chicot aquifer system. The Chicot aquifer system is used primarily in Cameron Parish, Louisiana, however, the Chicot and Evangeline aquifers are thought to be hydrologically connected in southwestern Louisiana (Baker Jr, 1978). The base of the lowermost USDW is located approximately at the base of the Chicot aquifer’s 700-Foot Sand or the uppermost portion of

the Evangeline aquifer. The following sections provide details on the local hydrostratigraphic units for the defined aquifer systems from deepest to shallowest intervals.

Local Hydrostratigraphy

The two main aquifers of local interest, in ascending order, include:

- The Chicot aquifer (Pleistocene), and
- the Evangeline aquifer (Pliocene).

The geologic units that make up these two hydrogeologic units, in ascending order, include:

- Fleming Formation / Lagarto Clay (Miocene),
- Goliad Sand (Pliocene),
- Willis Sand (Pleistocene),
- Lissie Formation (subdivided into the Montgomery and Bentley formations) (Pleistocene),
- Beaumont Formation (Pleistocene), and
- Holocene Alluvial sediments.

Most of the information provided below is derived from Calcasieu Parish, directly north of Cameron Parish where Project Minerva is located. Project Minerva is located in a specific area in Cameron Parish where freshwater exists.

Evangeline Aquifer

In the area of Project Minerva, the Evangeline aquifer predominantly contains saline groundwater (greater than 10,000 mg/l TDS). Upper and lower boundaries to the Evangeline include the Goliad Formation and the upper part of the Fleming Formation, respectively. The Evangeline and Chicot aquifers are usually separated by thin layers of confining clay that comprise the top of the Goliad Formation. However, when this clay is absent, the geologic boundary between the two aquifers is indistinguishable with the Goliad grading into the Willis Formation. In general, the Evangeline aquifer tends to have greater sand to clay ratio with individual sand beds up to several tens of feet thick.

Figure 2.1.2-6 is a Piper diagram demonstrating a graphical representation of the chemistry of water samples in the Lake Charles area to best represent the water chemistry at Project Minerva. This water chemistry data helps in understanding the sources of the dissolved constituent salts in water samples taken from each of the local aquifers. According to Figure 2.1.2-6, the Evangeline aquifer of Lake Charles area contains a sodium-potassium bicarbonate type of water chemistry with an ionic composition of sodium and potassium cations and bicarbonate type anions. The hydrochemical facies of the Evangeline aquifer is predominately sodium bicarbonate waters.

Because the Evangeline aquifer is mostly saline within the Project Minerva area, it is not considered USDW and is not used for groundwater in Cameron Parish.

Chicot Aquifer

In the area of Project Minerva, the major aquifer system is the Chicot aquifer. The Chicot aquifer is divided into distinct, shallow alluvial sands: (1) the “200-foot” sand, (2) the “500-foot” sand, and (3) the “700-foot” sand, named after their depths of occurrence, in the Lake Charles area (Figure 2.1.2-7). The eastern most side of Calcasieu Parish, and northeast into Cameron Parish in Louisiana, the Chicot aquifer is divided into the “upper sand” (i.e., “200-foot” sand), the “lower sand” (i.e., “700-foot” sand), and the “500-foot sand” being largely isolated between the two sands. The sands are separated by confining layers except where the “500-foot” sand merges with the “700-foot” sand further north of Calcasieu Parish, Louisiana (DEQ of Louisiana, 2017).

Salt water occurs within the Chicot aquifer near the coast and in isolated bodies north of the modern coastline (DEQ of Louisiana, 2017). In the area of Project Minerva, the “200-foot sand,” “500-foot sand,” and “700-foot sand” contain freshwater although saltwater encroachment does occur southward toward the Louisiana Gulf Coast (Milner & Fish, 2009).

According to Figure 2.1.2-6, the Chicot aquifer of Lake Charles area contains a mixed type of water chemistry with an ionic composition of sodium and potassium cations and bicarbonate-chloride type anions. The hydrochemical facies of the Chicot aquifer is predominately sodium bicarbonate-chloride waters.

200-Foot Sand

The “200-foot sand” is stratigraphically equivalent to, and continuous with, the “upper sand” of the Chicot aquifer. It is a shallow aquifer sand, with the sand grading from fine to medium sand in the uppermost portion to coarse sand or gravel at the base. The “200-foot sand” is used mainly to supply water for irrigation and domestic purposes. In the western part of Calcasieu Parish, the Chicot aquifer is thin, providing water strictly for domestic purposes, and in the central part of the parish, it provides water for industrial purposes (Harder, 1960).

The “200-foot sand” has a chloride content generally less than 100 parts per million (ppm), whereas in the eastern part of Calcasieu Parish, it increases up to approximately 300 ppm and the dissolved solids increase up to approximately 700 ppm. The “200-foot sand” contains the lowest TDS concentration waters in the Chicot aquifer. According to Figure 2.1.2-6, the “200-foot sand” of Lake Charles area contains a mixed type of water chemistry with an ionic composition of sodium and potassium cations and bicarbonate type anions. The hydrochemical facies of the “200-foot-sand” is predominately sodium bicarbonate waters.

The top of the “200-foot sand” dips southward (from the aquifer’s recharge outcrop in Beauregard Parish, Louisiana) at a rate of 4 ft/mile to 10 ft/mile; however, variance in thickness locally may change the dip to vary considerably, as in the southwestern part of Calcasieu Parish where it increases to 50 ft/mile (Harder, 1960).

500-Foot Sand

The "500-foot sand" is the most well-developed aquifer portion and the principal aquifer of Calcasieu Parish, Louisiana. The "500-foot sand" is composed of gray to brownish sand ranging from fine sand in the uppermost portion to coarse sand and gravel near the base. The "500-foot sand" is used in about all industries and supplies water to many irrigation wells. The "500-foot sand" is not utilized largely as a source of supply in the southeastern part of Calcasieu Parish, where the sand is relatively thin and consists of mainly fine sand (Harder, 1960).

The average dissolved solids content is 302 ppm, and the chloride content is generally low in the northern and central parts of Calcasieu Parish, where the average well supplies 30 ppm. According to Figure 2.1.2-6, the "500-foot sand" of Lake Charles area contains a mixed type of water chemistry with an ionic composition of sodium and potassium cations and bicarbonate type anions. The hydrochemical facies of the "500-foot-sand" is predominately calcium-sodium bicarbonate waters.

The dissolved solids increase up to more than 600 ppm, where the "500-foot sand" directly overlays salt dome structures (i.e. Vinton Dome). At Vinton Salt Dome, the "500-foot sand" is between depths of 410 ft and 600 ft and contains a clay unit between 470 ft and 500 ft. The "500-foot sand" dips southward (from the aquifer's outcrop area in central Beauregard and Allen Parishes, Louisiana) at an average rate of 18 ft/mile (Harder, 1960).

700-Foot Sand

The "700-foot sand" is thick and continuous throughout Calcasieu Parish. Clay units divide the Chicot aquifer into two or three separate layers; however, because the clay layers are not continuous, the sands are hydrologically connected. The "700-foot sand" is tan to grayish sands grading from fine in the uppermost portion to coarse at the base. The "700-foot sand" supplies water to industries and irrigators and is the source for public water supply in the area of Lake Charles, Louisiana.

The chloride content of water in the "700-foot sand" is greater than that in the "200-foot sand" and "500-foot sand." According to Figure 2.1.2-6, the "700-foot sand" of Lake Charles area contains a mixed type of water chemistry with an ionic composition of strictly sodium and potassium cations and bicarbonate-chloride type anions. The hydrochemical facies of the "700-foot-sand" is predominately sodium chloride-bicarbonate waters.

The regional dip of the sand is generally southward at about 10 ft/mile (Harder, 1960).

2.2 MAPS AND CROSS-SECTIONS OF THE AOR

The following sections discuss the data collection efforts employed by GCS to interpret the subsurface and the workflows followed to integrate the data into a geostatistical model for dynamic simulation and mapping.

2.2.1 Subsurface Interpretation and Integration

Continual peer review and critical assessment of model inputs, outputs and assumptions by the GCS technical team and GCS senior advisors ensures reasonable results and ongoing model refinement.

The following steps provide an overview of the full-cycle GCS data, model, and simulation workflow:

- **Extensive data collection** effort primarily from Stream proprietary sources, TGS Well Dataset services and the LDENR Strategic Natural Resources Information System (SONRIS). All well header information, geophysical well logs (digitized and TIFFs), core data and formation tops were built into a Petra database. Additional information drawn from public sources, including published literature and publicly available shapefiles (i.e., geological trend info, regional fault zones, and map culture). An extensive effort to digitize static well logs was conducted.
- **Regional stratigraphic and petrophysical analysis** across east Texas and southwestern Louisiana were evaluated. More than 1,700 regional geophysical wells were analyzed to generate an in-depth understanding of the structural and thickness trends of the late Oligocene and Miocene intervals overburden. A detailed analysis of structural closures and migration pathways. Injection Zone, Confining Zone and Secondary Confining Zone were defined, and the location of Project Minerva was narrowed down to Cameron, Louisiana.
- **Detailed mapping petrophysical analysis** completed on more than 470 wells with available log and core data, centered around Project Minerva. The upper Frio Formation within the Injection Zone is subdivided into 11 intervals based on sequence stratigraphic interpretation of maximum flooding surfaces. A detailed property (i.e., shale content, facies, porosity, permeability) modeling was also performed for all layers.
- **Analysis of local geophysical oil and gas wells and historical production** to confirm depletion of the upper Frio Formation is not an issue for CO₂ injection and containment.
- **3D seismic data imported and interpreted** to provide the seismically derived framework of the geostatistical model. Structural formation tops and resulting surfaces generated in Petrel, a software platform by Schlumberger Information Solutions, from log data combined with seismic horizons to extend the regional geostatistical model beyond the available seismic data. Detailed structural interpretation completed throughout available 3D seismic coverage.
- **Petrophysical analysis and facies modeled combined with the structural model** generates the static geo-model. Probabilistic property distribution is used to reduce data uncertainty.
- **Model outputs are used to apply a rigorous set of subsurface constraints** on the

controlled acreage to identify the optimal location for CO₂ injection.

- **Geo-model upscaled and imported to REVEAL software** to create the “reservoir simulation model.” Full suite of engineering data and assumptions used to build and iterate a robust geo-mechanical model to simulate AoR and CO₂ plume.
- **Based on the results and key learnings from the simulation runs, the inputs were then optimized, and the model is rerun.** This process commenced initially on a regional scale, and then ultimately allowed the geological characterization to focus on the areas that are of higher interest to injection. These iterations, which now number more than 700, have been key to GCS’s understanding of the key parameters and mechanisms and have ultimately allowed GCS to accurately define how CO₂ injections will occur.

2.2.1.1 Available Data Sets

History of Subsurface Data Development

The state of Louisiana was the 9th largest producer of crude oil and 4th largest producer of natural gas in the U.S. in 2018 (U.S. Energy Information Administration (EIA), 2020). The Frio Formation, including the Anahuac Formation, is the largest producer of hydrocarbons from the Paleogene in the Gulf of Mexico. Project Minerva is located in a highly productive and extensively developed Frio Formation (including the Anahuac Formation) “play” (i.e., a geological reservoir group) where millions of barrels of oil (MMBO) have been produced along the Texas and Louisiana Gulf Coast (Swanson, Karlsen, & J, 2013).

As such, the project benefits from a substantial dataset including geophysical well logs, core samples, production data, regional studies, and seismic surveys.

History of exploration at Project Minerva includes the following:

- In the 1920’s, early wells targeted the crest and flanks of the Vinton Dome and Black Bayou Domes in which included relatively few shallow Miocene wells drilled.
- From the 1930’s to the 1950’s, there was a big increase in drilling (hundreds of wells, targeted salt dome flanks with wildcat wells extending further afield; large, less structurally complex fault block traps were targeted in the Miocene reservoir).
- From the 1960’s to the 1980’s, there was an increase of two dimensional (2D) seismic use which encouraged the expansion of drilling into deeper reservoirs (Miocene and Frio Formation) and more structurally complex areas of the salt dome flanks (e.g. southern flank of Vinton Dome). The peak of Miocene reservoir drilling took place during the 1970’s just before decreasing in the 1980’s.
- In the early 1990’s, there was a dramatic drop in drilling before the advent of 3D seismic in the late 1990’s. This allowed imaging of deeper Hackberry sandstone reservoirs and better understanding in the development of structural traps. A new phase of drilling deeper, over pressurized wells occurred.

The drilling of deeper, over pressurized wells is important to Project Minerva as it provides a



45031 & 45032

modern, analogous data set for the project area (i.e., the upper Frio and Anahuac Formations).

- In the Early 2000's, there was a great increase in Miocene and Oligocene drilling across the flanks of Vinton Dome and Black Bayou Dome. Deep well targeted the Hackberry sandstone channels away from salt dome structures, notably in the structural, notably in the structural low targeted by Project Minerva. The deeper wells targeting the Hackberry were enabled by the extensive 3D seismic (90's-early 2000's). Modern well logs suites were acquired in these wells providing a critical data source for the Project Minerva analysis.
- From the mid-2000's to the present day, the more recent drilling has continued at a much-reduced rate, mainly targeting previously overlooked accumulations in fault blocks around Vinton Dome, Black Bayou Dome and Phoenix Salt Dome with vertical and directional wells.

Historic subsurface development has provided a wealth of information and knowledge about the Injection Zone and Confining Zone. Adjacent production has predominately been from the shallower Miocene or deeper Hackberry (mid to lower Frio Formation). Within the Project Minerva AoR, there are no productive intervals within the proposed Injection Zone (upper Frio Formation).

Well Data

A substantial amount of time was dedicated to building a comprehensive database. All geophysical well logs are derived from proprietary Stream family records, TGS Well Dataset services, the LDENR SONRIS and the Texas Railroad Commission (TRRC) databases.

A large part of the data-mining process involved digitizing proprietary hardcopy of well log data acquired from the Stream family, as well as regional, publicly available TIFFs of well log data. ArcGIS was also extensively used for spatial analysis of wells vs data such as infrastructure, and terrain. Petrel was used to combine well and seismic data analysis for use in geostatistical and reservoir simulation modeling.

Seismic Data

GCS has access to over 422 mi² of proprietary and licensed 3D seismic. The available seismic data extends from southeast Texas to Lake Calcasieu River, across Project Minerva. The dataset was collected in the late 1990's and has since been used in the entire seismic database as set forth below. In the mid-2010's, the inventory and digitization exercise of the historical 3D seismic survey began, which has since been upgraded from analog to digital to enable the full realizations of data volatility. The different seismic surveys have been reprocessed and merged into a new survey called *Alligator Cove 3D Survey*, which is marketed by Seismic Exchange Inc. All surveys merged were used to assess different degrees in response to the complexity of the geology overall. The surveys include:

- Big Island 3D Survey,
- Black Bayou 3D Survey,



45031 & 45032

- Vinton Dome 3D Survey, and
- Alligator Cove “merged” 3D Survey.

The seismic surveys were permitted, along with *Black Bayou 3D Survey*, in August of 1998 by Seitel Inc. The seismic survey was conducted by Seitel Inc., and the data was processed by Vector Seismic Data Processing. Data delivery under the permit occurred in March, April and July of 1999.

Big Island 3-Dimensional Survey

The *Big Island 3D Survey* was conducted in Calcasieu Parish, Louisiana, primarily in Township 10 and 11 South and covers a combined total live seismic area of approximately 55.26 mi². The seismic dataset contains both gathered field data and processed data. GCS utilizes the Pre-Stack Time Migration (PSTM) processed data set. The PSTM data file for the survey has a data record length of 5.996 seconds with 4 millisecond sample intervals, and a bin size of 110 ft by 110 ft. Although located in adjacent parish, Calcasieu Parish, the seismic lines from the *Big Island 3D Survey* were not used in the permit application for Project Minerva. The header for the PSTM is set forth in Figure 2.2.1-1.

Black Bayou Dome 3-Dimensional Survey

The *Black Bayou 3D Survey* was conducted in Calcasieu Parish, Township 11 South and Cameron, Parish, Louisiana Township 12 and 13 South covering a combined total live seismic area of 82.99 mi². The seismic survey contains one field data set and two processed data sets. GCS utilizes the PSTM processed data set. The PSTM data set is a Stacked Migration with Noise Reduction (MIGNR) and has a data record length of 8.5000 seconds with four millisecond sample intervals, and a bin size of 110 ft by 110 ft. The *Black Bayou 3D Survey* is the only seismic survey used in evaluating Project Minerva as the seismic lines cover the entirety of the AoR. The header for the MIGNR processed data set is set forth in Figure 2.2.1-2.

Vinton Dome 3D Survey

The *Vinton Dome 3D Survey* is a radial seismic survey acquired with receivers placed along radial-lines and sources on concentric arcs. A Vertical Seismic Profile (VSP) was available in ‘Well G-23’ located on the northwestern flank of the Vinton Dome. Concentric circles approximate source locations, with shot spacing being 165 ft along the arc. The seismic source consisted of 5.5 lb. pentolite charges set off at 60 ft depth. The receiver line interval on the surface is variable, ranging from approximately 900 ft to 1,200 ft, with alternating long and short line segments spaced at 5 increments. The receiver station spacing was 165 ft along a receiver line segment.

The *Black Bayou 3D Survey* was conducted in Calcasieu (Township 11 South) and Cameron (Township 12 and 13 South) Parishes, Louisiana, covering a combined total live seismic area of 82.99 square miles. The seismic survey contains one field data set and two processed data sets. GCS utilizes the PSTM processed data set. The PSTM data set is a Stacked Migration with Noise Reduction (MIGNR) and has a data record length of 8.5000 seconds



45031 & 45032

with four millisecond sample intervals, and a bin size of 110 ft by 110 ft.

The *Alligator Cove 3D Survey* was conducted in Calcasieu Parish, Louisiana covering approximately 50 mi² of Stream properties with a total live seismic area of 260.63 mi². The *Alligator Cove 3D Survey* is a merger of the following projects:

- *Big Island 3D Survey*,
- *Vinton Dome 3D Survey*,
- *Garter 3D Survey*,
- *Sulphur 3D Survey*,
- *Gillis 3D Survey*,
- *Houston River 3D Survey*, and
- *Pine Ridge 3D Survey* (which includes Calcasieu River, South Sulphur, and South Lake Charles 3D seismic surveys).

The project contains two gathered data sets and seven stacked data sets, and deliverables including three data type products:

- Raw Pre-stack Time Migration (RPSTM),
- Enhanced Pre-stack Time Migrations (EPSTM),
- Enhanced 1,
- Enhanced 2, and
- Amplitude Verses Offset (AVO) Pre-stack Time Migration (APSTM).

The APSTM included three angle sub-stacks (near, mid and far), and a Velocity model in SEG-Y format. The *Alligator Cove 3D Survey* has a record length of 7.988 seconds with two milliseconds sample intervals. The bins for all data sets are 110 ft by 110 ft. Data delivery for reprocessing occurred in July of 2019.

Limitations and Assumptions of the 3-Dimensional Datasets

As with any other seismic reflection survey, the surveys utilized in Project Minerva have limitations related to their different vintages, acquisition parameters, processing and reprocessing sequences applied, and ultimately their ability to distinguish between two features from one another. This is known as 'seismic resolution.'

There are two distinct types of seismic resolution: (1) vertical and (2) horizontal seismic resolution. Vertical seismic resolution represents the distance between two interfaces as separate reflectors, determining the thickness of the beds, such as two close seismic responses corresponding to different depths. Horizontal seismic resolution recognizes two lateral displaced features on the single interface, determining the termination of beds by

using seismic reflection. GCS assumes Rayleigh's Limit of Resolution, a measurement of the minimum resolvable separation between two-point sources, that two events should be separated by half seismic cycle model.

To solve for thickness:

$$\Delta h \geq \frac{\lambda}{4}$$

To solve for thickness, where (h) corresponds to the thickness and (λ) to the wavelength. The vertical resolution can be calculated from the length of the propagation wave and the layer thickness below $\frac{\lambda}{4}$ for resolving limits of beds. It is possible to detect layers down to $\frac{1}{32\lambda}$, and hence why in some cases in the presence of faults, the reflections are not completely disassociated but seem more continuous but with unexplained changes in their dipping angles.

Vertical seismic resolution varies, normally decreasing with depth as the earth works as a filter rapidly attenuating high frequency. As high frequencies play a key role in defining the vertical seismic resolution, the low frequencies play a role in penetration. Therefore, the importance of seismic surveys is of having a broad frequency spectrum.

Utilizing Rayleigh's Limit of Resolution, an average vertical seismic resolution at reservoir depth level has been calculated for the seismic surveys as follows:

- Big Island 3D Survey, $\frac{\lambda}{4} \cong 82$ ft,
- Black Bayou 3D Survey, $\frac{\lambda}{4} \cong 85$ ft,
- Vinton Dome 3D Survey, $\frac{\lambda}{4} \cong 90$ ft (decreases with proximity to Vinton Dome), and
- Alligator Cove “merged” 3D Survey $\frac{\lambda}{4} \cong 90$ ft.

These $\frac{\lambda}{4}$ are average values calculated using frequency spectrums generated with two different types of wavelets (statistical and deterministic) at several well locations used for the seismic-to-well tie via zero-offset synthetic seismogram generation. The seismic resolution will be less in areas where there are steep events, such as around the Vinton Dome where the fault illumination will be degraded, and with depth, as the high frequencies will be rapidly attenuated.

The difference in the vertical seismic resolution between the seismic surveys is almost undetectable, therefore, they can be combined, including the Alligator Cove 3D Survey, which has handled this difference well.

Although the vertical seismic resolution was calculated for all surveys, the one seismic survey used at Project Minerva is *Black Bayou 3D Survey*. This is due to the seismic lines of *Black Bayou 3D Survey* appropriately covering the furthest extent of the AoR at Project Minerva. No other seismic lines were necessary to use as the only other survey overlapping *Black Bayou 3D Survey* is *Big Island 3D Survey* in which seismic lines overlap just at the top of the county line between Calcasieu and Cameron parishes (Figure 2.2.1-3).

2.2.1.2 Seismic Interpretation Workflow

Petrel was used to analyze data throughout the subsurface workflow, enabling a shared vision of the reservoir and aiding in decisions with a clear understanding of both opportunities and risks. The interpretation of the subsurface workflow is summarized below.

Reconnaissance Viewing of Data

This process consists of a rapid screening of the entire seismic dataset aimed at:

1. Making a visual QC of the different seismic surveys available in the project and make a decision on which ones to use and for what specific purpose. The three seismic surveys used for the interpretation have very similar vertical resolution at reservoir level. The main difference can be seen in the fault illumination which is slightly better on the Big Island and Big Bayou 3D surveys due mainly to their higher high frequency content. Within the Vinton Dome, the Vinton Dome radial 3D survey offers a better fault definition, which is the main reason why GCS will perform a detail mapping exercise using this survey and will integrate the results once finalized. After running the reconnaissance viewing GCS made the decision to use the Big Bayou and Big Island surveys for horizon and fault mapping all over their extension, and the Alligator Cove survey filled in the easter side where neither of the two others are present.
2. Familiarize the interpreter with the structural styles present in the area such as faulting in terms of strike, dip, trough and heaves, and other such as the different domes. The type of faulting present in the area is extensive, with no inversion seen so far, meaning that no extensional fault has been reactivated in the opposite direction to its original movement. Fault troughs vary significantly, going from being within the data's detectability, to faults with considerable trough (Figure 2.2.1-4).
3. Familiarize the interpreter with the interval of interest in terms of horizon continuity. The upper Frio Formation (Injection Zone) and the middle Frio Formation (Lower Confining Zone) horizons are fairly continuous reflections within the three seismic surveys, only affected by normal faulting, therefore no complications should be expected in terms of mapping. The Anahuac Formation (Upper Confining Zone) is an unconformity mainly defined by a trough but on occasions it is a zero crossing. The Anahuac Formation is not a straightforward pick, as is common with many unconformities with spatially varied lithologies beneath the unconformity.



45031 & 45032

Synthetic Seismogram Generation for Seismic-To-Well Tie

Wavelet estimation as well as the seismic-to-well tie are at the core of every seismic interpretation workflow, with the wavelets representing the ultimate link between the seismic data and the stratigraphy as well as the rock properties of the subsurface. Seismic wavelet estimation is normally done to deconvolve the seismic trace, tie the well log to the seismic data, and design inversion operators. GCS used them to evaluate the quality of the seismic surveys and for calibration purposes.

The seismic wavelets must be known to interpret geology correctly; however, it is typically unknown and assumed to be both broad band and zero phase, meaning that they are symmetrical with a maximum at time zero.

GCS used two different methods for wavelet estimation. The Statistical method, which estimates the wavelet from the seismic data only, and the Deterministic method, which requires a direct measurement of the source wavefield or the use of well log data.

With the wavelets estimated for a shortlist of wells spread over the entire area covered by the seismic surveys, zero-offset synthetic seismograms were generated and used as the fundamental tool to link the reflection seismic data to the well data and to determine which geological picks are associated with which reflections on the different seismic surveys used.

In order to generate synthetic seismograms sonic (DT) and density (Rho) logs are needed, however, in this area, the majority of the wells targeted deeper intervals, and therefore the density logs were only recorded in the deeper section, resulting in little to no use for the synthetic seismogram generation. As a workaround, pseudo density logs were generated using the Gardner equation for some wells, and for others, a simple constant density value was used to test the tie. Due to the proximity of the wells, in principle, there was no need to acquire numerous sonic logs either, so the available number is relatively low, but enough to have a good spread over the area. All the DT logs have been QC'd and calibrated prior to being used to generate the synthetic seismograms.

The calibration process suggested that the best seismic-to-well tie was achieved with the Deterministic wavelets, which ended up with average correlation coefficients of 75% at reservoir level, within a 600 ms window.

The well-to-seismic tie helped define the onset type of the three main geological markers of interest. Following the SEG (Society of Exploration Geophysicist) convention, where a peak is defined as an increase in acoustic impedance (+) and a trough as a decrease in acoustic impedance (-), below is the list of markers with their respective onset types:

- Upper Confining Zone: Trough (decrease in acoustic impedance), and in some areas a zero crossing (\pm),
- Injection Zone: Trough (decrease in acoustic impedance), and
- Lower Confining Zone: Trough (decrease in acoustic impedance).

Horizon Interpretation

The starting point for all the horizon interpretation was the wells to which the seismic surveys have been tied to since these represent the ground truth. As picking complexities appeared, interpretation from other wells was extended to a point where the areas with uncertainties were reduced to a minimum.

The three horizons of interest (listed above) have been picked every 16 inlines and crosslines over the entire surveys, with refinement done in more structurally complex areas or where data quality deteriorates using a tighter grid of four inlines by four crosslines.

An additional nine horizons have been picked from which seven are within the Miocene section, and two are intra-reservoir picked for guidance purposes. The Miocene horizons picked are listed below:

- Miocene Middle (peak),
- Miocene Lower V2 (trough),
- Intra Miocene 1 (trough),
- MFS10 Robulus L Oakville (trough),
- Intra Miocene 2 (trough),
- MFS11 Marginulina A (trough),
- MFS12 Siphonia Davidi (trough).

Both intra-reservoir horizons are troughs and have been named in order of occurrence, intra-reservoir one and two, respectively.

Furthermore, and due to the high volume of normal faults, the horizon and fault interpretation has been done iteratively as a cycle. This technique allowed the horizon correlation to be easier in both sides of the faults, foot and hanging-wall. In the case of some smaller faults, the interpretation grid used was reduced to every four in lines and/or crosslines.

Fault Interpretation (Including Fault Polygon Generation)

The initial picking grid used was 16 inlines and/or crosslines, which for smaller faults, was lowered to a very tight four inlines and/or crosslines. Only on very rare occasions were faults picked on both inlines and crosslines. The standard workflow used was to select the seismic lines (inlines or crosslines) closest to being perpendicular to the fault's strike (line representing the intersection of the fault with a horizontal plane). Also, in very rare occasions, random lines were used to pick faults with strikes close to N45°E or N45°W.

A first pass to pick the faults around the Vinton Dome was done combining the *Big Island 3D* and the *Alligator Cove Merged 3D Surveys*, followed by a second pass or finetuning process done with the *Vinton Dome 3D Radial Survey*. This last one allowed a more detailed

interpretation of the complex structural style, which it is known to consist of a counter-regional faulting, three peripheral fault sets (already identified with the first pass mapping), and a small sub-seismic scale polygonal fault system in the entire dome. Similar polygonal faults in the Central North Sea and in Alberta Basin, have been interpreted to be formed by dewatering processes. The similarity of polygonal faulting in the Vinton dome suggests similar mechanisms and deformation by salt movement (Dewhurst, Cartwright, & Lonergan, 1999; Haskell, Nissen, & Hughes, 1999).

The faults related to the Black Bayou dome have been picked with the *Black Bayou 3D Survey*.

[Creation of Structural Time Maps](#)

The horizons of interest have all been grided in Petrel constraining their contours with their associated fault polygons and filling the gaps of no seismic data presence with well tops information.

[Velocity Model Generation & Time-To-Depth Conversion](#)

A layer-cake velocity model has been generated using interval velocities generated from the processing stacking velocities from the *Alligator Cove Merged Survey*, the TDR (Time-to-depth relationships) generated from the seismic-to-well ties, and the mapped horizons in Two Way Time (TWT).

The model was used directly in Petrel to depth convert the time structural maps, followed by correction at well locations to reduce the uncertainty due to the different resolution between the wells and the seismic data.

2.2.1.3 Petrophysical Workflow

The following outlines the steps taken in the initial petrophysical workflow focused on the upper Frio Formation (Injection Zone):

- Raw log data collated for the Project Minerva area
 - Digital logs and scanned raster images, where available. Data collected from log header data to understand the well and logging parameters
 - Where only a scanned or paper image existed, the log data was digitized to enable petrophysical calculations
 - Data loaded and organized into an interpretation software tool (Petra)
- Log data quality checked and normalized/conditioned
 - Based on the regional understanding baseline adjustments were used to calibrate the data. This is typically done using zones that are consistent, for example using a clean sand interval within the upper Frio Formation, or a shale baseline from the Anahuac Formation and/or Hackberry shale. Data points

and wells with results that were outliers were re-examined and discarded if not believed to be representative of the zone.

- Issues such as log splicing identified and/or corrected; logs with poor data (e.g. run through casing) eliminated from the data set
- Shale volume (Vshale) analysis carried out using SP logs. Gamma Ray logs were used when SP logs were not available. Unfortunately, as a lot of the wells in the area of interest logged only the section beneath the upper Frio with a full suite of logs as the primary target was sandstones within the Hackberry Trend
 - SP curve drift corrected for depth-related salinity variation, if appropriate
 - Clean sand baseline taken from thick, blocky sand interval within the upper Frio
 - 100% shale baseline generally taken from the underlying Hackberry shale interval. The shale within the Anahuac Formation was used in some instances where the Hackberry Trend was not logged
- Porosity and sonic logs corrected for compaction effects
- Vshale used to correct porosity log
- Effective porosity (PHIE) generated across upper Frio Formation interval
 - Used to calculate net-to-gross and create a facies model for use in the geostatistical model

2.2.1.4 Geostatistical Model Workflow

To accurately represent the subsurface over the wider context, GCS has developed a regional mapping workflow. The steps of the workflow are as follows:

- The upper Frio Formation has been divided into 11 regionally correlated, geological sequences, Frio 0, Frio 0.5, Frio 1 through 9 (Figure 2.2.1-5 and Figure 2.2.1-6). The shallower upper Frio sandstones represent thicker more proximal deposition in the NW of the mapping area, with these units thinning towards the SE across the main injection area. The deeper upper Frio sandstone layers, which are relatively thin in the NW of the mapping area, thicken over the injection area and are ultimately thicker but shale-rich in the depositional offshore section towards the SE. Table 2.2.1-1 summarizes the geologic sequences according to the name and depths of the geostatistical model and the associated simulation layer and correlates the layers to the respective regulatory zones.

- Outputs from the seismic interpretation workflow in Section 2.2.1.2 (Seismic Interpretation Workflow Overview) were integrated with well log data. Key outputs: depth-converted surfaces (middle Frio, upper Frio, and Anahuac Formations) and a fault model.
- A litho-facies scheme was created in wells that penetrate the upper Frio Formation and have log data. Two litho-facies types were interpreted in the upper Frio depositional system using a spontaneous potential log or calculated sonic porosity log: “High Quality Sandstone” units, generally displaying effective porosities greater than 10% and “Shaley-Interbedded” units that are generally more shale dominated with thin interbedded sands having less than 10% effective porosity.
- Effective porosity (PHIE) was calculated by using Vshale logs (calculated from spontaneous potential and/or gamma ray logs) to correct density, sonic and neutron porosity logs for shale content. The input to the modeling workflow is effective porosity.
- Using all the available data points, along with mapped trends such as facies probability maps, sequential and gaussian simulation is used to calculate facies and porosity maps.
- Horizontal and vertical permeabilities are calculated from the porosity-permeability relationships identified in the core samples (Figure 2.2.1-7).

The porosity and permeabilities calculated represent the averages in the geostatistical model:

- Anahuac Formation (all lithologies) – 4.8% porosity, 0.18 millidarcies (mD) horizontal permeability, 0.0184 mD vertical permeability (porosity values from log calculation and permeability from core derived porosity to permeability transform)
- Upper Frio Formation (High Quality Sandstone) – 18.3% porosity, 306 mD horizontal permeability, 190 mD vertical permeability.
- Upper Frio Formation (Shaley Interbedded) – 2.5% porosity, 0.18 mD horizontal permeability, 0.018 mD vertical permeability.

To balance model size and achieve a sufficient level of detail, the properties of the cells in the geostatistical model were vertically upscaled to a coarser grid over the central part of the reservoir simulation model (Figure 2.2.1-8). While outside of the central part of the reservoir simulation model the areal size of the grid cells has been increased laterally, resulting in a less detailed picture of the subsurface (Figure 2.2.1-8).

2.2.1.5 Reservoir Simulation Model Workflow

A comprehensive overview of the reservoir simulation model is set forth in a separate document: Area of Review and Corrective Action Plan (Attachment A). The following is a high-level summary of the full workflow and output.

The reservoir simulation model was used in two phases; the first was a regional, coarse-gridded study to find potential injection sites; and the second incorporating a refined grid around the chosen injection sites modeled the fine-scale behavior of the CO₂ and pressure plumes.

GCS began using a large-scale regional grid with coarse cells based on an interpretation of proprietary seismic and petrophysical data to find potential injection sites. The CO₂ plume exhibited an up-dip migration from buoyancy away from the injection site along higher permeability paths, so a combination of structure and permeability determined the direction and speed of dispersal. GCS sought to avoid areas such as the Vinton Dome, which might increase the risk to successful containment. The initial search tested eight separate injection sites. GCS discovered two Primary sites, now referred to as the North and South injection sites.

Over a series of simulations, GCS optimized the grid (extending it to ensure the best representation of the boundary conditions, centralizing it around the injection sites and added grids to represent the overlying Anahuac Formation. The simulation results were used to determine improvements to the geostatistical model in a combined active and continuous iteration workflow. The simulation results drove the development of the geostatistical model, and, in turn, the geostatistical model drove the reservoir simulation model.

GCS decided to use two injection wells at each of the two sites to provide the project with sufficient injectivity and redundancy.

The choice of injection site was predicated on a set of constraints. The constraints are:

- Sufficient horizontal permeability to ensure injection pressures stayed well below fracturing pressure at the required injection rates
- The injection depth deeper than approximately 9,000 ft true vertical depth subsea (TVDSS) to ensure a large vertical distance between the injection point and the confining Anahuac Formation, and to utilize the high pressure to ensure efficient use of the storage volume (Table 2.2.1-1)
- Sufficient distance between neighboring injection wells to avoid interference and hence reduced injectivity; sufficient distance from faults (greater than 500 ft per fault) to reduce the risk of reactivating the fault
- That local dip directs the CO₂ plume away from areas which may compromise containment, such as the Black Bayou Dome

The reservoir simulation model grid has 180 hexahedral grid cells in the X-direction, 158 grid cells in the Y-direction and 63 grid cells in the Z-direction, forming a structured grid. The total number of grid cells in the model's domain is 1.7 million, of which 1.5 million are active.

The simulation software uses units of feet for grid dimensions, and units of temperature are degrees centigrade.

The grid is approximately 17 x 15 miles. The grid cells are 500 x 500 ft in both X- and Y-directions across the entire model domain. Vertically, the cell thickness varies as a proportion of the mapped gross geological thickness for each zone divided by the number of grid layers in each zone. The total number of grid cells in the model's domain is 1.7 million, of which 1.5 million are active.

The reason for using a non-uniform grid, which is standard oil and gas industry practice, with increasing grid size (along the horizontal axes but not the vertical axes) is to reduce the number of grid cells to enable model efficiency and efficacy. There is less need for higher resolution (smaller) grid cells at the boundaries of the model where there is no CO₂ plume, and the pressure change is minimal. Instead, computing effort is concentrated around the injection wells and within the CO₂ plume and the region within and just beyond the boundary of the calculated AoR.

The upper Frio Formation (Injection Zone) and Anahuac Formation (Upper Confining Zone) are modeled. Analytical aquifers are applied at the top of the Confining Zone (to account for the behavior of the overlying Lower Miocene interval) and base of the Injection Zone (to account for the behavior of the Mid Frio Formation, Lower Confining Zone). Analytical aquifers are also applied along the edges of the model to account for the hypothetical lateral continuation of the Injection Zone. The area of review is calculated using outputs from the simulation and a depth grid of the lowermost USDW.

The trapping mechanisms are buoyant trapping of CO₂ against local and regional shales, capillary trapping of CO₂ and dissolution of CO₂ within reservoir brine. CO₂ mineralization trapping is not modeled. No communication with USDW is evidenced in the reservoir simulation model.

The modeling period is up to 500 years. Within this time period, CO₂ stability and the maximum extent of the pressure front can be defined. A delineated AoR is visualized on maps.

The pressure front shrinks rapidly after the injection ceases and the pressure dissipates. Within 5 years the pressure front no longer exists in the model. The CO₂ plumes continue to move up-dip and reach stability at 75 years after injection starts (45 years after injection ceases).

2.2.2 Cross-Sections

The cross-sections for Project Minerva represent two dimensional views of three-dimensional geological features below ground. The geological cross-sections are constructed from data collected from publicly available data sources and online databases. The cross-sections are centered north-south and west-east on the area of Project Minerva. The cross-sections fully illustrate the subsurface structural features below ground and are referenced to TVDSS. Subsurface structural features include faults, formation tops and

estimated thicknesses, USDW, and zones of interest. Dashed lines are used when well data log coverage is insufficient, and formations are interpreted.

The following geological intervals are defined by the following:

— Base of the Lowermost USDW

The base of the lowermost USDW is identified by a 2-ohm limit resistivity well logs (See Section 2.7.2.1 (Determination of the Base of the lowermost USDW)) for a detail discussion.

— Secondary Confining Zone

The Secondary Confining Zone is the shale-rich Miocene interval overburden. This unit is identified by an interval of high frequencies alternating between low and high on Spontaneous Potential (SP), Gamma Ray (GR), and resistivity well logs. The alternating low and high frequencies can be interpreted as alternating sand-silt-shale beds originating from a long period of consistent environments by transgressions and regressions during the Miocene Epoch.

— Upper Confining Zone

The Upper Confining Zone is the Anahuac Formation of late Oligocene age. This stratigraphic unit is identified by an interval of consistent, uniform high frequencies in SP, GR, and resistivity well logs. The consistent high frequencies can be interpreted as dominantly shale-rich intervals containing minimal sand intervals, primarily at the base of the formation. The regional continuity of sand intervals is not clearly interpreted from well log data used.

The top of the Confining Zone is identified as distinct by a sharp drop in well-log values and an increase in log variability (serrated log character); indicative of a regional unconformity related to a drop in sea level and a transition to a period of frequent transgression and regression.

— Injection Zone

The Injection Zone is the upper Frio Formation of middle Oligocene age. This stratigraphic unit is identified as an interval with frequent fluctuations between high and low values on SP, GR, and resistivity logs. Intervals of low resistivity, GR and SP are interpreted to be sand-rich units. The interval thickness is very variable and may be up to 100 ft thick or less than 5 ft. Intervals of higher resistivity, GR and SP are interpreted to be shale-rich units. Transition between sand-rich and shale-rich intervals may be sharp, creating blocky well log character, gradual, with fining or coarsening upwards trends, or a combination.

The top of the Injection Zone is marked variably by a sharp or gradational increase in SP, GR and resistivity and a transition to more uniform well log character.

— Lower Confining Zone

The Hackberry Trend of the middle Frio Formation is identified within the Project Minerva area as an interval of uniform log character punctuated by sporadic, infrequent deviations in log values. The log character varies depending on proximity to the paleo-shoreline and

intersection of deep marine channel/turbidite sandstones and basin floor fan complexes. Across the Project Minerva area and up-dip (proximal), the middle Frio Formation interval typically appears uniform in log character, with infrequent deviations, interpreted as shale-dominated strata punctuated by isolated submarine channel/turbidite sandstones. Correlation of sand-rich intervals is generally not possible with the density of data available. Distal areas, downdip of Project Minerva, may exhibit very variable, serrated log curves, or similar character to that described above. Variability may be linked to sampling of sandy basin floor turbidite fan complexes.

Top of the Hackberry Trend at Project Minerva is typically defined by an increase in SP log values and an increase and a reduction in the variability of SP and resistivity.

Figure 2.1.2-1 shows the local cross sections for Project Minerva, with Figure 2.1.2-2 showing north-southwest oriented cross-section that is approximately parallel to strike and Figure 2.1.2-3 showing west-east oriented cross-section that is approximately parallel to dip. All data logs used in cross-sectional figures are provided in Appendix V.

2.2.2.1 North-Southwest Cross-Sections

Figure 2.1.2-2 provides a regional dip-line view through Project Minerva, from North (proximal/continental platform) to the Southwest (distal/Gulf of Mexico Basin):

- The Injection and Confining Zones are demonstrably regionally continuous from north to southwest across Project Minerva.
- Some variability in interval log character from up-dip (proximal) to downdip (distal) depositional areas – zones are typically thinner and more coarse-grained in the north and thicker, with high interpreted shale content in the south, towards the deeper water setting.
- Some thinning of both zones is evident over the top of the Vinton Dome. This is due to syndepositional upward movement of the salt dome (decrease in accommodation space) during the deposition of the Frio and Anahuac Formations. Additionally, the dome structure includes complex radial faulting and a large fault cutting across the crest with counter-regional throw (to the NW). Local thickness changes are likely also linked to these structural complexities.

2.2.2.2 West-East Cross-Section

Figure 2.1.2-3 provides a regional strike-line view through the Project Minerva area, from West to East:

- The Injection and Confining Zones are demonstrably regionally continuous from west to east across Project Minerva.
- Relatively uniform log character in each defined interval along strike. Depositional environment interpreted to vary most strongly North-South.
- The upper Frio Formation thickens into the syncline structure at Project Minerva.

Likely linked to accommodation space creation by syndepositional fault movement and early Jurassic salt movement beneath, creating bathymetric changes on the paleo sea floor. Sediment may also have been preferentially deposited or redeposited off surrounding highs to east and west.

2.2.3 Structure Maps

The structure maps displaying the elevation of the formations of interest for Project Minerva are provided as:

- Figure 2.2.3-1 Top of Anahuac Formation (Upper Confining Zone)
- Figure 2.2.3-2 Top of Upper Frio Formation (Injection Zone)
- Figure 2.2.3-3 Top of Middle Frio (Lower Confining Zone)

Faults, shear zones, unconformities, or any other geological features are illustrated on the structure maps. Dashed lines are used when well data log coverage is insufficient, and formations are interpreted. Structural interpretation of the formations and regulatory zones is described in Section 2.4.2 (Description of the Injection Zone and Confining Zone System).

All structure maps are constructed from data collected from all publicly available data sources and online databases. This data is the most up-to-date subsurface data available. Data used to construct the structure maps include boreholes, wells, and seismic data. See Section 2.2.1.1 (Available Datasets) for a detailed discussion. Table 1.1-1 lists all wells and well data used to construct the maps. Table 1.1-1 includes, for each well, the operator's name, well name, well number, state serial number, total depth (TVD and MD if directional), and reference elevation.

2.2.4 Isopach Maps

The isopach maps for Project Minerva displaying the variation in thickness of the formations of interest for Project Minerva are provided as:

- Figure 2.2.4-1 Anahuac Formation (Upper Confining Zone)
- Figure 2.2.4-2 Upper Frio Formation (Injection Zone)
- Figure 2.2.4-3 Middle Frio (Lower Confining Zone)

All faults, shear zones, unconformities, or any other geological features are illustrated on the structure maps. Dashed lines are used when well data log coverage is insufficient, and formations are interpreted. Discussion of the gross thickness and lateral continuity of the formations of interest and regulatory zones is provided in Section 2.4.2 (Description of the Injection Zone and Confining Zone System).

The isopach maps are constructed from data collected from all publicly available data sources and online databases. This data is the most up-to-date subsurface data available. Data used to construct the isopach maps includes boreholes, wells, and seismic data. See Section 2.2.1.1 (Available Datasets) for a detailed discussion. As previously discussed above in Section 2.2.3 (Structure Maps), Table 1.1-1 lists all wells and well data used to

construct the maps. Table 1.1-1 includes, for each well, the operator's name, well name, well number, state serial number, total depth (TVD and MD if directional), and reference elevation.

2.3 FAULTS AND FRACTURES

2.3.1 Description of Faulting

In the area of Project Minerva, the direction of the faulting is relatively parallel to the edge of the Louisiana Gulf Coast. The faulting is a result of deposition of large quantities of sand and mud along the margins of the Gulf of Mexico resulting in rapid sedimentation creating large growth fault systems near the downdip edge of each sediment wedge within the area of maximum deposition. This growth faulting and rapid subsidence of Cenozoic shelf margins in the northwest Gulf of Mexico is also related to large-scale, deep-seated gravity sliding of the continental slope (Swanson, Karlsen, & J, 2013).

(Swanson, Karlsen, & J, 2013) discusses deeper, thick Jurassic salt mobilized by the weight of the overburden into a series of ridges and troughs. Local faulting connected to the growth and presence of numerous salt features originating from Black Bayou Dome to the southeast of Project Minerva adds complexity to structural architecture. Faults located further from Black Bayou Dome tend strike between 70° and 90°, although, radial faults originating from Black Bayou Dome have a wide variation in strike due to the complex structural regime associated with diapiric salt structures regionally. Salt related faults extend radially from the salt dome and have smaller displacement, and much larger densities than the regional west- to southwest- and east- to northeast trending regional faults.

A basemap of all structural features in the area of Project Minerva, including faults from the Anahuac Formation and upper Frio Formation are provided in Figure 2.2.3-1 and Figure 2.2.3-2.

All 3D seismic data is represented in the following figures:

Figure 2.3.1-1	Figure 2.3.1-2	Figure 2.3.1-3	Figure 2.3.1-4	Figure 2.3.1-5
Figure 2.3.1-6	Figure 2.3.1-7	Figure 2.3.1-8	Figure 2.3.1-9	Figure 2.3.1-10
Figure 2.3.1-11	Figure 2.3.1-12	Figure 2.3.1-13	Figure 2.3.1-14	Figure 2.3.1-15
Figure 2.3.1-16	Figure 2.3.1-17	Figure 2.3.1-18	Figure 2.3.1-19	

All structural features, including faults from the Frio Formation and Anahuac Formation, are provided in the following figures:

- Figure 2.2.3-1 (Top of Anahuac Formation (Upper Confining Zone))
- Figure 2.2.3-2 (Top of upper Frio Formation (Injection Zone)), and
- Figure 2.2.3-3 (Top of middle Frio Formation (Lower Confining Zone)).

2.3.2 Fault Transmissivity

The transmissivity of fluids across a fault must be considered with respect to both lateral (horizontal) and vertical components, requiring an assessment of the likelihood of a sealing surface (top seal and/or lateral seal) being present. Faults, in and of themselves, do not seal. However, faults can place porous intervals against seals and form non-transmissive barriers (traps) (Downey, 1984).

In the Gulf Coast region, the Tertiary fault rock seals are utilized greatly for their outstanding trapping capabilities to prevent the upward migration of hydrocarbons. The sand and shales are very thick, and the juxtaposition of shale-to-shale or sand-to-shale beds across a fault form a vertical rock barrier (i.e., seal) for fluid flow due to their low-permeability (Downey, 1984).

The faults within the AoR at Project Minerva are not transmissive and do not allow vertical fluid migration from the Injection Zone. An additional low-permeability fault rock between the Injection Zone and Upper Confining Zone, as well as the USDW, is achieved by a barrier of thousands of feet of fault rock seals along the fault plane. A high, net-to-gross within the Injection Zone results in effective horizontal permeability across faults such that they are predicted to not be sealing in relation to pressure or CO₂ plume migration.

2.3.2.1 Fault Seals

In circumstances where faulted sandstones are juxtaposed, seal analysis is performed to predict the potential for fault seal to lateral flow. These analyses were primarily developed for the petroleum industry and highlighted the importance of fine-grained fault rock for locally reducing fault permeability in multilayer sand-shale sequences (Nicol, Seebach, McNamara, & Field, 2016).

In a sand-to-shale geologic sequence, faulting will result in the juxtaposition of like and/or unlike lithology across the fault plane in three manners:

- sand-to-sand,
- sand-to-shale, and
- shale-to-shale.

Fault planes are normally considered to be inconsequential to migrating fluids, and generally are of significance as sealing surfaces only because they may juxtapose rocks of differing capillary properties and fluid pressures (Downey, 1984; Smith, Theoretical Considerations of Sealing and Non-Sealing Faults, 1966). Each fault case, based on the juxtaposition of lithologies across the fault, must be considered during an assessment for both lateral and vertical transmissivity (Figure 2.3.2-1) (Smith, 1966; Downey, 1984; Smith, 1980).

The deeper, underlying geologic sequence from the lowermost USDW consists of predominately shales (present in the section between the lower Lagarto of the Fleming Formation and the Frio Formation injection interval), which provide extensive shale-to-shale beds along a fault plane. The shale-to-shale beds will prevent fluid migration out of the

Injection Zone. No evidence of vertical effects of fluid migration due to faulting has been indicated within the area during production operations from Black Bayou Dome. In addition, the laterally extensive and impermeable shale-to-shale beds of the Lagarto Formation are a necessary Secondary Confining Zone barrier to effectively restrict upward movement of fluid. The presence of such lithology between the Injection Zone and the base of the lowermost USDW provides considerable protection to the USDW.

2.3.2.2 Vertical Fault Transmissivity

The shales at Project Minerva are ductile at the depths of the intervals of interest, and the juxtaposition of shale beds or sand-to-shale beds across a fault form a vertical barrier (seal) to fluid flow, due to their very low vertical permeability. This property of viscoelastic deformation behavior will cause any fractures and faults to close very rapidly in response to the in-situ compressive stresses, like squeezing into the fault plane from both sides. This well-known ductile, or plastic, behavior of the Gulf Coast shales is demonstrated by the presence of shale diapir structures and the natural closure of uncased boreholes with time (Gray, Darley, & Rogers, 1980; Johnston & Greene, 1979; Warner, 1988; Warner & Syed, 1986).

An example of a worse-case scenario presented to the EPA is in 1991, the E.I. Du Pont de Nemours and Company (DuPont) Sabine River Works Plant, located approximately 3 miles west of Project Minerva, conducted a borehole closure test demonstrating that the plastic nature of the Gulf Coast shales and the rapidity of shale movement can seal off openings in the subsurface. The test demonstrates that the Miocene shales of the Gulf Coast will flow and seal off an open area in the subsurface relatively quickly. The test duration was one-week, during which time the formation pressure achieved equilibrium. The conclusive evidence resulted in, even under worse-case scenario, no fluid flow migrates, and the borehole closes naturally (Clark, Papadeas, Sparks, & McGowen, 1991).

The vertical sealing nature of shale-to-shale or sand-to-shale juxtaposed lithologies across the Gulf Coast region having fault traps where both the top and the lateral seals are provided by shale beds (Figure 2.3.2-1). Due to the very plastic nature, the natural sealing capabilities, and the potential deformation of shales faults can seal based on the juxtaposition of like and unlike lithology across the fault plane. The deeper underlying geologic sequence of predominately shales provide extensive shale-to-shale contacts along the fault plane which will prevent CO₂ migration from the Injection Zone.

2.3.2.3 Lateral Fault Transmissivity

Lateral fault seal can arise from juxtaposition of porous and permeable reservoir rock against nonporous or no permeable rock, or by the development of fault rock having a high entry pressure. While faults may not act as seals themselves (Downey, 1984), they can place porous intervals against seals that form non transmissive barriers (traps). Fault planes are normally inconsequential to migrating fluids, and generally are of significance only in the circumstance of shallow, near-surface faulting in an overall tensional regional stress environment.

An example in such cases, of field observations and theory from (Secor Jr, 1965) discusses that the fault plane may act as an open transmissive fracture. However, the process of faulting may result in a "disturbed" fault zone between the offset lithologies. Therefore, a two-tiered analysis approach may be required:

1. First-order fault seal analysis involves identifying reservoir juxtaposition areas over the fault surface using mapping techniques.
2. Second-order fault seal analysis ascertains whether the reservoir-to-reservoir contact is likely to support a pressure difference. Several mechanisms have been recognized whereby fault planes can act as seals.

This includes:

- Juxtaposition, in which reservoir rock are juxtaposed against a low-permeability unit with a high entry pressure
- Clay smear or entrainment of clay/shale into the fault plane, thereby giving the fault "disturbed zone" a high entry pressure
- Cataclasis, which is the crushing of sand grains to produce a fault gouge of finer grained material, giving the fault "disturbed zone" a high capillary pressure
- Diagenesis, where preferential cementation along a previously permeable fault plane may partially or completely remove porosity, creating a hydraulic seal (Knipe, 1989; Nicol, Seebach, McNamara, & Field, 2016).

Juxtaposition seals can be recognized by mapping the contact of the various units across a fault. To identify or predict sealing via clay smear, cataclasis, or diagenesis requires an ability to relate these mechanisms to measurable properties or processes in the subsurface. The initial host rock is an important control on the fault disturbed zone material and properties, and thus, on seals. The host-rock properties that exert the most influence are the clay or phyllosilicate content, porosity, and permeability (Knipe, 1997; Nicol, Seebach, McNamara, & Field, 2016).

A criterion can be developed from these considerations and approach to potentially determine which faults surrounding the AoR at Project Minerva are laterally transmissive or are laterally sealed. The criteria include:

- Where the sand-to-shale ratio of the faulted geologic section indicates a substantial amount of impermeable shale ($\geq 25\%$ in shale beds) is present. The shale can be expected to be smeared along the fault plane during the growth of the fault. This clay smear would impede fluid movement laterally against the juxtaposed sand, resulting in a laterally non-transmissive fault.
- A fault is laterally sealing where the entire injection interval of sand is juxtaposed with a low-permeability layer such as clay or shale.
- A fault is laterally, non-sealing where sections of the same sandstone section (excluding shale beds within a sandstone unit) are juxtaposed (Knipe, 1997; Smith,

Theoretical Considerations of Sealing and Non-Sealing Faults, 1966; Nicol, Seebach, McNamara, & Field, 2016).

2.3.3 Faulting within the AoR

Within the AoR at Project Minerva, all faults are mapped where 3D seismic data is available. This is best represented in the following figures:

Figure 2.3.1-2	Figure 2.3.1-3	Figure 2.3.1-4	Figure 2.3.1-5	Figure 2.3.1-6
Figure 2.3.1-7	Figure 2.3.1-8	Figure 2.3.1-10	Figure 2.3.1-11	Figure 2.3.1-13
Figure 2.3.1-14	Figure 2.3.1-15	Figure 2.3.1-18		

A basemap of structural features, including faults in the AoR transecting the Frio Formation or Anahuac Formation, is provided in Figure 2.3.3-1 and mapped in the following figures:

- Figure 2.2.3-1 (Top of Anahuac Formation),
- Figure 2.2.3-2 (Top of upper Frio Formation), and
- Figure 2.2.3-3 (Top of middle Frio Formation).

The faults interpreted throughout the area of Project Minerva are not active at the present day. No growth faults within the shallow formations have been interpreted on seismic data represented in the figures listed above, and no surface representation of fault movement has been mapped by (USGS, 2024). According to (USGS, 2024), the gulf-margin normal faults in Louisiana are assigned as 'Class B' structures because of their low seismicity and because they may be decoupled from underlying crust making it unclear if they can generate significant seismic ruptures causing damaging ground motion. Although there are no growth faults within the AoR, there are listric faults restricted to the deeper Jurassic and Upper Cretaceous sedimentary intervals significantly below the Injection Zone. For a detailed discussion on seismic events associated with faulting, see Section 2.6 (Seismic History).

2.3.3.1 Fault Mapping and Modeling

The faults identified and interpreted throughout the area of Project Minerva on the 3D seismic datasets have been mapped and modeled with detail. The seismic horizons and faults were used to construct a structural framework within the geologic model. The model was populated with several properties, including shale content, which, combined with fault thickness (calculated from using a fault displacement-fault thickness ratio) used to determine fault permeability (Jolley, et al., 2007).

2.3.3.2 Fault Slip Potential Study

A fault slip potential study was carried out using the Fault Slip Potential (FSP) tool. The FSP is a free tool for deterministic and probabilistic screening of the rupture stability of existing faults in contact with a reservoir undergoing a pore pressure change, typically near injection wells (Walsh, et al., 2016-2018). The tool combines Mohr-Coulomb analysis with either an imported pressure model or semi-analytic pressure modeling, and either hypothetical or known faults. Faults are assumed to be in contact with the injection interval and out-of-zone

effects and poroelasticity are not considered. Initially developed by ExxonMobil and the Stanford Center for Induced and Triggered Seismicity; now housed at the University of Texas Bureau of Economic Geology and Center for Injection and Seismicity Research.

Appendix VI provides an overview of the complete Fault Slip Potential study.

Overview of Methodology

1. The Mohr-Coulomb pore pressure to slip on each fault is calculated using a deterministic approach
2. A Monte-Carlo analysis of the same parameter is run on each fault, which yields the probability of each fault slipping as a function of pore pressure increase on it
3. A pressure model created from the reservoir simulation is used as a deterministic hydrologic model. This is used to assess specific injection scenarios and relate injection to pore pressure changes
4. The code provides a simple radial flow-based model for pressure changes due to injection. The output of the hydrologic model is used as the pore pressure input to the probabilistic fault slip model, which yields an estimate of the cumulative probability of the fault slipping as a function of time
5. The Monte-Carlo approach to uncertainty can optionally also be applied to the included hydrology model to calculate probability of pressure increase on each fault

The FSP tool provides a relatively quick and cost-effective method for assessing fault slip risk in injection scenarios. It allows for rapid assessment of risk and uncertainty based on relative influence of key factors such as fault orientation, crustal stresses, and pressure changes. FSP predicts failure state for a pre-existing, arbitrary fault plane. FSP does not predict probability of a felt earthquake being produced by injection activity or fault slip, only the conditions required to cause fault failure, and the probability of failure based on site conditions over time. Results are sensitive to fault orientations, crustal stress orientations (which are not well-defined for project area), pressures, and other inputs that may have wide uncertainty ranges.

Data Inputs

Four faults intersect the AoR and were included in the analysis: Fault F02, Fault F13, Fault F03, Fault F19 (Figure 2.3.3-1).

- Fault geometries were exported as point data from the geostatistical model
 - Three sets of points were provided for each fault, 500+ points in total
 - Each point was assigned a fault dip, fault strike, and annual pressure delta through
- To simplify the analysis and make FSP results more meaningful, fault data were binned / upscaled
 - The “middle” points from each fault to establish a fault trace for input to FSP

- Faults were segmented according to strike direction:
 - Figure 2.3.3-2 (Fault F02)
 - Figure 2.3.3-3 (Fault F13)
 - Figure 2.3.3-4 (Fault F03)
 - Figure 2.3.3-5 (Fault F19)

Key assumptions

- Initial reservoir pressure gradient of 0.457 psi/ft, provided by GCS
- Fault friction coefficient of 0.85, estimated from published ranges
 - 0.68-0.72 (Engelder, 1974)
 - 0.6-0.85 (Byerlee, 1978)
 - Various references to ranges of >0.3-1
- Vertical stress gradient of 1 psi/ft, estimated from published ranges
 - 1 psi/ft commonly used as a starting point for onshore overburden
 - (Eaton, 1969) predicts ~0.93-0.95 psi/ft for Gulf Coast strata at GCS project depths
- Fault orientation and depth data extracted from geostatistical model
- Max horizontal stress direction – estimated
 - Three cases: N60E, +/-15 deg
 - Sources: World Stress Map; GIS data obtained from (Lundstern & Zoback, 2020)
- A phi - estimated from near offset control points
 - GIS data obtained from (Lundstern & Zoback, 2020)

Key findings from FSP analysis

- Deterministic model
 - For the mid-case SHmax orientation of N60E, no fault segments across any of the faults see pressure delta required to slip over the life of Project Minerva
 - Pressures to slip are generally more pessimistic for N75E SHmax and more optimistic for N45E SHmax
- Probabilistic FSP analysis
 - Maximum probability of fault slip:
 - ~0.28 for one segment (Fault 3)
 - ~0.23 for a second segment (F02)

- ~0.14 for a third segment (F02)
- All other fault segment have slip probabilities of less than 10%
- Highest-sensitivity inputs are SHmax azimuth, strike of fault, and dip of fault
- Fault slip potential at a project level is slow
 - Assuming SHmax N60E, the overall probability of slip is low (most segments <10%)
 - The western tip of F02 and eastern tip of Fault 3 have highest slip potential probabilities (20-30%) but over relatively short segment lengths and not the entire fault
 - However, a higher SHmax azimuth could increase slip risk to unacceptable levels for more segments (i.e., pressure required to slip becomes less than modeled pressure on fault)
- Induced seismicity risk
 - The Gulf Coast is considered at low risk of seismic activity overall
 - It is not known whether partial failure of a fault would trigger a felt earthquake
 - Growth faults along the Gulf Coast are generally not associated with seismic hazards

[Site-specific data likely to help reduce uncertainty in modeled assumptions](#)

- Obtain local stress orientation data
- Confirm and update fault segment geometries
- Apply updated pressure model based on operational data over life of project

[Monitoring](#)

If required by LDENR, microseismic data will be collected to monitor seismicity at Project Minerva.

2.4 INJECTION ZONE AND CONFINING ZONE SYSTEM DETAILS

The Injection Zone is defined as the zone capable of accepting fluids and of sufficient areal extent, thickness, porosity, and permeability to receive carbon dioxide through a well(s). Additionally, an adequate Injection Zone must be confined by formations that prevent the migration of fluids from the zone.

A sufficient Confining Zone System must provide upper and lower containment of the Injection Zone and provide isolation between the Injection Zone and the base of the lowermost USDW. The Confining Zone System consists of the Lower Confining Zone, Upper Confining Zone, and Secondary Confining Zone.

Figure 2.4.2-1 illustrates a cross-section of the geostatistical model layers intersecting MS CCS 1 and MS CCS 2 and identifies the regulatory zones, the respective proposed depths,

and the associated formations. Table 2.2.1-1 summarizes the information presented in Figure 2.4.2-1 by correlating the regulatory zones to the geostatistical model formation top depths and the simulation layers.

2.4.1 Geologic Summary

At Project Minerva, the regional and local geology demonstrates ideal geologic conditions for CO₂ injection and storage. The massive, fluvial-deltaic sandstones of the Middle Frio Formation offer effective injection reservoirs in terms of the lateral extent, mineralogical composition, and petrophysical characteristics of the formation. These injection reservoirs have the permeability, porosity, thickness, and lateral continuity to accept and contain injected materials. The underlying aquiclude layers in the Middle Frio Formation are thick, impermeable, and have lateral continuity to confine the injected fluids in the Injection Zone.

The Anahuac Formation and the shale-rich Miocene interval are sufficient confining units and have effective barriers to prevent upward fluid migration. The Confining and Secondary Confining Zone are regionally extensive and are extensively less permeable than the underlying injection reservoir and aquiclude layers. The multiple sand-shale layers between the top of the Injection Zone and the base of the lowermost USDW ensures additional confinement and protection of a USDW.

2.4.2 Description of the Injection Zone and Confining Zone System

At Project Minerva, the Injection Zone has the permeability, porosity, thickness, and lateral continuity to accept injected materials. Both the Upper Confining and Secondary Confining Zone are impermeable units with sufficient thickness and low permeability necessary to meet the confining criteria to be an effective barrier for upward fluid migration. A description of the Injection Zone and the injection intervals, as well as the Upper Confining and Secondary Confining Zones are discussed below in detail.

2.4.2.1 Injection Zone

The Injection Zone at Project Minerva is the upper Frio Formation. The Frio Formation is comprised of three intervals, informally referred to as, in ascending order: (1) The lower Frio Formation, (2) the middle Frio Formation, and (3) the upper Frio Formation. The upper Frio Formation is comprised of stacked shoreline sandstones interbedded with shales. The middle Frio Formation is comprised of channel-turbidite sandstones isolated in thick shales intervals. Both the upper and middle Frio Formation are prolific hydrocarbon producers and are consequently most frequently sampled during well logging. The upper and middle Frio Formation intervals have been extensively developed in southwest Louisiana, however, at Project Minerva, the upper Frio Formation is wet and sparsely penetrated by historic wells targeting the deeper middle Frio Formation Hackberry turbidite/channel sandstones.

The Injection Zone extends from the upper Frio Formation, where the Anahuac Formation contacts the Frio Formation, to the top of the middle Frio Formation (Figure 2.1.2-2 and Figure 2.1.2-3). Gross thickness varies from approximately 1,400 ft to approximately 1,700 ft in the Project Minerva's AoR. Gross thickness trends are shown in Figure 2.2.4-2.

The upper Frio Formation is a well-defined seismic reflector mappable in 3D seismic data

across Project Minerva's AoR. Seismic sections within the AoR are represented in the following figures:

Figure 2.3.1-1	Figure 2.3.1-2	Figure 2.3.1-3	Figure 2.3.1-4	Figure 2.3.1-5
Figure 2.3.1-6	Figure 2.3.1-7	Figure 2.3.1-8	Figure 2.3.1-9	Figure 2.3.1-10
Figure 2.3.1-11	Figure 2.3.1-12	Figure 2.3.1-13	Figure 2.3.1-14	Figure 2.3.1-15
Figure 2.3.1-16	Figure 2.3.1-17	Figure 2.3.1-18	Figure 2.3.1-19	

Some variability in interval log character from up-dip (proximal) to downdip (distal) depositional areas – zones are typically thinner and more coarse-grained in the north and thicker, with high interpreted shale content in the south, towards the deeper. Depth varies from 8,000 ft TVDSS to 10,200 ft TVDSS at Project Minerva. Figure 2.2.3-1, Figure 2.2.3-2, and Figure 2.2.3-3 demonstrate the local structure at Project Minerva. The structure maps were generated using high quality 3D seismic data in conjunction with logs/formation tops to create a depth surface. Modeled structural dip is variable and derived primarily from 3D seismic.

Log data within the Injection Zone indicate individual or stacked sand-rich beds alternating with shale-rich intervals and/or siltstones:

1. Sand-rich intervals,

- Interpreted as a negative deflection in spontaneous potential, resistivity, and gamma ray log value,
- Multiple feet to >100 ft thick,
- May appear as induvial beds or amalgamated/stacked,
- Variably sharp or gradational upper- and lower-unit boundaries give log curves a blocky or serrated character, and
- May be correlated laterally at the scale of the AoR and are therefore interpreted to be laterally extensive shoreface sandstones.

2. Fine grained/shale-rich intervals,

- Interpreted as a positive deflection in spontaneous potential, resistivity, and gamma ray log values, and
- Multiple feet to hundreds of feet thick.

This interpretation conforms with published analysis of Oligocene Gulf Coast depositional environments: the middle Oligocene Frio Formation is described as a thick sequence of mainly regressive sand-rich sediments interbedded with silts/shales, deposited rapidly in alluvial, lagoonal, marginal marine and deep marine environments, forming a major progradational wedge along the Gulf (Swanson, Karlsen, & J, 2013).

Sand-rich beds correlated across the AoR are relative pay intervals and are likely to have very good lateral communication and variable vertical communication through intra-Frio shales/siltstones.

Relatively limited core data is available and is located north of Vinton Dome (Table 2.4.2-1, Figure 2.4.2-2). Sidewall core data and petrophysical analysis of well logs indicate that sand-rich units appear to average approximately 8% porosity (with some samples exceeding 25 %), 42.6 mD horizontal permeability, and 16.7 mD vertical permeability. XRD analysis is available in the upper Frio Formation in the M Gray G Well, 85 (API: 17019216270000). Data indicates that the upper Frio Formation sand-rich intervals typically comprise 69-80% quartz 6-11% clay minerals, with the rest consisting of 5-7% feldspar and 3-4% calcite (Table 2.4.2-2 and Table 2.4.2-3). Site-specific data will be collected in pre-operational data testing prior to commencement of injection to verify this data.

The top of the Frio Formation is a well-defined seismic reflector that is mappable across the 3D seismic dataset. As can be seen from the interpreted seismic lines are represented in the following figures:

Figure 2.3.1-1	Figure 2.3.1-2	Figure 2.3.1-3	Figure 2.3.1-4	Figure 2.3.1-5
Figure 2.3.1-6	Figure 2.3.1-7	Figure 2.3.1-8	Figure 2.3.1-9	Figure 2.3.1-10
Figure 2.3.1-11	Figure 2.3.1-12	Figure 2.3.1-13	Figure 2.3.1-14	Figure 2.3.1-15
Figure 2.3.1-16	Figure 2.3.1-17	Figure 2.3.1-18	Figure 2.3.1-19	

As depicted in the above-referenced figures, the lateral and vertical continuity of the Injection Zone can be confidently interpreted throughout the AoR and the study area.

2.4.2.2 Upper Confining Zone

The Confining Zone is defined as the zone overlying the Injection zone that acts as a barrier to fluid movement above an Injection zone. The Confining Zone must have sufficient rock strength, permeability, areal extent, and thickness to confine injected fluids within the Injection zone.

The confining formation overlying the Injection Zone, identified as the Upper Confining Zone, is the Anahuac Formation which conformably overlies the upper Frio Formation. The Anahuac Formation acts as a very effective, thick regional seal to many prolific hydrocarbon fields and so can be assumed to be rich in sealing lithologies (Swanson & Karlsen, 2009).

SP, GR, and resistivity log data indicate that the Anahuac Formation has high shale content regionally. Current available core data samples of the Anahuac Formation have preferentially targeted high porosity intervals and thus average skewed recorded porosities towards higher values (Table 2.4.2-4). (Clark, 1981; Porter & Newsom, 1987) were used to characterize the petrophysical properties of the Anahuac Formation at Project Minerva, including two Core Laboratory reports (Core Laboratories, 1987; Core Laboratories, 1987)

and an End-Of-Well report (The Dow Company, 2020) for a waste disposal well for the DuPont de Nemours company in Jefferson County, Texas.

(Clark, 1981) reports on groundwater flow in deep saline aquifers, with examples from the Wolfcamp aquifer system (Palo Duro Basin, West Texas), the Mount Simon aquifer (Northern Ohio), the Lower Floridan aquifer (Northwest Florida), the Wilcox aquifer (Gulf Coastal Plain, Mississippi) and the Frio aquifer (Harris County, Texas). This report also discusses the permeability and porosity of the sealing units (i.e., shale formations) overlying these deep saline aquifers. (Clark, 1981) states the following:

1. Formation water flow speeds in the deep saline aquifers are on the scale of ~1 ft/yr (in contrast to those in shallow fresh-water aquifers with flow rates of ~100 ft/year).
2. Gulf Coastal Plain shales the vertical flow rate through the sealing shale formations is the order of 1 ft in 10,000 yrs.

(Clark, 1981) discusses the sluggish circulation within the deep saline aquifers and state "demonstrates that geological confinement is effective on both a local and regional scale."

For permeability, the minimum value for the Anahuac Formation was set to $1E^{-6}$ mD; the maximum value is assumed to be $1E^{-3}$ mD. The most likely value is $1E^{-4}$ mD. This is weighted towards the minimum value because more of the measured data occurs at the lower end of the range of values (Clark, 1981).

At Project Minerva, the porosities for the Anahuac Formation were determined using correlations developed for Gulf Coast shales as presented in (Porter & Newsom, 1987).

The "effective" shale porosity, which discounts the bound water within the clay structure as well as water contained in dead-end pores, represents an appropriate choice of a porosity value for such a calculation. At the depths of interest, an effective clay/shale layer porosity is detailed in Table 2.4.2-4 (Porter & Newsom, 1987). Using this relationship for the minimum effective porosity in a shale versus depth, the maximum porosity in the Upper Confining Zone was taken to be 0.11 (fraction), with a most likely (midrange) value of 0.09 (fraction) and a minimum of 0.08 (fraction) for the model. We assume a vertical to horizontal permeability ratio of 0.1.

Rock compressibility's were estimated by combining data from taken from (Zheng, Zhuang, & Espinoza, 2019; Zimmerman, 1991; Yale, Nabor, Russell, Pham, & Yousef, 1993). It was assumed that the minimum (min), most likely and maximum (max) formation compressibility for the Upper Confining Zone were: 3 (min), 6 (most likely) and 10 (max) E^{-6} pound per square inch (psi)⁻¹.

At Project Minerva, the Anahuac Formation extends from -6,600 ft TVDSS near Black Bayou Dome to over -9,200 ft TVDSS at the base of a syncline structure located northeast of the AoR (Figure 2.1.2-1, Figure 2.1.2-2, and Figure 2.2.3-1). Depth across the AoR varies from -7,000 ft to -8,400 ft TVDSS.

The Anahuac Formation forms a syncline structure within the AoR area through the interplay of the regional dip towards the Louisiana Gulf (southeastwards at Project Minerva) with

northwards dip off Black Bayou Dome (Figure 2.2.3-1). Areas of increased dip coincide with large-scale normal faults.

Project Minerva proposed injection wells are located >1,000 ft from major faults in areas of low-moderate dip. The Anahuac Formation thickens in a broad wedge geometry, from north to south. Gross thickness varies between 750 ft to >1,200 ft in the main AoR area (spanning).

The Anahuac Formation thickens from 800 ft, north of the project area, to over 1,100 ft, south (Figure 2.2.4-1).

Figure 2.2.4-1, Figure 2.1.2-1, Figure 2.1.2-2, and Figure 2.1.2-3 clearly demonstrate the lateral continuity of the mapped Upper Confining Zone across the AoR. Log character and interval thickness are demonstrably consistent in cross-section and isopach. At the top of the Anahuac Formation is a seismically complicated reflector, and it is hard to consistently map across the entire 3D seismic dataset. However, due to a good spread of well-to-seismic ties made, GCS has consistently mapped the Anahuac Formation from the interpreted seismic lines in the following figures:

Figure 2.3.1-1	Figure 2.3.1-2	Figure 2.3.1-3	Figure 2.3.1-4	Figure 2.3.1-5
Figure 2.3.1-6	Figure 2.3.1-7	Figure 2.3.1-8	Figure 2.3.1-9	Figure 2.3.1-10
Figure 2.3.1-11	Figure 2.3.1-12	Figure 2.3.1-13	Figure 2.3.1-14	Figure 2.3.1-15
Figure 2.3.1-16	Figure 2.3.1-17	Figure 2.3.1-18	Figure 2.3.1-19	

The lateral and vertical continuity of the Upper Confining Zone can be confidently interpreted throughout the AoR, and the study area.

2.4.2.3 Lateral Extent of the Injection and Confining Zones

The Injection Zone (upper Frio Formation) and the Upper and Lower Confining Zones (Anahuac Formation and middle Frio, respectively) are regionally extensive along the Gulf Coast, Texas and Louisiana. Figure 2.2.4-1, Figure 2.2.4-2, and Figure 2.2.4-3 illustrate the combined gross thickness and mappable large-scale extent. Additionally, Figure 2.1.2-1, Figure 2.1.2-2, and Figure 2.1.2-3 demonstrate the regional continuity of the zones across Project Minerva. Within the AoR the base of the lowermost USDW, Upper Confining Zone and top/base Injection Zone are clear, consistent picks in the available well log data. The Upper Confining Zone and Injection Zone are represented by and mapped on well-defined seismic reflectors in 3D seismic data, as depicted in the following figures:

Figure 2.3.1-1	Figure 2.3.1-2	Figure 2.3.1-3	Figure 2.3.1-4	Figure 2.3.1-5
Figure 2.3.1-6	Figure 2.3.1-7	Figure 2.3.1-8	Figure 2.3.1-9	Figure 2.3.1-10
Figure 2.3.1-11	Figure 2.3.1-12	Figure 2.3.1-13	Figure 2.3.1-14	Figure 2.3.1-15
Figure 2.3.1-16	Figure 2.3.1-17	Figure 2.3.1-18	Figure 2.3.1-19	

The Injection and Upper Confining Zones are demonstrably laterally extensive, exhibiting no evidence of pinchout of sand-rich intervals within the main AoR. Within the Injection Zone, some local variations in interval thickness and extent occur, however these have been factored into the reservoir model, and do not negatively impact the overall behavior of the reservoir in terms of storage capacity, injection rates or safety of the USDW.

The lateral extent of the Injection, Upper Confining and Secondary Confining zones is demonstrated by the well log data cross-sections, Figure 2.1.2-1, Figure 2.1.2-2, and Figure 2.1.2-3. The extent of the Upper Confining Zone and Injection Zone are demonstrated on the the isopach maps, Figure 2.2.4-1 and Figure 2.2.4-2; and the well-defined seismic reflectors in 3D seismic data, as depicted in the following figures:

Figure 2.3.1-1	Figure 2.3.1-2	Figure 2.3.1-3	Figure 2.3.1-4	Figure 2.3.1-5
Figure 2.3.1-6	Figure 2.3.1-7	Figure 2.3.1-8	Figure 2.3.1-9	Figure 2.3.1-10
Figure 2.3.1-11	Figure 2.3.1-12	Figure 2.3.1-13	Figure 2.3.1-14	Figure 2.3.1-15
Figure 2.3.1-16	Figure 2.3.1-17	Figure 2.3.1-18	Figure 2.3.1-19	

2.4.2.4 Secondary Confining Zone

The Secondary Confining Zone is located within the Miocene Lagarto Formation and consists predominantly of impermeable shale. The dominance of shale versus sand within this Secondary Confining Zone is readily apparent on Figure 2.1.2-2, and Figure 2.1.2-3. More than 7,000 ft of shale-rich strata accumulated at the Project Minerva site, providing a thick, robust secondary seal to the Injection Zone (upper Frio Formation).

This Secondary Confining Zone lithology is composed primarily of interbedded sand and shales, whose shales have very low permeabilities in the range of 10^{-5} mD. Table 2.4.2-5 shows analogous permeabilities for the confining shale layers near the base of this zone. Core plugs, for the analogous Lagarto shale analysis, were taken from Class I Well at the DuPont Beaumont Works Plant (WDW188). Additional information is contained in the report on "Shale Porosity and Permeability" by (Porter & Newsom, 1987).

Interbedded sand units within the Secondary Confining Zone provide an additional level of safety as buffer aquifers that could capture and retain any fluids that might migrate vertically through an undetected potential breach in the Injection Zone (upper Frio Formation) and the Secondary Confining Zone (Anahuac Formation).

2.4.2.5 Lower Confining Zone

The confining formation underlying the Injection Zone, identified as the Lower Confining Zone, is the Hackberry Trend of the Frio Formation. The Hackberry Trend is interpreted as shale-dominated strata punctuated by isolated submarine channel/turbidite sandstones. Correlation of sand-rich intervals is generally not possible with the density of data available. Top of the Hackberry Trend at Project Minerva is typically defined by an increase in SP log values and an increase and a reduction in the variability of SP and resistivity.

The base of the middle Frio in the area of Project Minerva is not well defined by seismic interpretation or well control. Stream 34 Well No. 001 (SN 224971, Map ID 1), located approximately 1 mile north of the proposed injection wells, was drilled and logged to approximately 14,000 feet TVDSS within the middle Frio Formation, nearly 3,300 feet below the top of the middle Frio Formation. Figures 2.1.2-2 and 2.4.2-1 depicts the location of Stream 34 Well No. 001 relative to the proposed injection wells and indicates there is sufficient thickness to serve as a lower confining unit.

Figure 2.1.2-1 shows the base map of the local cross sections for Project Minerva, with Figure 2.1.2-2 showing north-southwest oriented cross-section that is approximately parallel to strike and Figure 2.1.2-3 showing west-east oriented cross-section that is approximately parallel to dip. GCS has designated the top 500 ft of the middle Frio Formation as the Lower Confining Zone and provided the required isopach of the Lower Confining Zone as Figure 2.2.4-3. As indicated on the above-referenced cross-sections and the isopach for the Lower Confining Zone, there is sufficient confinement below the Injection Zone to provide containment.

2.4.2.6 Regional Pressure Sources and Sinks

To identify all critical activities in the Injection and Upper Confining Zones, including pressure sources and sinks, a REVEAL reservoir simulation model of the project area was built.

- All available production data (including hydrocarbons and water) were acquired from the Enverus Drilling Info database, dating from 1950 to August 2020. Data was pulled in August 2020.
- Production was assigned to geological intervals – Hackberry, Frio, Anahuac, Miocene and other.
- Water production and re-injection is available post-1970; the data were allocated to each geological interval.
- The production of oil and gas and the re-injection of produced water were modelled in three regions: Phoenix Lake, Black Bayou and Vinton Dome

Limitations of the available dataset:

- The naming convention for “producing interval” is very variable between regions (Phoenix Lake, Black Bayou and Vinton Dome) and by state (Louisiana vs Texas). This increases the potential error on allocating production/injection to the correct geological interval.
- “Producing interval” may at times be misreported – this becomes evident when comparing the reported depth of the perforated interval of a well to interpreted formation tops in well log data
- Production is reported on a lease basis, rather than well-by-well

- Water production and injections were not reported in Texas and Louisiana prior to 1970

Key conclusions:

- Given the huge size of the upper Frio Formation's connected aquifer and its large average permeability, the pressure change, at the present day, due to all this activity is not significant in the area of Project Minerva.
- Following the steep decline of production from the mid 1970's until today, pressure has recovered in the region of Project Minerva to close to its original value, within ± 5 psi. This uncertainty range is less than the current uncertainty in the current formation pressure (uncertainty range = -12 to +20 psi), which we estimate to be 3,662 pounds per square inch absolute (psia) at a datum depth of 8,000 ft TVDSS. This was backed up by an analytical material balance calculation.

Plan to address limitations of current dataset:

- The assumption that there is a hydrostatic pressure equilibrium at present in the upper Frio Formation will be tested using newly acquired pressure data
- Pressure data will be collected at each injection well and at an in-zone monitoring well.

2.5 GEOMECHANICAL AND PETROPHYSICAL INFORMATION

Geomechanical and petrophysical characterization of the Injection and Upper Confining Zones will be undertaken during construction of injection wells, as outlined in the Pre-Operational Logging and Testing Plan (Attachment C). In the absence of core material from a dedicated stratigraphic well, data has been generated from published sources for the Frio Formation.

2.5.1 Geomechanical Information

2.5.1.1 Existing Data Sources

Two published studies were used as sources to inform the analogous geomechanical properties of the upper Frio Formation for Project Minerva: Frio Formation CO₂ Injection Pilot Project (Hovorka, et al., 2005) and In-Situ Stress Predictions and Measurement in an Unconsolidated Sandstone Formation, the lower Frio Formation, East Texas (Ramos, Katahara, Keck, & Batzle, 1994).

The upper Frio Formation CO₂ injection pilot project was conducted in October 2004 on the flank of a salt dome within the South Liberty oil field, near Dayton, Texas (Figure 2.5.1-1). The Frio "C" Injection Zone was described as a subarkosic, fine grained, moderately sorted quartz and feldspar sandstone, with minor amounts of illite or smectite and calcite (Kharaka, Hovorka, Cole, & Gunter, 2006). The zone had a mean porosity of 32% and a permeability of 2-3 Darcy. Situated immediately above the "C" sandstone, the "B" sandstone had an approximately 13 ft thick, reworked fluvial sandstone bed at the top, but had more shale and

siltstone beds, including an approximately 23 ft thick transgressive marine shale bed at the bottom.

The cores were obtained (Zheng, Zhuang, & Espinoza, 2019) from measured depths (MD) of 5,053 – 5,056 ft MD and 5,063 – 5,066 ft MD. The initial porosity measured by logging tools was approximately 33%, by MICP 32.5%, and by manometric method it was 33.8%. In the interval 5,053 – 5,056 ft, most of the grains were larger than 10 μ m with a mean of approximately 100 μ m.

Another study of the geomechanical behavior of the Frio Formation is reported in (Ramos, Katahara, Keck, & Batzle, 1994) (Figure 2.5.1-1). This was a field test at a depth of 5,000 ft in the lower Frio Formation in Jasper County, East Texas. The target sand occurred from 4,430 to 4,585 ft in depth and was bound above by a 130 ft thick shale, and below by a series of shale/sand sequences that extended down to the Yegua sand at 6,500 ft.

2.5.1.2 Stress

In the absence of measured local data, we used published sources (Trevino & Meckel, 2017; Nicholson, 2012; Zoback & Zoback, 1980) to set the orientation of the principal horizontal stresses. These were set to 54.1° for the maximum horizontal stress and 324.1° for the minimum horizontal stress, Figure 2.5.1-2 (Nicholson, 2012).

The directions of principal stresses were determined using regional fault-strike statistics. (Nicholson, 2012) calculated the average fault strike for 297 faults or fault segments, which was 54.1°, roughly parallel to the coastline and in agreement with onshore values for the maximum horizontal stress azimuth found by (Zoback & Zoback, 1980).

As reported below, there is uncertainty in the magnitudes of the principal stresses, particularly the horizontal stresses.

Vertical total stress: S_v

The overburden stress, S_v , for normal-fault stress regimes is assumed to be an average of 1.0 psi/ft (Nicholson, 2012). This is equivalent to the lithostatic pressure exerted by rock with an average density of 2.3 g/cm³ (Hovorka, Tutton, & Trevino, 2018). (Trevino & Meckel, 2017) assumed a value of 1.0 psi/ft. This data was used for studies of the Lower Miocene in the Texas Gulf of Mexico.

GCS took the most likely total vertical stress gradient to be 1.0 psi/ft.

This compares with a value of 0.9 psi/ft (from the density log) reported by (Ramos, Katahara, Keck, & Batzle, 1994). (Ramos, Katahara, Keck, & Batzle, 1994) derived values for the principal horizontal stress gradients from an unconventional differential strain curve analysis (DSCA). The rock samples were poorly consolidated, and this prevented a conventional DSCA. Based on this data, we estimate the error in the total vertical stress gradient to be approximately ± 0.1 psi/ft.



45031 & 45032

Total minimum horizontal stress; $S_{h,min}$

(Nicholson, 2012) assumed a value of 85% of S_v , values consistent with work published by (Engelder, 1974). (Trevino & Meckel, 2017) assumed a value of 0.85 psi/ft (85% of 1 psi/ft for the vertical stress gradient).

GCS took the most likely value of the minimum horizontal stress gradient to be 0.85 psi/ft.

(Ramos, Katahara, Keck, & Batzle, 1994) reported a value of $0.74 * 0.9$ psi/ft = 0.66 psi/ft. Based on this data, we estimate the error in the total minimum horizontal stress gradient to be approximately ± 0.15 psi/ft.

Total maximum horizontal stress; $S_{h,max}$

GCS took a value equal to the average of the gradients of the total vertical and minimum horizontal stresses, 0.93 psi/ft (to 2 decimal places), with an error of ± 0.07 psi/ft. Our estimate of the error is the range between our most likely total vertical and minimum horizontal stress gradients. (Ramos, Katahara, Keck, & Batzle, 1994) reported a value of $0.81 * 0.9$ psi/ft = 0.73 psi/ft from six DSCAs, so we may be underestimating the error. It is half the error we report for the total minimum horizontal stress. This is because of the extra “information” carried by constraining the expected value to lie between the total vertical and minimum horizontal stress gradients.

Biot Coefficient

(Zheng, Zhuang, & Espinoza, 2019) reported a value of 0.944 (± 0.056), in the effective stress range 3.5 – 7 MPa (500 – 1,000 psi). (Ramos, Katahara, Keck, & Batzle, 1994) assumed a value of 1.0. We assume a value of 1.0. The error is approximately ± 0.06 , assumed from (Ramos, Katahara, Keck, & Batzle, 1994).

Poisson's ratio

This is taken from (Zheng, Zhuang, & Espinoza, 2019), partly reproduced below, GCS took the unloading process values with an average of 0.23 ± 0.04 . (Ramos, Katahara, Keck, & Batzle, 1994) reported an average core value of 0.21, based on static tests.

Young's modulus

Young's modulus is taken from (Zheng, Zhuang, & Espinoza, 2019) (Figure 2.5.1-3). We take the unloading process values with an average of 5.5 ± 0.5 Gpa.

(Ramos, Katahara, Keck, & Batzle, 1994) measured a value of 1.7 Gpa, and with a cohesive (shear) strength of less than 3.4 Mpa (500 psi). It was also noted that the elastic moduli of the sandstones were about twice that of the shale but that the shear strength of the shale was about twice that of the sandstone.

Cohesion, C

Cohesion is assumed to be zero, (Trevino & Meckel, 2017).

Coefficient of friction, μ

Coefficient of friction is equal to 0.6, (Trevino & Meckel, 2017).

Poro-elastic, thermo-elastic and linear thermal expansion coefficients

Figure 2.5.1-4 is taken from the Petroleum Experts' REVEAL manual and shows the definitions of the poro-elastic and thermo-elastic coefficients used in REVEAL.

The poro-elastic coefficient translates the effect of fluid pressure to the reservoir stress field as $\Delta S \sim \partial S / \partial P * \Delta P$, where ΔS is the change in stress, $\partial S / \partial P$ is the poro-elastic coefficient and ΔP is the change in pressure. The expected value of the poro-elastic coefficient is $6.77E^{-7}$ psi⁻¹.

The thermo-elastic coefficient translates the effect of temperature to the reservoir stress field, as $\Delta S \sim \partial S / \partial T * \Delta T$, where ΔS is the change in stress, $\partial S / \partial T$ is the thermo-elastic coefficient and ΔT is the change in temperature. The expected value of the thermo-elastic coefficient is 21.5 psi °C⁻¹. The thermo-elastic coefficient requires an additional item of data, the linear thermal expansion coefficient. We take the default value in REVEAL of $2.16E^{-5}$ °C⁻¹.

REVEAL calculates the stress field in the model grid using a finite element grid which is separate from the grid used to solve fluid flow. This grid is generated automatically. The stress is calculated as a function of the *in-situ* stress, temperature, pressure, Poisson's ratio, Young's modulus and the poro- and thermo-elastic coefficients.

REVEAL simulation software also has a fracture model, where it is possible to investigate the possibility of fracture initiation and growth geometry within a dynamically coupled reservoir and wellbore system.

2.5.2 Petrophysical Information

Pre-Operational Testing will involve the acquisition of customized log suites, fluid samples, and cores from both the Injection Zone and Upper Confining Zone. A Triple-Combo log suite will be obtained for formation evaluation, which will be used to gather measurements such as density, porosity, and resistivity. These measurements will allow for the calculation of petrophysical properties, including total porosity, effective porosity, hydrocarbon saturations, and facies characterization. Additionally, if necessary, a nuclear magnetic resonance (NMR) log may be acquired for advanced characterization, particularly if other methods prove insufficient. The NMR log provides detailed information on pore size, permeability, hydrocarbon properties, vugs, fractures, and grain size.

GCS plans to implement a core program after the well is drilled, where whole cores and sidewall cores will be collected and analyzed for calibration. These core samples will undergo routine core analysis to test storage capacity (total and effective porosity), flow units (permeability), and saturation levels. A lithoscan test will be conducted to determine parameters such as photoelectric factor (PEF), bulk density, lithology, and VP-VS (compressional and shear wave velocities). The data gathered from these tests will enable

the calibration of petrophysical workflows for the Project Minerva site, with improvements in petrophysical outputs feeding into the geostatistical and reservoir simulation models.

Rock mechanics testing will also be performed, including combined triaxial and ultrasonic testing with Mohr-Coulomb borehole stability analysis. The following parameters will be measured under reservoir stress conditions: Young's modulus, Poisson's ratio, compressive strength, Biot's coefficient, and Brazilian tensile strength.

2.5.2.1 Core and Rock Data Description

Core data in the project area was available only from older vintage wells located around the Vinton Dome (Table 2.5.2-1, Figure 2.4.2-2). All the available core samples are percussion side-wall core (SWC) and are not ideal for the analysis of porosity and permeability due to potential damage during the acquisition. However, as no other sources of core data were available, 482 side-wall core samples have been analyzed for permeability and porosity in the area – 350 from the Injection Zone (Frio Formation) and 132 from the Upper Confining Zone (Anahuac Formation) (Tables 2.4.2-1 and 2.4.2-4). It should be noted that samples taken from the Upper Confining Zone targeted high porosity and permeability intervals and are thus skewed towards higher value ranges. Site-specific shale samples from the Upper Confining Zone will be collected during the preoperational testing phase. Analog Gulf Coast shale porosity values were also factored into porosity/permeability ranges (Table 2.5.2-2).

The available samples were used to normalize the 28 porosity logs, which were then used to characterize the porosity of the Injection and Upper Confining Zones. Permeability was calculated using a porosity – permeability relationship established from side-wall core sample results (Figure 2.2.1-7). Mineralogical analyses have been performed on two samples (Tables 2.4.2-2 and 2.4.2-3).

There were also five other samples analyzed using X-Ray diffraction to establish their mineralogical composition. These samples were likely taken from the Injection Zone, from depths ranging between -5,426 to -5,446 ft below KB, and showed only qualitative results, which indicates that the sands consisted mostly of quartz, and contained no carbonates. Because of the questionable location where the samples were taken, these results could not be used to further characterize the analyzed formations.

Prior to operations at Project Minerva, and consistent with the Pre-Operational Testing Program, whole core samples from the Injection and Upper Confining Zones will be acquired and analyzed for porosity, permeability, and mineralogy. The geostatistical and reservoir simulation models will be updated with the newly acquired site-specific data and submitted for review with the Pre-Operations Completion Report and Site Reassessment (Attachment F).

2.5.2.2 Geochemical Data

Data currently unavailable – to be collected during Pre-Operational Testing.

2.5.2.3 Rock

Data currently unavailable – to be collected during Pre-Operational Testing.

2.5.2.4 Fluid

Data currently unavailable – to be collected during Pre-Operational Testing.

2.5.2.5 Reservoir Engineering Data

Site specific data will be collected as part of the Pre-Operational Testing and Logging Plan (Attachment C). In the meantime, we have conducted a thorough literature review of the available data pertinent to Project Minerva.

This data is separated into three sets. The first set is the generic data sourced from a carbon capture and storage project in a saline system. Second set is the data unrelated to the upper Frio Formation but relevant as analog data. Finally, the third set is data specific to the upper Frio Formation (Injection Zone).

As an example, GCS cites the relative permeability and capillary pressure data. Data from generic studies are utilized such as (Zeidouni, Pooladi-Darvish, & Keith, 2009; Ghanbari, et al., 2006; Juanes, Spiteri, Orr Jr, & Blunt, 2006; Kumar, et al., 2005).

Capillary pressure data from core samples which have been specifically analyzed for CCS purposes has been given by (Krevor, Pini, Zuo, & Benson, 2012). GCS uses the data to sense-check our characterization of CO₂ /brine capillary pressures for the Project Minerva work.

For studies specific to the Frio formation, we have capillary pressure data from (Jung & Wheeler, 2017; Doughty, Freifeld, & Trautz, 2015; Hovorka, et al., 2005). Lastly, the data from GEM simulation model from the Bureau of Economic Geology (Hosseini, 2019). Data for two rock types has been generated. Rock type 2 – Data appeared to be for a sandstone, whereas rock type 1 – Data was for a tighter (potentially shale or mud stone) rock with a lower relative permeability to water and much larger capillary pressures. These had been history matched to measured data from the upper Frio Formation CO₂ CCS pilot project (Hovorka, Tutton, & Trevino, 2018) and therefore have added weight.

Other types of reservoir engineering data include; the formation pore pressure and temperature gradients and initial values at datum depth, salinity, rock compressibility, PVT properties of the in-situ formation fluids and CO₂ (density and viscosity as functions of pressure, temperature, salinity and dissolved CO₂ concentration), rock and fluid thermal properties (conductivities and heat capacities); the temperature, pressure and injection rates of the injected CO₂, assumed well locations, perforated intervals and injection depths, composition of the injected fluids, aquifer properties (depth, length, thickness, permeability, porosity), geo-mechanical data (initial stress state, Biot coefficient, Young's modulus and Poisson's ratio versus depth, cohesion, coefficient of friction and the poro-elastic and thermo-elastic expansion coefficients), and the data to model CO₂ dissolution (equilibrium constant, fugacity coefficient and activity coefficient as functions of pressure, temperature and salinity).



45031 & 45032

All the assembled data was then incorporated into a software tool called “REVEAL” to create what is referred to in all submitted permit documents as the “reservoir simulation model”.

Details of the analysis of this data, with a complete bibliography, and its use in the REVEAL reservoir simulation model, are described in other documents submitted to LDENR as part of the permitting process, such as the Post-Injection Site Care and Site Closure Plan (Attachment F) and Area of Review and Corrective Action Plan (Attachment A) documents.

REVEAL is a reservoir simulation package produced by Petroleum Experts Limited of Edinburgh, UK (Petroleum Experts Limited, 2019)). The versions used for modelling during this project were IPM Version 11, until 1Q 2020, and IPM V12 thereafter. REVEAL is a fully functional compositional, three-phase reservoir simulator, with black-oil functionality if required. GCS uses two phases: a gaseous phase for the injected supercritical CO₂ and an aqueous phase for the in-situ formation fluids.

REVEAL models fluids using the Peng-Robinson equation of state (Peng & Robinson, 1976). Hysteresis in the saturation functions (from drainage to imbibition) may be modelled too. REVEAL has full aqueous phase geochemistry modelling via an interface to PHREEQC, which stands for PH (pH) RE (redox) EQ (equilibrium) C (program written in Q) (Parkhurst & Appelo, 2024).

REVEAL solves a complete energy balance equation. REVEAL has geo-mechanical modelling capability, including fracture modelling, and uses a finite element grid. It has advanced parallel solver options with a 5-point or 9-point template to formulate the finite difference equations for fluid flow. GCS used the 9-point option to minimize grid orientation effects.

REVEAL is fully compatible with other modelling tools produced by Petroleum Experts, such as Prosper (a well modelling tool, (Petroleum Experts Limited, 2019), PVTP (a fluids modelling package, (Petroleum Experts Limited, 2019) and GAP (for injection and production network modelling, (Petroleum Experts Limited, 2019). These are oil industry standard software packages with many years of development and use by oil and gas companies worldwide.

GCS uses REVEAL because it takes the effect of pressure and temperature into account when calculating the density and viscosity of CO₂, and the effects of any contaminants such as methane on these properties of the gaseous phase. These are important factors in determining its distribution under buoyancy-drive and an imposed pressure gradient. It also models the dissolution of CO₂ into the aqueous phase as a function of pressure, temperature and salinity, an important trapping mechanism; and it calculates the effect of gas trapping during imbibition, accounting for hysteresis in the saturation functions. It allows the modeling of geo-mechanical effects to assess, for example, the risk of thermal fracturing as cool CO₂ is injected into a warmer formation.

2.6 SEISMIC HISTORY

2.6.1 Gulf Coast Basin Seismic History

As previously discussed in Section 2.3.1 (Description of Faulting), in the area of Project Minerva, the majority of seismic sources in the Gulf Coast Basin involve faulting. The direction of most faulting is parallel to the edge of the Gulf Coast. The faulting is a result of deposition of large quantities of sand and mud along the margins of the Gulf of Mexico resulting in rapid sedimentation creating large growth fault systems near the downdip edge of each sediment wedge within the area of maximum deposition.

Faulting in the Gulf Coast Basin is predominantly two types: (1) listric normal growth faulting and (2) radial faulting associated with shale or salt piercement structures. Growth faults form contemporaneously with sedimentation so that their throw increases with depth and strata on the downthrown side are thicker than the correlative strata on the upthrown side of the fault. The faults form in clastic sequences that build out into unconfined depositional sites that have prograded to the edge of the continental margin, resulting in contemporaneous failure of the prograding sediments (Jackson & Galloway, 1984). Although growth faults can be common throughout the Gulf Coast Basin regionally, none are present within or immediately surrounding Project Minerva's AoR. The listric faults are locally present but are restricted to the deeper Jurassic and Upper Cretaceous sedimentary intervals significantly below the Injection Zone.

2.6.2 Project Minerva's Seismic History

The Gulf Coast of Louisiana and Texas is historically an area of low seismicity with rare, naturally occurring earthquakes of exceptionally low magnitude (USGS, 2018). Project Minerva is located in an area recognized by the USGS Earthquake Hazards Program having low level of seismic risk in the US (Figure 2.6.2-1).

At Project Minerva, there are no growth faults within the AoR but there are listric faults restricted to the deeper Jurassic and Upper Cretaceous sedimentary intervals significantly below the Injection Zone.

2.6.2.1 Data Sources

All historical seismic events were sourced from the USGS Earthquake Hazards Program Earthquake Catalog, a part of the program's interactive map in which recorded recent and historic seismic events can be searched with custom parameters for the US and worldwide. Other data of historical seismic events along the Gulf Coast of Texas and Louisiana was sourced from publicly available published literature from the USGS.

Utilizing the USGS Earthquake Hazards Program Earthquake Catalog, parameters were set to search and identify closest proximity seismic events to MS CCS 1 and MS CCS 2 bottom-hole locations. These custom parameters include a min magnitude (M_{blg}) of 0.5 to a max of 9, and a start date and time of 00:00:00 UTC on January 1st, 1901, to present day (i.e., May of 2024) (USGS, 2024). The seismic events identified are discussed in detail below.

2.6.2.2 Historical Seismic Events

According to the USGS Earthquake Hazards Program Earthquake Catalog, within a 100-mi radius of MS CCS 1 and MS CCS 2 bottom-hole locations, there is only one recorded earthquake (Figure 2.6.2-2). The earthquake occurred 1 km (0.62 mi) west to northwest of the City of Sulphur in Calcasieu Parish, Louisiana ($30^{\circ} 24' 3''$ N, $093^{\circ} 03' 93''$ W) approximately 5 km (3.1 mi) deep. The earthquake had a Mblg of 3.8 and had a time of 19:40:50 Universal Time Coordinated (UTC) on October 16th, 1983, (USGS, 2024). Notes from (USGS, 2024) state the earthquake impact was felt at Hackberry, Hayes, Sulphur, Westlake, and in the Lake Charles area.

According to the USGS Earthquake Hazards Program Earthquake Catalog, within 115-mi radius of MS CCS 1 and MS CCS 2 bottom-hole locations, and other than the two previously discussed earthquakes, there are three recorded earthquakes in Texas (Figure 2.6.2-2). The third closest proximity earthquake occurred 5 km (3.1 mi) west to northwest of the City of San Augustine, Texas ($31^{\circ} 05' 45''$ N, $094^{\circ} 01' 62''$ W) approximately 5 km (3.1 mi) deep. The earthquake had a Mblg of 2.1 and had a time of 06:40:56 UTC on February 3rd, 2013, (USGS, 2024). Notes from (USGS, 2024) state the impact of the earthquake was felt at Garrison and Timpson, Texas. The next two closest proximity earthquakes occurred 5 km (3.1 mi) west to southwest of the City of Chireno, Texas. The next closest at ($31^{\circ} 28' 22.8''$ N, $094^{\circ} 23' 52.8''$ W) approximately 6.4 km (4.0 mi) deep and the second at ($31^{\circ} 28' 22.8''$ N, $094^{\circ} 24' 14.4''$ W), approximately 7.6 km (4.7 mi) deep. The closest earthquake had a ml of 2.6 and had a time of 02:21:41 UTC on May 4th, 2024, and the second earthquake had a ml of 3.0 and had a time of 22:17:27 on April 2nd, 2024, (USGS, 2024). Table 2.6.2-1 describes the seismic events within the 115-mi radius of MS CCS 1 and MS CCS 2 bottom-hole locations.

At Project Minerva, the likelihood of an earthquake caused by natural forces, fluid injections, and/or oil and gas production is considered exceptionally low. At Project Minerva, injection of carbon dioxide is anticipated to be at comparatively low pressures taking place into deep, high porosity and high permeable formations. These formations are regionally extensive and are not subject to natural earthquakes. Therefore, the probability of an earthquake occurring and causing damage to Project Minerva's injection capabilities is exceptionally low.

2.6.3 Project Minerva's Seismic Risk Analysis

A preliminary seismic risk evaluation was conducted for Project Minerva. As previously discussed in Section 2.6.2.2 (Historical Seismic Events), Project Minerva's Seismic History, Project Minerva is located in an area recognized by the USGS Earthquake Hazards Program having low level of seismic risk in the US. The low-level risk is based on the following:

- Low intensity and frequency of seismic events (i.e., natural earthquakes) in the area of Project Minerva, with maximum ground motion on the surface being less than or

equal to an intensity range of Modified Mercalli Intensity (MMI) = V (i.e., Moderate)² (USGS, 2024),

- Low population density in Cameron Parish, Louisiana, which limits exposures and impacts, with only about 5,617 total population in the area of Project Minerva,
- Lack of injection-induced seismicity in Underground Injection Control (UIC) Class I hazardous and non-hazardous injection wells operating in Tertiary sediments along the Gulf Coast of Texas and Louisiana, and
- Injection pressures are less than those required to induce slip along pre-existing faults.

Additional information according to Federal Emergency Management Agency (FEMA) Earthquake Hazards Maps, the Gulf Coast of Texas and Louisiana is assigned in the lowest seismic design category (SDC) (Figure 2.6.3-1). In the area of Project Minerva, an SDC, or map color, of A/white is assigned indicating there is a very small probability of experiencing damaging earthquake effects if affected (FEMA, 2024).

2.6.3.1 Model Earthquake at Project Minerva

A “model” earthquake is used to evaluate the potential effects, if any, of natural earthquakes on structures associated with the sequestration project. In general, a source mechanism is required when designing a “model” earthquake. In these cases, it is usual to have a “known” active fault system with a measured strain or stress field. In more active regions of the earth, faults with strain (i.e., movement across the fault without rupture) develop at a rate of up to 5 centimeters (cm)/year, or more (Leeds & Associates, 1989). As a meter or more of strain develops, stress accumulates and eventually the system releases this stored strain energy in the form of elastic waves (i.e., an earthquake).

Although the Gulf Coast of Texas and Louisiana contain several geological features capable of storing and releasing stored energy, all are weak or ineffective in terms of generating even modest ground motion (Leeds & Associates, 1989).

Salt structures develop gravimetrically by the flow of lower density salt through weaker zones of the thick Tertiary sediments. The salt is generally so plastic that it tends to flow rather than develop large fractures. The surrounding sediments are badly faulted by the intrusion of salt and are almost as physically incompetent as the salt, also having low densities, poor cementation, and low shear strength with resulting low shear moduli. It is doubtful that the salt dome as a seismogenic source could develop earthquakes with magnitudes greater than 3.0 and intensity MMI>IV (Leeds & Associates, 1989). These events could be felt locally but are unlikely to propagate damaging ground motions. The events might be perceptible, but the level of shaking could not be considered damaging.

² According to Modified Mercalli Intensity Scale (MMI) by the USGS Earthquake Hazards Program, a V (i.e., Moderate) is described as “Felt by nearly everyone; many awakened. Some dishes, windows broken. Unstable objects overturned. Pendulum clocks may stop (USGS, 2024).



45031 & 45032

Growth faults have also developed along the Texas/Louisiana Gulf Coast which may be responsible for seismic activity. Considering the Gulf Coast as a whole, a level of $M_b=4.2$ is considered an upper level for this kind of source in this area (Leeds & Associates, 1989). The several low magnitude events within about 50 miles of the coastline are probably attributable to this mechanism.

The possibility that growth faults may be triggered by faults in the basement is suggested by Stevenson and Agnew (1988) in their discussion of the Lake Charles Earthquake. Details of the event were developed from recordings of Department of Energy (DOE) supported microseismic networks deployed for monitoring geothermal experiments (withdrawal and injection) in southern Louisiana. The interpreted depths $\geq 14+$ km for these events are deeper than have previously been reported and well beneath anticipated injection depths for the sequestration project. Additionally, none of the events were attributable to the geothermal extraction/reinjection operations (Stevenson (pers comm.), in (Leeds & Associates, 1989).

Design Earthquake for Seismic Risk Analysis

In the evaluation of the potential effect of seismicity on a Class I Injection Well Facility located near the western margins of Project Minerva, (Leeds & Associates, 1989) used a modeled seismic event with a body-wave magnitude, M_b of 4.2 ± 0.2 as a conservative working model for the design earthquake and presumed that the source area for the event would be along one of the nearby coast parallel growth faults.

The maximum ground motion on the surface generated by the design earthquake would be within the intensity range of $MMI=V$. This intensity equates to a horizontal surface acceleration of 0.05 grams (g) (Leeds & Associates, 1989). This is the same value used as an "Operating Basis Earthquake" (OBE) for Gulf Coast nuclear power plant electric generating stations. The Nuclear Regulatory Commission (NRC) estimates the risk each year of an earthquake intense enough to cause core damage to the reactor at River Bend (north of Baton Rouge) was 1 in 40,000, according to an NRC study published in August 2010 (Hiland, 2010). The empirical correlation between intensity and acceleration has a wide spread of data, with recordings varying from horizontal accelerations of 0.025 g to 0.15 g for intensity $MMI=V$ event.

The design earthquake for seismic risk analysis at Project Minerva is based on the empirical data of normal shallow focus (<12 miles) earthquakes on soft sites (Leeds & Associates, 1989). (Leeds & Associates, 1989) assumes that in the Gulf coastal seismic environment, the release of energy from less competent materials than usual, would result in longer surface rise times; therefore, the ground motion would be biased to longer periods with lower frequencies and result in low accelerations, large displacements, and long durations.

Studies over the years of the effect of depth on seismic ground motion have all noted the attenuation that is realized with depth. Observations in deep mines and boreholes have confirmed this phenomenon. The data strongly indicates dampening of amplitude with depth and are an average of one-half, or less, of the ground motion. The motion may be as

low as one-fifth and for small motions, where the materials remain completely elastic, the diminution of amplitude may be as small as one-tenth (Leeds & Associates, 1989).

The effect of ground motion on saturated granular soils is the buildup in pore water pressure. If the water table is located near the surface (within about 15 ft to 20 ft), if the sands are reasonably well sorted and clean (free of clay), and if ground accelerations exceed about 0.25 g, a type of soil failure known as liquefaction can occur (Leeds & Associates, 1989). Liquefaction causes a loss of shear strength of the soil and may result in ejection of sand and water to the surface (sand boils), and collapse of the foundations of structures supported by soils. In extreme cases, multistory buildings have rolled over (Niigata, Japan Earthquake in 1964) and buried tanks have “floated” to the surface (Leeds & Associates, 1989). Following liquefaction, there is settlement and ensuing densification of the soil. Project Minerva does not meet the conditions expected to trigger liquefaction since the acceleration levels (0.05g) are only about one-fifth that required (Leeds & Associates, 1989).

As depth increases there is attenuation and reduction of motion. While pore pressures could increase, the soils framework is not used as support the lithostatic sediment column. Additionally, within the short duration of shaking, there is insufficient time or place for the fluid to go to. Thus, it remains incompressible. (Leeds & Associates, 1989) concludes that possible interactions between sedimentary horizons due to casings penetration and cement are minimal since there are only minor differential movements as the seismic wave passes through the matrix. They conclude that there might be only several centimeters of displacement over the wavelength of the seismic waves and that the normal elasticity of well casing and tubing is sufficient to accommodate the strain (Leeds & Associates, 1989). It is only in extreme cases, such as in Kern County, California, where surface accelerations can reach 0.5 g and there are many miles of surface rupture, that existing wells may be affected. The 1952 event, approximately 2% of the wells in the area had some surface damage due to settlement of surficial soils (Leeds & Associates, 1989). This event caused some subsurface damage including collapsed tubing near the surface due to the sharp rise in causing pressure accompanied the shock. However, all wells returned to normal status within 2-to-3 weeks of the event (Leeds & Associates, 1989).

2.6.4 Induced Seismicity

Seismicity related to fluid injections normally results from activity involving high pressures and large volumes, such as those associated with high-pressure water flood projects for enhanced oil recovery. The seismicity caused by increased pore pressure, which reduces frictional resistance, allows the rock to fail. Fluid withdrawals has caused land subsidence and earthquakes due to dewatering and differential compaction of the sediments. Earthquakes of a magnitude, ml of 3.4 to 4.3 on the Richter scale appear to have been caused by fluid withdrawal near some oil fields in east Texas (Davis, Pennington, & Carlson, 1989).

Since 2010, the occurrence of earthquakes with a magnitude, ml of ≥ 3.0 have increased from 20 events/year (from 1967-2000) to ≥ 100 events/year (2010-2013) in the central and eastern US regions (Ellsworth, 2013). The increased rate of occurrence in previously inactive seismic

areas has been correlated with the increased use of injection wells located near faults. Fluid injections induced by earthquakes are mostly caused by the increased pore pressure from injection operations which have reduced effective stress of faults leading to failure. This mechanism has been used to explain the best-known cases of injection-induced seismicity which was first studied in the Rocky Mountain Arsenal near Denver, Colorado. New case studies have increased the use of wastewater injection wells associated with hydraulic fracking. In many sites, smaller seismic occurrences have been shown to be precursors to larger events. More data has become available since the Rocky Mountain study in the 1960's, leading to a better understanding of factors and processes associated with induced-seismicity.

One of the most notable regional cases of induced seismicity associated with injection wells occurred in Youngstown, Ohio. In 2011, a total of 12 low-magnitude seismic events occurred along a previously unknown fault line (ODNR, 2012). These events occurred less than a mile from Class II injection well, Northstar I. Previously, the area was seismically inactive, with earthquakes beginning a few months after the injection of wastewater. The injectable pressure at Northstar I increased twice over 6 months (ODNR, 2012) and may have reduced the effective stress on a fault. After the well was shut down by the ODNR, the seismic activity declined. As a result of this case, seismic monitoring prior to injection and after injection has become common in Class II sites.

A case study in the Dallas-Fort Worth area tied small seismic events to a Class II injection well. There are 11 hypocenters in which have been observed at a focal depth of 4.4 km and 0.5 km from a deep saltwater disposal (SWD) well (Frohlich, Potter, Hayward, & Stump, 2010). Injection at this well began 8 weeks prior to the first recorded seismic event. A northeast trending fault is located approximately at the same location as the DFW focus (Frohlich, Potter, Hayward, & Stump, 2010). As a result of fluid injection into the disposal well, the stress upon the fault had been reduced and thus reactivated the fault (Frohlich, Potter, Hayward, & Stump, 2010). All the seismic events associated with the DFW focus are small magnitude events (less than 3.3) and occur very shortly after initial injection.

In Oklahoma, one of the largest earthquakes in the state's history may have been a result of wastewater injection at a Class II disposal site. In 2011, Prague, Oklahoma was the location of a 5.7 magnitude earthquake that was followed by thousands of smaller aftershocks. Wastewater had been pumped continuously into an old oil well for 17 years. As the pore spaces filled, the wellhead pressure increased to continually inject the wastewater. This reduced the effective stress upon the Wilzetta fault located 650 meters from the well (Keranen et al., 2013). The fluid was injected into the same sedimentary strata at which 83% of the aftershocks originated (Keranen et al., 2013). In this case, the seismic event occurred years after the initial injection phase. Since the area was considered low risk seismically, there is no data on smaller earthquakes that may have proceeded with the event in 2011.

In north-central Arkansas, multiple earthquakes have been triggered because of a Class II injection well. Since the operation of the disposal well in 2009, the site has experienced an increase from two events in 2008 to 157 events in 2011 (Horton, 2012). It was also tied to the discovery of a new vertical fault. 98% of earthquakes within this area occurred within 6 km

of one of three waste disposal sites (Horton, 2012). The depth of the earthquake foci occurred between 6.7 and 7.6 km. Injection of fluid occurred at a depth of 2.6 km. At this disposal site, E-W trending (Enders Fault) cut into the aquifer in which the fluid was injected and then acted as a conduit to the new fault at the depth of 6.7 to 7.6 km (Horton, 2012). The disposal wells were shut down in 2011 by the Arkansas Oil and Gas Commission. The rate and size of the earthquakes steadily decreased following the shutdown of the wells (Horton, 2012).

In Texas there are at least two known examples of previously seismically inactive areas becoming seismically active after major injection programs began. One site is located in the Central Basin Platform, near Kermit, and the other is in the Midland Basin near Snyder. In both cases, large scale, high pressure, oil field related, water flooding projects were under way, and earthquakes with a magnitude of over 4.0 on the Richter

2.7 HYDROLOGIC AND HYDROGEOLOGIC INFORMATION

2.7.1 Data Sources

All hydrologic and hydrogeologic data was sourced from the LDENR, Strategic Online Natural Resources Information System (SONRIS), TWDB Submitted Drillers Reports Database (SDRD), and publicly available published literature from the TWDB and USGS.

The SONRIS database was used to source all water well data for the state of Louisiana and the TWBD SDRD was used to source all water well data for the state of Texas. Well log data was used to construct maps using the well locations and depths as control points and calculate formation fluid salinity by determining the resistivity of the formation fluid (R_w). See Section 2.7.2.1 (Determination of the Base of the Lowermost USDW) for a detailed discussion. All publicly available published literature was sourced for published cross-sectional maps, isopach and structural maps, graphs and charts regarding thickness and depth, and/or research regarding characteristics and properties of hydrogeologic units.

2.7.1.1 Water Wells and Data Sets

Water well data was sourced from the LDENR SONRIS database. The SONRIS database includes the best available sources of well data for the state of Louisiana. Water well data is current through August 2024.

All water wells were searched and identified within Project Minerva's AoR and are represented on Figure 2.7.1-1. Table 2.7.1-1 includes data for water wells within the AoR as well as water wells within a conservative 2-mile radius from Project Minerva's AoR.

Within the AoR, there is only one water well (58911Z) (Figure 2.7.1-1 and Table 2.7.1-1). Water well 58911Z is an active well completed at 400 ft below ground level and withdraws from the Chicot aquifer, with the "200-foot sand" as the main water supply. Water is not withdrawn from the deeper Evangeline aquifer for public use within Project Minerva's AoR.

2.7.2 USDW within the AoR

The base of the lowermost USDW is identified across Project Minerva based upon 91 publicly available well log data. Figure 2.7.2-1 shows the locations of well log data used to determine the lowermost USDW and the structural interpretation of the base of the USDW at Project Minerva. Figure 2.7.2-2 and Figure 2.7.2-3 show the lateral extent of the lowermost USDW across Project Minerva's AoR.

The nearest well to MS CCS 1 and MS CCS 2 that logs the base of the lowermost USDW is Watkins Well No. 80 (Map ID 5, SN 46471) (Figure 2.7.2-1). Based on SONRIS, the base of the USDW was identified on the log at approximately -1,020 ft KB, however the base of the sand unit that contains the USDW is interpreted at approximately -1,090 ft KB (Figure 2.7.2-3).

The lowermost USDW is consistent with the base of the “700-foot sand” in the Chicot Aquifer at Project Minerva. The base of the lowermost USDW does not follow the stratigraphic formations and the units above the lowermost USDW are hydraulically connected. Therefore, the lowermost USDW varies from the upper portion of the Evangeline aquifer into the base of the “700-foot sand” of the Chicot aquifer based upon the conservative 2-ohm resistivity cutoff.

The position and depth of the lowermost USDW is influenced by the proximity of well log data to the adjacent Black Bayou Dome. Near the Black Bayou Dome, the lowermost USDW deepens slightly from approximately -1,000 ft to approximately -1,250 ft MSL. The lowermost USDW is located approximately at the base of the Chicot aquifer’s 700-Foot Sand (Figure 2.1.2-5, Figure 2.1.2-6, and Figure 2.1.2-7). However, the sands of the aquifers are mostly saline groundwater at Project Minerva and are not usable groundwater sources in Cameron Parish, Louisiana.

The top of salt at Black Bayou Dome is deep, and saline influence from the salt dome on the overlying aquifers is prevented due to a thick caprock covering the dome. However, as the strata dips towards the Louisiana Gulf Coast, evidence of saltwater encroachment into the deeper aquifers, such as the Evangeline aquifer and Jasper aquifer exist in the southernmost portion of Calcasieu Parish and in Cameron Parish, Louisiana due to pumping operations. The Chicot Aquifer though less impacted by the increase in groundwater withdrawals and saltwater encroachment.

2.7.2.1 Determination of the Base of the Lowermost USDW

The most accurate method for determining formation fluid properties is through the analysis of formation fluid samples. In the absence of formation fluid sample analyses, GCS has sourced data from well logs to calculate formation fluid salinity by determining the resistivity of the formation fluid (R_w) by converting the resistivity value into a salinity value.

The two primary methods to derive resistivity of the formation fluid (R_w) from well log data are: (1) the “Spontaneous Potential (SP) Method” and (2) the “Resistivity Method.” The “SP Method” derives resistivity of the formation fluid (R_w) from the resistivity of the mud filtrate, and the magnitude of the deflection of the SP response of the formation. The “Resistivity

Method" determines resistivity of the formation fluid (R_w) from the resistivity of the formation (R_i) and the formation resistivity factor (F), which is related to formation porosity and a cementation factor (Schlumberger, 1989).

Spontaneous Potential (SP) Method

The SP curve on a well log records the electrical potential (voltage) produced by the interaction of the connate formation water, conductive drilling fluid, and certain ion selective rocks (shales). The SP curve usually defines a straight line (called the shale baseline), while opposite permeable formations (i.e., sands or limestones), the SP curve shows excursions (deflections or not a straight line) away from the shale baseline. The deflection may be to the left (negative) or to the right (positive), depending primarily on the relative salinities of the formation water and the drilling mud filtration. A negative deflection occurs when formation salinities are greater than the drilling mud filtrate salinity. A positive deflection occurs when the formation salinities are less than the drilling mud filtrate salinity. When formation salinities and the drilling mud filtrate are similar, no SP deflection opposite a permeable formation will contrast (Schlumberger, 1989).

The deflection of the SP curve away from the shale baseline in a relatively "clean sand" is related to the equivalent resistivities of the formation water (r_{we}) and the drilling mud filtrate (r_{mf}) by the following formula:

$$SP = -K \log \left(\frac{r_{mf}}{r_{we}} \right) \quad \text{Equation 2.7-1}$$

For NaCl solutions, $K = 71$ at 77°F and varies in direct proportion to temperature by the following relationship:

$$K = 61 + 0.133T^{\circ} \quad \text{Equation 2.7-2}$$

In the equations above, by knowing the formation temperature, the resistivity of the mud filtration, and the SP deflection away from the shale baseline, the resistivity of the formation water can be determined (Figure 2.7.2-4). From the formation water resistivity and the formation temperature, the salinity of the formation water can be (Figure 2.7.2-5).

Resistivity Method

The "Resistivity Method" determines formation fluid resistivity from resistivity of the formation (R_i) and the formation resistivity factor (F). The resistivity of a formation (R_t in ohmmeters) is a function of: (1) resistivity of the formation fluid (R_w), (2) the amount and type of fluid present, and (3) the pore structure geometry. The rock matrix can have zero conductivity (infinitely high resistivity) except for some clay minerals, and therefore is not a

factor in the resistivity log response. Induction well logs determine resistivity (R_t) by inducing electrical current into the formation and measuring conductivity, a reciprocal of resistivity. The induction logging device investigates deep into a formation and is focused to minimize the influences of borehole effects, surrounding formations, and invaded zone. Therefore, the induction well log measures the true resistivity of the formation (Schlumberger, 1989). The conductivity measured on the induction well log is the most accurate resistivity measurement for the “Resistivity Method” under 2 ohmmeters.

Electrical conduction in sedimentary rocks almost always results from the transport of ions in the pore-filled formation water and is affected by the amount and type of fluid present and pore structure geometry. In general, high-porosity sediments with open, well-connected pores have lower resistivity, and low-porosity sediments with sinuous and constricted pore systems having higher resistivity (Schlumberger, 1989). (Schlumberger, 1989) established experimentally that the resistivity of a clean, water-bearing formation (i.e., one containing no appreciable clay or hydrocarbons) is proportional to the resistivity of the saline formation water. The constant proportionality for this relationship is called the formation resistivity factor (F), where:

$$F = \frac{R_t}{R_w} \quad \text{Equation 2.7-3}$$

The formation resistivity factor (F) remains nearly constant for all values of R_w below 1.0 ohmmeter. For fresh, more resistive waters, the value of F may decrease as R_w increases. (Schlumberger, 1989) suggests given formation water, the greater the porosity of a formation, the lower the resistivity of the formation (R_t) and the lower the formation factor. Therefore, the formation factor is inversely related to the formation porosity. (Archie, 1942) proposed the relationship (commonly known as Archie’s Law) between the formation factor and porosity based on experimental data:

$$F = \frac{\alpha}{\phi^m} \quad \text{Equation 2.7-4}$$

where:

ϕ = porosity

α = a pore-geometry factor or empirical constant

m = a cementation factor or exponent

The value α is a pore-geometry factor (i.e., tortuosity factor) in which researchers gave or used various values for different lithologies (Salem & Chilingarian, 1999). The value m is the cementation factor (i.e., shape factor) in which is not a constant value but is a variable depending on many physical parameters and lithological attributes of porous media (Salem & Chilingarian, 1999). Table 2.7.2-1 shows Archie’s formula for different lithologies. In sandstones, the cementation factor is assumed to be a value of two but can vary from a value of 1.2 to 2.2. In shallower sandstones, as sorting, cementation, and compaction decrease, the cementation factor can also decrease (Stolper, 1994). On the Gulf Coast, research found that low mud resistivities are not common. The effects of mud resistivity are generally of little

importance, except when dealing with high formational resistivities or extremely low mud resistivities. With the present advanced knowledge of mud control, invasion of mud filtrate into sands can be minimized, thereby increasing the dependability of the electrical well log (Archie, 1942).

Archie's Law assumes:

$$\alpha = 0.81$$

$$m = 2$$

where:

The value α is a proportionality constant varying from 0.6 to 1.5, and the value m is a cementation factor that varies between 1.3 and 3:

$$F = \frac{0.81}{\phi^2}$$

Combining the equations for the Humble relationship and the definition of the formation factor, the resistivity of the formation water (R_{we}) is related to the formation resistivity (R_t) by the following:

$$R_t = \frac{R_{we} \times 0.81}{\phi^2} \quad \text{Equation 2.7-5}$$

2.7.2.2 Methodology Used in the Evaluation of Project Minerva

To determine the resistivities of the formation water (R_{we}) in a particular zone, the drilling mud filtrate (R_{mf}), in which is obtained from the log header at the depth of a particular zone must first be determined. Resistivities of saline solutions vary as a function of NaCl concentration and temperature. The relationship between temperature, NaCl concentration, and resistivity are typically shown in the form of a nomograph for computational ease (Figure 2.7.2-5). As seen on Figure 2.7.2-5, the resistivity of the drilling mud filtrate (R_{mf}) can be corrected to the temperature of the zone of interest. Next, a shale baseline is established on the SP curve. A chart containing the graphic solution of the SP equation can be seen on Figure 2.7.2-4. The SP equation provides the solution $(R_{mf})/(R_w)$ for the ratio between the resistivity of the drilling mud filtrate (R_{mf}) and resistivity of the formation fluid (R_w). The resistivity of the formation fluid (R_w) at formation temperature can be determined from the $(R_{mf})/(R_w)$ ratio and converted to the equivalent NaCl concentration from Figure 2.7.2-5. Lastly, the base of the lowermost USDW is established by identifying the formation resistivity (R_t) cut-off on the deep induction log using Equation 2.7-5.

Figure 2.7.2-4 and Figure 2.7.2-5 show resistivity of the formation fluid (R_w) of 0.35 ohm-m corresponds to a salinity of 10,000 mg/l TDS. At a temperature of approximately 90°F, a resistivity of the formation fluid (R_w) of 0.45 ohm-m corresponds to a salinity of 10,000 mg/l TDS. Deeper intervals with higher temperatures will have a higher resistivity cut-off for analysis.

Using the value from resistivity of the formation fluid (R_w) and an estimate of formation porosity, a formation resistivity (R_t) cut-off can be calculated. For the Project Minerva site, the lowermost USDW is projected to be relatively shallow, thus a resistivity of the formation fluid (R_w) of 0.35 ohm-m is used. Using an assumed formation porosity of 34% (shallow unconsolidated sands) and solving for the total formation resistivity, gives the following result:

$$R_t = \frac{R_w \times 0.81}{\phi^2}$$

$$R_t = \frac{0.35 \text{ ohm-m} \times 0.81}{0.34^2}$$

$$R_t = 0.35 \text{ ohm-m}$$

Therefore, it is conservatively calculated that the sands with a formation resistivity of greater than 2.0 ohm-m were considerably USDWs. The site-specific calculation agrees with the LDENR guidance, which indicates that the USDW should fall between:

- ground surface to -1,000 ft: 3.0 ohms or greater is considered USDW,
- -1,000 ft to -2,000 ft: 2.5 ohms or greater is considered USDW, and/or
- -2,000 ft and deeper: 2.0 ohms or greater is considered USDW.

To be conservative in the current analysis, the base of the lowermost USDW across the evaluated well logs was placed at the base of the deepest sand with a deep resistivity greater than 2.0 ohms. Additionally, for continuous sand beds with higher resistivities at the top, the USDW was placed at the bottom of the next deepest sand. At Project Minerva, the USDW is identified at a depth range of approximately -1110 ft to -1,200 ft KB, based on the 2.0 ohm-m cut-off.

2.8 GEOCHEMISTRY

Per the Pre-Operational Logging and Testing Plan (Attachment C), GCS will collect cores samples from the Upper Confining Zone and Injection Zone during the drilling of MS CCS 1 and MS CCS 2, as well as native fluid from the Injection Zone.

2.8.1 Sources of Data

No site characterization or formation testing has been completed at this time. However, GCS has performed an extensive literature review, leveraged offset well data and commissioned a third-party geochemical modeling study. By integrating this information, GCS has gained comprehensive understanding of the chemical interactions between CO₂-saturated brine and the Injection Zone.

2.8.1.1 Literature

Mineral composition of the Injection Zone and the Upper Confining Zone is defined by a regional petrographic study (Loucks et al., 1977) and scanning electron microscopy with

energy-dispersive X-ray fluorescence scanning (SEM-EDS) of 75 cuttings samples from well (E W Brown Jr #1, Serial Number 130259; API 17019202320000) in the Project Minerva area.

Analogous Injection Zone sandstones in the area are quartz arenites to quartzose subarkoses, with minor (predominantly metamorphic) rock fragments (Loucks et al., 1977). Sandstone samples are dominated by quartz grains. Other sandstone minerals that could potentially react with dissolved CO₂ include (in order of abundance): calcite, dolomite, Na-feldspar (albite-oligoclase), K-feldspar and biotite. All of these appear as detrital grains in cuttings; the carbonates are likely bioclastic (shell) fragments, and possibly some early diagenetic cements. Proportions of carbonate grains in sandstones are estimated to be less than 5%. Feldspars appear as occasional detrital grains. Biotite is present in very small proportions (< 1%). In addition to the detrital grains, very small proportions of illite may be present as coatings on quartz grains.

Among the sandstone minerals, carbonates are likely to be most reactive with CO₂ (Vafaie et al., 2023; Bickle et al., 2017; Raistrick et al., 2009). The dissolution rate of silicates (quartz clay and feldspars) is up to nine orders of magnitude slower than calcite (Vafaie et al., 2023). CO₂ reactions with K-feldspars can be important in some cases, buffering reaction with carbonates (Raistrick et al., 2009). Biotite is relatively reactive with CO₂ (but present in very small quantities in the Injection Zone), whereas Na-feldspars and illite exhibit low reactivity (e.g., Bickle et al., 2017). Reaction of CO₂ with carbonates, feldspars and biotite could result in local dissolution and precipitation of new minerals, including carbonates, kaolinite, albite or dawsonite (Vafaie et al., 2023; Bickle et al., 2017). Dissolution is expected to affect isolated detrital grains (mostly carbonates), or possibly local diagenetic cements. Reactions may locally increase or reduce porosity and permeability (Vafaie et al., 2023); this is expected to affect small reservoir volumes, reflecting the relatively small proportion of reactive mineral grains, buffering of aqueous CO₂ concentrations and limited contact of dissolved CO₂ with reservoir rocks.

Shales in the Injection Zone and Upper Confining Zone are dominated by illite and quartz, with lesser amounts of smectite or illite/smectite mixed-layer clays, and minor proportions of kaolinite. Calcite and dolomite are present as separate fragments in cuttings, likely representing bioclastic fragments as well as diagenetic cements (possibly concretions). Minor amounts of pyrite are also present. The dominant minerals (illite and quartz) exhibit low reactivity with CO₂; the more reactive minerals (carbonates and smectite (Bickle et al., 2017)) are present in much smaller proportions. CO₂ reactions in shales may involve mineral dissolution (especially carbonates) and/or precipitation (Vafaie et al., 2023; Skurtveit et al., 2019), which may increase or decrease capillary entry pressure and permeability (Hou et al., 2022; Sorai, 2017). Several laboratory experiments show little reaction (e.g., Ilgen et al., 2018; Dewhurst et al., 2020).

CO₂ reactions in shales are generally limited by high capillary entry pressure and very low permeability. Among natural analogues, CO₂ intrusion into cap rocks is 50 ft or less (e.g., Lu et al., 2009; Kiraly et al., 2017; Liu et al., 2012; Watson et al., 2005). CO₂ is thus unlikely to significantly penetrate the much greater thickness of the Upper Confining Zone (>900 ft gross thickness at Project Minerva site).

Injection may cause near-wellbore precipitation from highly saline pore waters near injection wells, due to water vaporization into the CO₂ (Miri & Hellevang, 2016). This is characteristic of very saline formation fluid. The moderate salinity of Injection Zone formation fluid (predicted to be 115,000 ppm TDS) indicates that this is unlikely to occur at the Project Minerva site. In any event, minor salt precipitation can be easily remediated. Similarly, the low concentrations of solutes in Injection Zone pore waters indicates the likelihood of precipitation of new minerals due to reaction with injected CO₂ is very low.

In conclusion, CO₂ injection streams conforming to the proposed specification are compatible with the mineralogy and pore waters of the Injection Zone and the Upper Confining Zone. Although small-scale, localized mineral reactions may occur, they are highly unlikely to materially affect CO₂ injection operations or CO₂ storage integrity.

2.8.1.2 Offset Injection Zone Data

GCS analyzed analogous data from an offset well located nine miles away from Project Minerva, (CECOS, WDW No. 004, Serial Number 975888; API 17019882140000). The offset data obtained provided valuable insights into the composition of the local subsurface fluid and rock.

Below is a list of data obtained and specifics can be referenced in Appendix VII-1 (CECOS, WDW No. 004 Completion Report).

- Upper Frio Formation (Injection Zone) Fluid Laboratory Analysis
- Conventional Core Plug Analysis
- Conventional Core Particle Size Analysis
- Conventional Core X-Ray Diffraction
- Advanced Core Analysis Study (Upper Confining Zone Sample)

An understanding of the Injection Zone water chemistry is essential to anticipating how the injected CO₂ will interact with the formation fluid and move through the reservoir. The core analysis covered both the Upper Confining Zone and the Injection Zone, this data enhanced GCS's understanding of various key reservoir characteristics, such as porosity, permeability, mineral composition, and formation lithology. Accurate water chemistry and formation characterization data is essential for calibrating geochemical models.

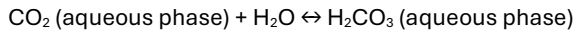
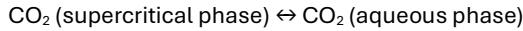
2.8.2 Geochemical Modeling

Geochemical modeling is crucial for predicting how CO₂ will behave after it has been injected into subsurface formations. The interactions between CO₂, brine and the rock matrix can trigger various chemical reactions that may alter the porosity and permeability of the storage sites (i.e. rock formations), which could impact their capacity and safety.

2.8.2.1 GCS Geochemical Review

Geochemical modeling was confined to the dissolution of CO₂ into the formation fluids.

The principal chemical reaction we wish to model in REVEAL was the dissolution of CO₂ into the formation brine and its dissociation into H⁺ and CO₃²⁻.



Only a small fraction of the dissolved CO₂ exists as the acid H₂CO₃, the equilibrium constant being equal to 1.3 E⁻³ typically. The time scale to form H₂CO₃ is of the order of seconds. Other possible geochemical reactions are not considered in the current study.

To specify this reaction, we defined the following species in the REVEAL /PHREEQC model:

- CO₂ (supercritical phase) – injected CO₂
- CO₂ water (CO₂ in the aqueous phase)
- H⁺ (protons)
- e⁻ (electrons, to balance the electrical charge of the protons)
- CO₃²⁻ (the corresponding anions to the protons)

To initialize the composition of the aqueous phase the aqueous species were set at the following concentrations:

- CO₂water (CO₂ in the aqueous phase) – this is calculated by PHREEQC
- H⁺ (protons) at pH = 6.7, (Kharaka et al., 2006)
- e⁻ (electrons) -9.6432 pe (default REVEAL value)
- CO₃²⁻ at 100 ppm (Kharaka et al., 2006)

In REVEAL the unit of 1 ppm is equivalent to 1 mg of solute per kg of solvent. The unit pe for electron concentration or activity is analogous to pH (pe = -log [e⁻]). A value of 100 ppm was assumed for the initial concentration of CO₃²⁻.

No uncertainty ranges were set. Measured values from formation water samples would allow the setting of the uncertainty ranges for the initial concentrations of the active species in the aqueous phase.

REVEAL uses PHREEQC (USGS, 2021) as its geochemical modeling engine. REVEAL provides input to PHREEQC and outputs the results. Two versions of PHREEQC are available: version 2.4.2 (the default) and version 3.1.5. The analysis for Project Goose Lake utilizes version 2.4.2 of PHREEQC.

The dissolution model is partitioned between the two codes as illustrated in Figure 2.8.2-1.

The following description of method for modeling CO₂ dissolution in brines is taken from (Gundogan, 2011).

The CO₂ solubility model is:

$$K\Phi PCO_2 = \gamma mCO_2 \quad \text{Equation 2.8-1}$$

where K is the equilibrium constant for the equilibrium reaction between CO₂ in the gas and aqueous phases, Φ is the fugacity coefficient of CO₂ in the gas phase, PCO₂ is the partial pressure of CO₂ (gas phase), γ is the activity coefficient and mCO₂ is the molality of CO₂ in the aqueous phase.

In essence, this says that the ratio of the effective mole fraction of CO₂ in the aqueous phase to the effective partial pressure of CO₂ in the supercritical phase is equal to the equilibrium coefficient, K.

(Diamond & Akinfiev, 2003) published CO₂ solubility data (mol% of CO₂ dissolved in pure water (i.e., with zero salinity) from 25 published data sources. They assembled a set of 362 measurements which satisfied their criteria for good quality data. The temperature range investigated was -1.5 to 100 °C and the pressure range was 0.1 to 100 Mpa.

Figure 2.8.2-2 is a visual comparison of CO₂ solubility data from (Diamond & Akinfiev, 2003) and REVEAL-zero salinity data. (Diamond & Akinfiev, 2003) shows a P-T diagram in which selected solubility contours of XCO₂ (aq) (concentration of dissolved CO₂ in mol%) from the measured data were plotted (a transparent plot with the same axes of the equivalent data calculated in REVEAL has been overlain on the original chart). The REVEAL data lies on a P, T grid with the solubility data (mol% dissolved CO₂) appearing in the label attached to each point. The agreement between the REVEAL data and the contours plotted in (Diamond & Akinfiev, 2003) is exceptional. The REVEAL data extends beyond the range of temperature reported by (Diamond & Akinfiev, 2003).

The brine density is also corrected for the effect of the dissolved CO₂ as,

$$\frac{1}{pw(+ \text{ dissolved CO}_2)} = \left[\left(\frac{CCO_2}{78} \right) + \left(\frac{(1-CCO_2)}{pw} \right) \right] \quad \text{Equation 2.8-2}$$

Here, pw is the density of the brine without dissolved CO₂, pw (+ dissolved CO₂) is the density of the brine with dissolved CO₂, CCO₂ is the concentration of dissolved CO₂ (kg CO₂/kg solvent – molality) and 78 is the effective saturated CO₂ density, in units of lb/ft³, (REVEAL manual p.124, Petroleum Experts).

2.8.2.2 Macro-Scale Simulation

GCS engaged Core Lab, in conjunction with University of Houston, to complete an independent geochemical review, through macro-scale modeling of CO₂/CO₂ saturated brine. The study objective was to develop an integrated model that quantifies the impact of rock mineral dissolution and precipitation during the convective and dispersive reactive flow of CO₂ saturated brines.

To create an accurate geochemical model, inputs must be sourced from accurate representations of the local reservoir rock properties. For this reason, the Injection Zone offset data was used as the foundational input. Model inputs included: water chemistry,

formation mineralogy, injection fluid composition, formation water salinity, and injection operations conditions (i.e. depths, pressure, injection rates, temperature, etc.). Tables 1-3 and Figure 1 from Appendix VII-2 (GCS Phase 1 Geochemical Modeling Report) outline the details of the geochemical model inputs.

The study was divided into two phases.

- CO₂ Injection Modeling: CO₂ Solubility in Brine
- Modeling CO₂ Injection: Reactive Flow with Mineralization/Dissolution

PHREEQC software was used to simulate the geochemical reactions in aqueous media. This software was coupled with continuity equations to dynamically update the model to reflect real-time changes in chemical and physical properties of the reservoir. As CO₂ is injected, the set of continuity equations tracks the flow and distribution of CO₂ and brine within the porous media (reservoir). Simultaneously, PHREEQC calculates the geochemical reactions occurring at each time step, providing updated saturation indices for various minerals. This coupled geochemical reactive workflow can be seen in Figure 4 of Appendix VII-2.

The results of the geochemical reactive modeling can be seen in Figures 7- 16 of Appendix VII-2. The Injection Zone does not show any potential for mineralization during the CO₂-saturated brine injection at reservoir conditions. No significant dissolution or precipitation was observed for the calcite, quartz and dolomite tested, meaning the porosity and permeability will not be impacted. Due to the high injection rate and similarity between the formation brine and injective fluid composition, there is a minimal impact from the chemical reactions that occur. The results of this study validate GCS' REVEAL modeling and ensure the integrity of the storage site based on the operations conditions tested.

2.9 OTHER INFORMATION

2.9.1 Magnetometer Survey

To perform due diligence on Project Minerva, GCS will hire a third-party vendor to conduct an extensive search to identify any potential undocumented artificial penetrations. The main objective is to locate potential leak points that could provide pathways for fluids to vertically migrate outside of the proposed Injection Zone. The search will cover an area of interest that encompasses approximately 10,400 acres and will incorporate drone-based aerial surveys to efficiently and non-invasively cover the large area. The figure on page 3 of Appendix VIII-1 demonstrates the search area, which includes the Project area of review and an additional 80 acres. While the AOR does not include any APs, GCS has extended the survey acreage in order to include the two known APs nearby.

One drone will conduct a magnetometer survey, with flight lines spaced at 50m with 500m spaced tie lines. During flight, the magnetometer will continuously record the magnetic field at 10 Hz intervals. A base station magnetometer will also be deployed to account for background magnetic variability. A second drone will capture RGB Imagery, which provides a 5 cm resolution image. GCS is including this add-on imagery map to rule out obvious cultural features, such as metallic infrastructures or hurricane debris. Once collection is

complete, all aerial data will be processed to remove noise and correct for any diurnal variations and maneuver errors. A magnetic interpretation expert will review the Total Magnetic Intensity data and RGB image together to map and identify any magnetic anomalies. The combination of these two data types will provide location accuracy of 5-30m. If any magnetic anomaly cannot be confidently identified by the interpretation expert, then ground truthing efforts will be deployed.

This project is scheduled to start September 25, 2024. The final interpretation report and all relevant deliverables will be added as Appendix VIII-2.

2.10 SITE SUITABILITY

2.10.1 Lithological Distribution

The intervals of interest at Project Minerva are the Oligocene and Miocene deposits of the Gulf Coastal Plain. The Oligocene and Miocene deposits are characterized by rapid subsidence in areas of high sediment loading through multiple cyclic depositional episodes. The Oligocene and Miocene deposits are subdivided according to depositional cycles and paleontological zones (Foote, 1984; Swanson, Karlsen, & J, 2013). Figure 2.1.1-5 represents the depositional cycles of the subdivisions listed below, in ascending order:

- Vicksburg Group (early Oligocene). Represents a transgressive phase (mainly shale and some sandstone lenses),
- Frio Formation (middle Oligocene). Represents a dominantly regressive phase. (Mixture of marginal marine and deltaic sandstones and shales, with localized deep marine shales and turbidite sandstones) Downdip equivalent of the continental Catahoula Formation (Swanson, Karlsen, & J, 2013). The upper Frio Formation is the Injection Zone and the middle Frio Formation is the Lower Confining Zone at Project Minerva,
- Anahuac Formation (late Oligocene). Represents transgression (marine shales and thin sandstones). This formation is the Upper Confining Zone at Project Minerva, and
- Fleming Formation (Miocene). Represents a very high number of alternating regressive and transgressive phases (progradational sandstones and retrogradational shales). This formation is additional secondary confinement to the Confining Zone.

The Secondary Confining Zone, Upper Confining Zones, Injection Zone, injection intervals, and Lower Confining Zone have been chosen based on each of the reservoir's permeability, porosity, thickness, and lateral continuity to accept and contain injected material. The massive fluvial-deltaic sandstones of the upper Frio Formation provide effective injection reservoirs in terms of their lateral extent, mineralogical composition, and petrophysical characteristics. The overlying aquiclude layers in the upper Frio Formation are sufficiently thick, impermeable, and laterally continuous to contain the injected fluids in the Injection Zone. Shales of the overlying Anahuac Formation and Fleming Formation possess the necessary Confining Zone criteria to be effective barriers for potential upward migration. The

thick Anahuac and Fleming Formation shales extend laterally across the region and are well over 1,000 times less permeable than the underlying injection reservoirs. Additionally, more than 7,000 ft of overlying, shale-rich Miocene section provides a Secondary Confining Zone. The existence of multiple sand/shale layers between the top of the Injection Zone and the base of the lowermost USDW ensures additional protection from the contamination of a USDW.

Lateral and vertical continuity of the Confining Zones, Injection Zone, and injection intervals can be confidently interpreted throughout the AoR. Figure 2.1.2-1, Figure 2.1.2-2, and Figure 2.1.2-3 demonstrate the mapped intervals of interest across the AoR.

2.10.2 Confinement

Project Minerva benefits from the following trapping mechanisms of the stratigraphic units:

- Buoyancy trapping against the Anahuac Formation,
- Relative permeability hysteresis,
- Dissolution of gaseous phase CO₂ into the formation's aqueous phase, and
- Localized buoyancy trapping within 4-way closures, where they might exist.

The Injection Zone will confine the CO₂ as local buoyant trapping in 4-way closures, immobilization by capillary trapping and dissolution. The Confining Zones are free of transmissive faults and fractures, and have sufficient areal extent and integrity to contain CO₂ stream and potential displaced formation fluids. No leakage pathways from existing wells within the AoR are identified.

2.10.3 CO₂ Stream Compatibility

Table 2.10.3-1 provides the proposed CO₂ stream specification for Project Minerva. This specification is designed to ensure safe operation of the project work and ensure no-endangerment of USDWs. Component concentrations were defined based on recommended impurity limits for different applications, including carbon steel pipelines, EOR, CO₂ saline storage and CO₂+ hydrogen sulfide (H₂S) saline storage. (Shirley & Myles, 2019) provides recommendations based on review of 55 different specifications from literature.

The logic of proposed component concentrations is as follows:

- Limited primarily by reservoir considerations include:
 - Total non-condensable gases affect CO₂ phase behavior and migration of the CO₂ plume in the subsurface. Value chosen to limit effects on plume migration and pressure propagation in the Injection Zone.
 - O₂ and H₂S are primarily limited for other reasons, but partly to limit possible reactions with minor mineral components in the Injection Zone and Confining Zone.

— Limited primarily for operational performance include:

- O₂ contributes to total non-condensable gases and is further limited to reducing the potential for corrosion of metallic facilities components in the presence of H₂O, SO₂ and/or NO₂. It is also limited to reduce potential reactivity with minor minerals in the reservoir and caprock.
- CH₄ contributes to total non-condensable gases and is further limited to reduce energy requirements for compression and pumping.
- Dense-phase CO₂ may carry considerable amounts of H₂O in vapor phase, which is not problematic. Total H₂O is limited to ensure there is no condensation of liquid H₂O anywhere within the facilities under the anticipated full range of operating conditions. CO₂ and other minor components (e.g., O₂, H₂S) form corrosive agents in the presence of liquid H₂O.
- H₂S is limited primarily for health and safety, but partly to limit the formation of corrosive compounds in the presence of liquid H₂O and/or O₂.

— Limited primarily to protect human health and safety and the environment include:

- H₂S, which carries significant risk (including toxicity) to humans and other organisms if introduced to the environment.
- Mercury (Hg), which is associated with long-term health risks and environmental degradation if introduced to the environment.

The proposed CO₂ stream (Table 2.10.3-1) is compatible with the mineralogy, petrology, and pore waters of the Injection Zone and the Confining Zone. No geochemical interaction between the injected CO₂ and the subsurface formations, beyond the dissolution of some gaseous CO₂ into the formation fluids is expected to occur at Project Minerva. As previously discussed in Section 2.8.2.2 (Macro-Scale Simulation), the Core Lab study confirmed the Frio Formation minerals remain largely unaffected by the CO₂ injection at reservoir conditions. Any interactions are highly unlikely to affect CO₂ injection operations or CO₂ storage integrity.

Well materials will be selected to be corrosion resistant throughout the life of the project (i.e., casing), or replaceable (i.e., production tubing).

Nippon Steel Corporation conducted a material selection analysis based on the provided CO₂ stream composition and well conditions. Super Duplex Stainless Steel (SM25CRW) is recommended as the best corrosive resistant option for expected conditions. Appendix IX (CO₂ Stream Compatibility) provides an overview of the study set up, analysis and results of the material section analysis for Project Minerva. The well material selections will be discussed in detail in Section 5 (Injection Well Construction).

2.10.4 Storage Capacity

The Injection Zone is a laterally extensive, high net-to-gross interval with substantial storage capacity, as demonstrated by extensive historical oil and gas development regionally. In the

Injection Zone, some local variations in pay sand interval thickness and extent occur. The total storage capacity of the Injection Zone at Project Minerva is more than 20.2 MMT of CO₂.

2.10.5 Modelling Approach and Simulation

The model area is approximately 255 mi². The simulation grid has 180 hexahedral grid cells in the X-direction, 158 grid cells in the Y-direction, and 63 cells in the Z-direction, forming a structural grid. The total number of grid cells in the model's domain is 1.7 million, of which 1.5 million cells are active in the reservoir simulation model.

To enhance computational efficiency, the reservoir simulation model employed a non-uniform grid. Grid cell size increased horizontally while remaining constant vertically. This optimization reduced the overall number of grid cells required. Given the minimal CO₂ plume and pressure changes at the model boundaries, lower-resolution grid cells were used in these areas. This approach concentrated computational resources on regions of critical interest, including the vicinity of injection wells, the CO₂ plume, and the area immediately surrounding the AoR.

The model served a dual purpose: (1) identifying potential injection sites through a regional, coarse-gridded analysis; and (2) simulating the fine-scale behavior of CO₂ and pressure plumes around selected injection sites using a refined grid.

A large-scale regional grid was initially developed based on seismic and petrophysical data to pinpoint promising injection locations. Subsequent modeling refined the grid around chosen sites (North and South) to accurately capture CO₂ and pressure plume dynamics. The model incorporated the overlying Anahuac Formation and iteratively refined the geostatistical model based on simulation results.

The model layers are as follows:

- Model grid layers K = 1 and K = 2 represent the Confining Zone, and
- Model layers K = 3 to 63 represent the Injection Zone.

The physical processes modeled in reservoir simulation model are:

- The injection of CO₂ is at cooler temperature than the *in-situ* formation temperature at constant rates over a 30-year period via two injection wells.
- The resultant cooling of the Injection Zone in the proximity of the injection wells, together with the change in effective geo-mechanical stress caused by the poro-elastic and thermo-elastic response of the rock therein and generally throughout the model domain.
- The change in density (the CO₂ is compressible) and viscosity of the injected CO₂ as its pressure and temperature change.
- CO₂ is modelled in its supercritical state (density typical of a liquid and viscosity typical of a gas).
- The advective flow (using Darcy's equation) of the CO₂ under the pressure gradient

induced by the injection wells and by its buoyancy with respect to the formation water.

- The advective flow (using Darcy's equation) of the aqueous phase.
- The advection (in the gaseous and aqueous phases) and conduction of heat within the model.
- The dissolution of some of the injected CO₂ into the aqueous phase (an important CO₂ trapping mechanism).
- The change in density (the aqueous phase is compressible) and viscosity of the aqueous phase as its pressure and temperature change (and as a function of its constant salinity).
- The relative permeabilities of the gas and aqueous phases are accounted for, together with hysteresis in the gas phase (an important CO₂ trapping mechanism).
- Geochemical reactions are not modelled beyond the dissolution of CO₂ into the aqueous phase. Long-term mineralization trapping is not modelled. (It is assumed that the time scales for this are many times (approximately 1,000x) longer than the lifetime of the project and, in this sense, our model is conservative in excluding a possible CO₂ sequestration mechanism).
- The geo-mechanical response of the rock to the changes in formation pressure and temperature is calculated.
- The precipitation of salt from the aqueous phase following dehydration by the injected CO₂, particularly at the well bores, is not modelled.
- The Joule-Thomson effect on the perforations is not modelled.
- The rock occurring in the Confining and Injection Zones is compressible.
- Table 2.10.3-1 details the CO₂ composition planned for Project Minerva. The compositional effects of CO₂, N₂ and CH₄ are modelled. The Peng-Robinson equation of state (Peng & Robinson, 1976) is used to model the CO₂-rich phase(s).

The model does not account for water evaporation into the gaseous phase. Multiple injection sites were evaluated within the regional model before selecting the South Site with its two injection wells.

Injecting 20 MMT of CO₂ in total through two injection wells at the South Site resulted in an AoR spanning approximately 4 miles across at its maximum extent. The CO₂ plumes extended roughly 3.75 miles across at their maximum extent 100 years of post-injection.

Simulation results indicate that CO₂ is primarily trapped through buoyancy against regional shales, capillary forces, and dissolution into reservoir brine. Reservoir model variations account for local zone differences without compromising storage capacity, injection rates, or underground source of drinking water (USDW) safety. The injected CO₂ was securely contained within the storage formation, and maximum injection pressures remained



45031 & 45032

significantly below estimated fracturing pressures.



45031 & 45032

3 AOR AND CORRECTIVE ACTION

3.1 PROJECT PLAN

The Area of Review (AoR) and Corrective Action Plan is provided as Attachment A of this Narrative. The AoR and Corrective Action Plan Report satisfies the requirements of LAC 43:XVII §3607.C.2.I, §3615.B.2, and §3615.B.3.

The report covers in detail the computational modelling approach to the delineation of the AoR, the Corrective Action Plan relating to existing well penetrations within the AoR, and the Reevaluation Schedule for AoR delineation once operations commence. A thorough review of the hydrogeology is also supplied, along with a comprehensive bibliography of references utilized during the AoR modelling execution and reporting phase.

3.2 GSDT SUBMISSION

The AoR and Corrective Action Plan Report (Attachment A) has been submitted via the *AoR and Corrective Action* module in GSDT. All tabs within the module that require input data have also been completed and submitted via the GSDT.



45031 & 45032

4 FINANCIAL RESPONSIBILITY DEMONSTRATION

4.1 FINANCIAL RESPONSIBILITY DEMONSTRATION REPORT

The Financial Responsibility Demonstration Report is provided as Attachment B of this Narrative. The Financial Responsibility Demonstration Report satisfies the requirements of LAC 43:XVII §3607.C.2.m.

4.2 GSDT SUBMISSION

The Financial Responsibility Demonstration Report (Attachment B) has been submitted via the *Financial Responsibility Demonstration* module in GSDT. The plan and supporting materials were uploaded within the *Cost Estimates* tab of the module. The remaining tabs that required input data or file uploads were completed and submitted via the GSDT.

5 INJECTION WELL CONSTRUCTION

GCS proposes to drill and complete two Class VI injection wells, MS CCS 1 and MS CCS 2, in compliance with LAC 43:XVII §3617, Well Construction and Completion requirements. GCS will ensure that all phases of Class VI well construction will be supervised by people who are knowledgeable and experienced in practical drilling engineering and are familiar with the special conditions and requirements of injection well construction.

Class VI injection wells are designed to ensure the permanent sequestration of CO₂ and prevent its movement into Underground Sources of Drinking Water (USDWs). The injection wells are constructed and operated to prevent fluid migration into or between USDWs, as well as into any non-approved zones. The design allows for the effective use of testing devices and workover tools, and supports continuous monitoring of the annulus between the injection tubing and long-string casing.

Key factors considered in the well design include the expected injection volume, rate, chemical composition, and physical properties of the injectate, including its potential corrosiveness and interactions with wellbore materials. Appendix XII (Operating Plans) provides detailed operational parameters and CO₂ injection composition.

MS CCS 1 and MS CCS 2 will be constructed and operated to effectively manage pore space utilization in the reservoir, contain CO₂ within the authorized injection interval, and comply with LAC 43:XVII §3617.

Figures 5-1 and 5-2 provide wellbore schematics for MS CCS 1 and MS CCS 2, respectively. MS CCS 1 is planned as a vertical well, while MS CCS 2 is planned to be drilled directionally. The proposed directional drilling plans are provided in Appendix X (Drilling Plans).

The surface wellhead design will be consistent for both injection wells. The proposed wellhead schematic is provided in Figure 5-3.

5.1 WELL CONSTRUCTION PLANS

The well construction plans for proposed injection wells MS CCS 1 and MS CCS 2 have been designed to prevent fluid movement from the Injection Zone into overlying formations. Each injection well will have six permanent barriers between USDW and the injection activities in the well interior: three casing strings with cement circulated to surface within each of the three annuli. Additionally, two further barriers will separate injection fluids from the USDW: a metal tubing wall and pressurized fluid in the tubing-casing annulus. In total, there will be eight man-made barriers and one natural barrier (the Anahuac Formation upper Confining Zone) to prevent fluids from migrating to the USDW.

5.2 CONSTRUCTION REQUIREMENTS

5.2.1 Prevention of Vertical Fluid Migration

The construction plans described in this section detail the steps required to drill and construct MS CCS 1 and MS CCS 2. These steps include drilling through the USDW and a substantial impermeable formation that confines fluids to the underlying Injection Zone.

The plan specifies drilling through the USDW to a depth that ensures sufficient formation strength to support the installation of 20 inch casing. The casing will be cemented with a sufficient volume of cement to circulate cement from the casing shoe to surface, providing complete coverage of the USDW with a bonded layer of steel and hardened cement.

Drilling will continue through the upper Confining Zone to approximately 150 ft (TVD) above the top of the Injection Zone. At this point, 13 $\frac{3}{8}$ inch casing will be installed and cemented to surface, providing further isolation and protection of the USDW.

After drilling to the Injection Zone, logging and sampling will be conducted in accordance with LAC 43§3617.4.b requirements. Details can be found in the Pre-Operational Logging and Testing Program (Attachment C). Then, the 9 $\frac{1}{2}$ inch casing will be installed and cemented with CO₂ corrosion-resistant cement with circulated returns to surface. Corrosion-resistant alloy (CRA) materials will be used across the injection and confining intervals to ensure sufficient corrosion resistance for CO₂ injection. This long-string casing provides an additional layer of steel and cement between the injection operations and the USDW.

A 4 $\frac{1}{2}$ inch tubing string and packer will be placed within the long-string casing. CO₂ will be injected down the tubing and through perforations in the long-string below the packer. The annular space between the tubing and long string will be filled with corrosion-inhibited fluid, pressurized, and continuously monitored, enabling prompt action if any leaks are detected.

The injection well designs will meet or exceed the following American Petroleum Institute (API) standards:

- API Specification 5CT
- API RP 5C1
- API RP 10D-2
- API Specification 11D1

All well materials to be used, including casing, cement, tubing, and packer, are compatible with the fluids they are expected to contact and will meet or exceed standards established by the American Petroleum Institute or comparable organizations.

In total, the wells will have eight permanent barriers installed between the USDW and the injection operations: three steel casing strings, three cement sheaths, a metal tubing wall, and pressurized annular fluid. Additionally, the upper Confining Zone (Anahuac Formation) acts as a natural barrier to prevent fluid migration out of the Injection Zone.

5.2.2 Drilling Practices and Contingencies

Class VI well construction will be supervised by personnel knowledgeable and experienced in practical drilling engineering, with specific familiarity in injection well construction and its unique requirements. Standard drilling practices will be employed to drill the well to total depth (TD), reaching the geologically favored target location.

The surface hole will be drilled vertically, with surveys conducted every 500 ft to accurately determine the well's subsurface position at -3,000 ft TVDSS. The remainder of the well will be drilled using directional drilling bottom-hole assemblies (BHAs), that incorporate a bent-housing mud motor and a measurement-while-drilling (MWD) tool. The MWD tool has accelerometers and magnetometers to determine the downhole position (surveys) in reference to the surface location (the center of the rotary table on the rig floor). Surveys will be taken at intervals of at least 95 ft to calculate the wellbore position, allowing for any necessary adjustments to be made using the mud motor to steer the bit back on the desired path.

All drilling tools (e.g. mud motors, stabilizers, drill collars, drill pipe) will undergo inspection before entering the wellbore. The integrity of the tool body and the threaded connections between tools will meet the standards of DS-1, Category 3. Any tools that do not meet body, thread, and shoulder specifications will be rejected, ensuring only reliable tools are used in the well. In the event that a downhole tool fails, the operable portion of the drill string will be pulled out of the hole, leaving a "fish" in the well. Accurate measurements of each tool's top are taken prior to entry, allowing an appropriately sized fishing tool to be used to latch onto the top of the failed component and recover it, if needed.

The well has been designed to set surface casing at a depth that extends into a confining bed—such as a shale—below the base of the deepest formation containing a USDW. This ensures that the formation strength, specifically resistance to fracturing, is sufficient to safely drill the remainder of the well to total depth.

Per LAC 43:XVII§3617.A.3.a, and A.3.a.i, after cementing each casing string but before drilling out the respective casing shoe, all casings shall be hydrostatically tested to verify casing integrity and the absence of leaks.

In accordance with LAC 43:XVII§3617.A.3.b, and A.3.b.i, after drilling out the casing shoe, the casing seat and cement of any intermediate and injection casings (i.e., long-string casing) will be hydrostatically tested. At least 10 ft of formation below the respective casing shoes shall be drilled before the test, test pressures shall never exceed the known or calculated fracture gradient of the appropriate subsurface formation.

Once drilling is complete, the long-string casing will be run and cemented, with cement densities and volumes specifically designed to avoid formation fractures at any depth. The long-string casings in both of these wells are planned to include a stage tool. Lost circulation due to imposed drilling or cementing forces is not expected. While lost circulation is not anticipated, plans are in place to address it if it does occur. If lost circulation occurs, lost circulation material (LCM) will be added to the mud to plug/block/seal the intervals

downhole where fluid loss is occurring. LCM will be available on-site throughout drilling operations.

All practices described above are standard oilfield best practices, allowing for safe and efficient drilling of MS CCS 1 and MS CCS 2.

5.2.3 Testing and Monitoring Devices Within the Borehole and Annulus

The long-string casing for MS CCS 1 and MS CCS 2 will have a 9 ½ inch outer diameter and an inside diameter of 8.535 inches. The injection tubing will have an outer diameter of 4 ½ inch, which comfortably fits inside the long-string casing, leaving an annular space of approximately 2.0125 inches. Distributed temperature sensing/distributed acoustic sensing (DTS/DAS) fiber optic cables will be clamped to the outside of the long-string casing from the surface to TD. An additional backup fiber optic cable will be installed from the surface to the depth of the intermediate casing shoe.

Annular measurements will also be taken at depth using downhole-deployed gauges fit with ¼ inch control lines, which are connected across the multiple tubing joints via clamps. Surface measurements of annular pressure will be collected with gauges installed on the wellhead, as illustrated in the cut-away schematic shown in Figure 5-3. These monitoring practices are essential to ensure well integrity and detect potential issues in real-time.

5.3 CASING PROGRAM

5.3.1 Injection Zone Depth

The Injection Zone for Project Minerva is the upper Frio Formation. The projected depths to the top and base of the Injection Zone in MS CCS 1 and MS CCS 2 are provided in Table 5.3.1-1.

5.3.2 Lithology of Injection and Confining Zones

The Confining Zone is the shale-rich Anahuac Formation, which conformably overlies the upper Frio Formation (Injection Zone). Offset resistivity, spontaneous potential, and gamma ray log data indicate that the Anahuac Formation has high shale content regionally. The upper Frio Formation is comprised of stacked shoreline sandstones interbedded with shales. Detailed summaries of both the injection and Confining Zones can be found in Section 2 of the Narrative (Site Characterization).

5.3.3 Borehole and Casing Size and Grade

5.3.3.1 Borehole Sizes

MS CCS 1 and MS CCS 2 are each designed with a 26 inch hole for the surface casing, a 17 ½ inch hole for the intermediate casing, and a 12 ¼ inch hole for the long-string casing, as depicted in Figures 5-1 and 5-2.

5.3.3.2 Casing Size and Grade

From surface to below the base of the USDW, the surface casing will be composed of a 20 inch, 133 lb/ft, L-80 Type 1 grade casing.

The intermediate casing string, extending from surface to significantly into the Confining Zone, will be composed of 13 $\frac{3}{8}$ inch, 68 lb/ft, L-80 Type 1 casing. L-80 Type 1 casing is a commonly used oilfield casing grade that offers sufficient minimum yield and tensile strength for injection operations.

The long-string casing will extend from the surface through the Injection Zone to total depth and will be composed of 9 $\frac{1}{2}$ inch, 53.5 lb/ft casing. For the interval from the surface to above the Confining Zone, L-80 casing with a premium connection (VAM-21 or equivalent) will be installed. From above the Confining Zone to total depth, Super Duplex 25 Chrome casing (Grade: 25CRW-125, specifically Nippon's SM25CRW-125[®]) will be tied into the L-80 casing with the same premium connection (VAM-21 or equivalent). Super Duplex 25 Chrome is a cold-hardened duplex stainless steel intended for corrosion resistance in sweet (CO₂) and mildly sour (H₂S) environments with high chloride content, requiring high strength up to 450°F. It has a high pitting resistance equivalence (PREN) greater than or equal to 40.

The size, grade, and depths of the surface casings, intermediate casings, and long-string casings are provided in Table 5.3.3-1 and depicted in Figures 5-1 and 5-2.

5.3.3.3 Casing Strength

Table 5.3.3-2 provides casing details including the tensile, burst, and collapse strength for MS CCS 1 and MS CCS 2. The casing has been designed to withstand expected forces, incorporating a substantial factor of safety, during injection operations. For example, each casing will be cemented with a sufficient volume of cement to circulate cement from the casing shoe to surface, with cement bond logs run to confirm proper bonding to both the casing and the formation.

Casing strength can be degraded if the wall thickness is reduced by corrosion or erosion. A baseline inside diameter of each long-string casing will be measured with a casing caliper log during pre-operational testing. This log can be repeated during the life of the well whenever the tubing is pulled. The critical section of the long-string casing is the packer setting area, which must retain sufficient wall thickness to maintain structural integrity, particularly hoop stress, throughout the injection activities' operational life. For this reason, corrosion-resistant (CRA) casing has been specified for this interval.

Expected loads on the surface casing, intermediate casing, long-string, and injection tubing were found to be within equipment specifications. Modeled loads (downhole stresses) with design limits and equipment specifications limits can be found in the following figures:

- 20 inch Surface Casing, MS CCS 1 (Figure 5.3.3-1)
- 20 inch Surface Casing, MS CCS 2 (Figure 5.3.3-2)
- 13 $\frac{3}{8}$ inch Intermediate Casing, MS CCS 1 (Figure 5.3.3-3)
- 13 $\frac{3}{8}$ inch Intermediate Casing, MS CCS 2 (Figure 5.3.3-4)



45031 & 45032

- 9 5/8 inch Long String Casing (Stage 2), MS CCS 1 (Figure 5.3.3-5)
- 9 5/8 inch Long String Casing (Stage 2), MS CCS 2 (Figure 5.3.3-6)
- 9 5/8 inch Long String Casing (Stage 1), MS CCS 1 (Figure 5.3.3-7)
- 9 5/8 inch Long String Casing (Stage 1), MS CCS 2 (Figure 5.3.3-8)

5.3.4 Downhole Temperature

The expected temperature at total depth is 201°F, which is not expected to adversely impact the cement, casing, packer element, or downhole gauges. The cement reaches a value close to its maximum compressive strength within days and gradually becomes more competent with time and bottomhole temperature.

Similarly, the crystalline structure of casing steel is not significantly affected at this temperature. The thermal effect at 201°F is minimal since it takes temperatures around 1,500°F to alter the crystalline structure of steel. Therefore, the casing will not experience detrimental effects from the anticipated downhole temperature.

5.4 CEMENTING PROGRAM

Centralizer placement will be designed utilizing the final cementing vendor's software and actual deviation surveys. Centralizers will be placed in all casings, as per the design, to aid in the centering of the casing in the openhole and optimize uniform cement placement behind pipe. Complete cement details have been provided in Tables 5.4-1.

5.4.1 Circulation of Cement

In all cases, multi-arm caliper logs will be run prior to running casing. Cement volumes will be calculated based on the recorded hole caliper, with an excess volume factored in to ensure the complete circulation of cement to the surface. All cement returns to the surface will be recorded in daily drilling reports.

5.4.2 Cement and Cement Additives

Additives used to achieve the desired properties of the cement slurry include defoamers, accelerators, and retarders. Table 5.4.2-1 lists the proposed additives for each cement slurry utilized in the well designs. The primary cement utilized in the well designs will be a CO₂ corrosion-resistant cement, such as PermaSet™ System Cement, which is a proprietary blend developed by Baker Hughes. For more details, refer to Appendix IX-2. The proprietary blend replaces calcium hydroxide [Ca(OH)₂] with calcium (alumino)silicate hydrate (C-(A)-S-H) phases to enhance resistance to acid-induced corrosion.

The secondary cement used in the well designs is Class H cement with the following additives to improve resistance to CO₂: tricalcium silicate (C₃S), dicalcium silicate (C₂S), tricalcium aluminate (C₃A), tetra calcium aluminoferrite (C₄AF).

5.5 TUBING AND PACKER

LAC 43:XVII§3617.A.4 requires that the tubing and packer must be compatible with the fluids they contact and meet or exceed recognized industry standards. Considering the potential

formation of carbonic acid from a mixture of water and CO₂, the injection tubing for Project Minerva is specified as 4 ½ inch, 25 CR-rated steel. The added chrome content in the steel replaces iron, reducing the amount of ionic activity available to react with carbonic acid. The 4 ½ inch outside diameter (OD) tubing size was selected by considering the total proposed injection volume of CO₂ during the project life. Additionally, premium tubing connections using gas-tight sealing surfaces (VAM-21 or equivalent) will ensure the integrity of the tubing string and mitigate weakness at the connections.

The packer will be comprised of CRA materials and installed inside the 53.5 lb/ft, 9 ½ inch long-string casing across an interval confirmed to be cemented near the top of the injection interval. The packer anchors the tubing string, provides structural stability, and isolates the overlying annular space from the injection interval, allowing the annulus to be monitored for potential tubing and packer leaks. The CRA retrievable injection packer will be manufactured using carbon dioxide-compatible elastomer materials and will be rated to withstand the pressure differentials during installation, workovers, and the injection phase, including an additional safety factor.

The following parameters are the basis of design for the tubing and packer:

- **Setting depth:** Approximately 9,000 ft TVDSS, or within 150 ft of the top perforations in the Upper Frio Formation. The setting depths for each well will be slightly different due to formation tops and geometry of the directional well; 9,000 ft is used as a generalization knowing that precise depths will be confirmed upon drilling and logging.
- **CO₂ stream specification:** Expected to be within specs shown in Table 2.10.3-1.
- **Maximum proposed injection pressure:** Approximately 3,200 psig at the surface during the injection period. This equates to downhole pressures of 4,880 psig and 4,807 psig in MS CCS 1 and MS CCS 2, respectively.
- **Annular pressure requirements:** In accordance with Class VI requirements, the annular pressure (between the tubing and long-string casing) will be maintained greater than the fluctuating daily injection pressure, which will vary due to ambient temperature changes.
- **Injection wells planned:** Two injection wells are planned for Project Minerva. Proposed injection rates and volumes are shown in Table 5.5-1.

The International Organization for Standardization (ISO) and the American Petroleum Institute (API) have created standards (ISO 14310:2001 E and API Specification 11D1) to guide packer selection. Project Minerva specifies packer validation level Q1, which provides maximum trace documentation, and a standard design-validation grade of V1.

Tubing and packer details are provided in Tables 5.5-2 and 5.5-3.

5.6 MECHANICAL INTEGRITY

Per LAC 43:XVII §3627A.1, a Class VI well has mechanical integrity if there are no significant leaks in the casing, tubing, or packer (internal integrity) and there is no significant fluid movement into the USDW through channels adjacent to the injection wellbore (external



45031 & 45032

integrity). Additional information about the internal and external mechanical integrity testing performed prior to operations can be found in the Pre-Operational Testing Program (Attachment C). The Testing and Monitoring Plan (Attachment D) covers specifics about internal and external mechanical integrity testing that will be performed over the operational life of the wells.

5.6.1 Internal Integrity

To demonstrate internal integrity, GCS will perform an annulus pressure test after initial well construction (LAC 43:XVII §3617.B.1.d.i) and once operational, at least once every 12 months and after performing any remedial work that involved unseating the tubing or packer (LAC 43:XVII §3627.A.2.a). GCS will ensure annulus pressure tests are witnessed by an LDENR Conservation Enforcement Agent.

Additionally, GCS will continuously monitor injection pressure, rate, and volume; downhole pressure monitoring of the tubing-casing annulus; and annulus fluid volume (LAC 43:XVII §3627.A.2.b). Continuous monitoring will allow GCS to identify any potential internal integrity issues between annual testing events and allow immediate response to potential integrity issues.

5.6.2 External Integrity

To demonstrate external integrity prior to operating the wells, GCS will perform an oxygen activation log, a noise log, and a casing inspection log (LAC 43:XVII §3617.B.1.d.ii-iv). Each of these logs will provide a baseline for future testing/logging throughout the operational life of the wells.

Once the wells are operational, GCS will perform a DTS MIT at least once every 12 months to identify any fluid movement through channels or cracks in the cement (LAC 43:XVII §3627.A.3 and LAC 43:XVII §3627.A.5). If there are any temperature anomalies that indicate a failure of well integrity, GCS will perform a noise or oxygen activation log per LAC 43:XVII §3627.A.3.a-b. Upon request by the Commissioner, GCS will perform a casing inspection log to determine the presence or absence of corrosion in the long-string casing (LAC 43:XVII §3627.A.4).



45031 & 45032

6 PRE-OPERATIONAL LOGGING AND TESTING

6.1 PROJECT PLAN

The Pre-Operational Logging and Testing Plan is provided as Attachment C of this Narrative. The Pre-Operational Logging and Testing Plan satisfies the requirements of LAC 43:XVII §3607.C.2.g.

6.2 GSDT SUBMISSION

The fully completed Pre-Operational Testing Plan (Attachment C) has been submitted via the *Pre-Operational Testing* module in GSDT. The plan and supporting materials were uploaded within the *Welcome* tab of the module.

7 WELL OPERATION

7.1 OPERATIONAL PROCEDURES

The Operating Plans for proposed MS CCS 1 and MS CCS 2 are provided in Appendix XII (Operating Plans).

GCS has defined the following key objectives for operation:

- Maintain and achieve a safe, reliable, and efficient sequestration system.
- Ensure operations remain within safe parameters.
- Maximize continuous injection of CO₂ and minimize cycling of the injection wells.

Per LAC 43:XVII§3617.A.2, GCS will prevent injection into the wellbore annulus of any casing protecting the USDWs.

Please see Table 7-1 for the operational parameters for injection well MS CCS 1 and MS CCS 2. Values for the operational parameters were calculated using PROSPER well modeling software and REVEAL, a well simulation program, each developed by Petroleum Experts Limited of Edinburgh, UK (Petroleum Experts Limited, 2019). Please see further discussion on the use of each program in Section 1.0 (Computation Modelling Approach) and 1.1.4.2 (Simulation Software) of the Area of Review and Corrective Action Plan (Attachment A).

GCS will implement a comprehensive testing and monitoring plan for Project Minerva, satisfying the well operation planning requirements outlined in LAC 43:XVII §3621.A, §3625.A, and §3627.A. Please refer to Appendix XII (Operating Plans) for operational parameters specific to each injection well and the Injection Zone. The Testing and Monitoring Plan (Attachment D) covers specifics about external mechanical integrity testing and the overall testing and monitoring approach for MS CCS 1 and MS CCS 2.

7.1.1 Injection Rate

Project Minerva will utilize a sequential completion strategy, starting with the bottom interval and progressing upwards. Targeted injection rates are set at 21 MMSCF/D for the bottom interval for 15 years, 19 MMSCF/D for the intermediate interval for 7 years, and 17 MMSCF/D for the top interval for 8 years. The project will inject a combined average of 0.674 million metric tons (MMT) of CO₂ per year over its 30-year lifespan, split between the two injection wells, as defined in Table 7-1.

7.1.2 Injection Pressure

Injection induced pressure will not exceed 90% of the fracture pressure of the zone. The bottom-hole pressures are significantly smaller than the estimated fracture pressure and induced seismicity pressure. The initial formation pressure is based on the most-likely initial formation pressure gradient of 0.457 psi/ft.

The most-likely value of the minimum horizontal stress gradient is assumed to be 0.85 psi/ft, as provided in Section 2.5.1.2 (Total Minimum Horizontal Stress) of the Project Minerva Narrative.

The depth of the deepest completion interval in MS CCS 1 is approximately 9,958 ft TVDSS, which calculates to a minimum horizontal stress of approximately 8,464 psia. The depth of the deepest completion interval in MS CCS 2 is approximately 9,832 ft TVDSS, which calculates to a minimum horizontal stress of approximately 8,357 psia.

Assuming a safety factor of 90%, this gives an estimate of the formation fracturing pressure to be approximately 7,618 psia at 9,958 ft TVDSS in MS CCS 1 and 7,521 psia at 9,832 ft TVDSS in MS CCS 2. This is a conservative estimate as it assumes no cohesion in the formation, i.e. the formation parts as soon as the effective minimum horizontal stress is less than zero. The induced seismicity pressure is estimated to be 9,958 psia at a depth of 9,958 ft TVDSS in MS CCS 1 and 9,832 psia at a depth of 9,832 ft TVDSS in MS CCS 2, at the pressure gradient of 1 psi/ft.

7.1.3 Stimulation Program

All stimulation activities will be approved by the LDENR Commissioner prior to conducting the stimulation. GCS will carry out the stimulation program in accordance with Appendix XI of this application.

7.1.4 CO₂ Volume

Project Minerva is designed to permanently store a total of 20.2 MMT. This volume will be achieved by injecting at an average rate of 0.674 MMT/yr for 30 years (Table 7-1).

7.1.5 CO₂ Stream Characteristics

Table 2.10.3-1 provides the proposed CO₂ stream specification for Project Minerva, designed to ensure safe operation and prevent endangerment of USDWs. Project Minerva will utilize CO₂ from multiple sources, all capable of meeting or exceeding the specified requirements, which the reservoir simulation model has fully accounted and explored.

7.2 PROPOSED CARBON DIOXIDE STREAM

The emissions that are anticipated for Project Minerva in the near term are likely to be high purity CO₂. Examples of high purity CO₂ anticipated to be economically capturable include natural gas processing and other natural gas derived processes including blue H₂ and LNG. The Gulf Coast region of Southeast Texas and Southwest Louisiana have a variety of currently operating or planned facilities for natural gas processing. Such applications can meet the CO₂ specification that GCS has proposed. Further, such specification of CO₂ is consistent with the existing CO₂ pipeline infrastructure in the Gulf Coast region.

Table 2.10.3-1 provides the proposed CO₂ stream specification for Project Minerva. This specification is designed to ensure safe operation of the project work and ensure no-endangerment of USDWs. Component concentrations were defined based on recommended impurity limits for different applications, including carbon steel pipelines, EOR, CO₂ saline storage and CO₂+H₂S saline storage. (Shirley & Myles, 2019) provides recommendations based on review of 55 different specifications from literature.

The logic of proposed component concentrations is as follows:

— Limited primarily by reservoir considerations include:

- Total non-condensable gases affect CO₂ phase behavior and migration of the CO₂ plume in the subsurface. Value chosen to limit effects on plume migration and pressure propagation in the Injection Zone.
- Oxygen (O₂) and H₂S are primarily limited for other reasons, but partly to limit possible reactions with minor mineral components in the Injection Zone and Confining Zone.

— Limited primarily for operational performance include:

- O₂ contributes to total non-condensable gases and is further limited to reducing the potential for corrosion of metallic facilities components in the presence of H₂O, sulfate (SO₄²⁻) and/or nitrogen dioxide (NO₂). It is also limited to reduce potential reactivity with minor minerals in the reservoir and caprock.
- CH₄ contributes to total non-condensable gases and is further limited to reduce energy requirements for compression and pumping.
- Dense-phase CO₂ may carry considerable amounts of H₂O in vapor phase, which is not problematic. Total H₂O is limited to ensure there is no condensation of liquid H₂O anywhere within the facilities under the anticipated full range of operating conditions. CO₂ and other minor components (e.g., O₂, H₂S) form corrosive agents in the presence of liquid H₂O.
- H₂S is limited primarily for health and safety, but partly to limit the formation of corrosive compounds in the presence of liquid H₂O and/or O₂.

— Limited primarily to protect human health and safety and the environment include:

- H₂S, which carries significant risk (including toxicity) to humans and other organisms if introduced to the environment.
- Hg, which is associated with long-term health risks and environmental degradation if introduced to the environment.

Under the proposed operational conditions (e.g., down-hole P/T) for the lifetime of the injection project, the proposed CO₂ stream specification is compatible with the mineralogy, petrology, and pore waters of the Injection Zone and the Confining Zone. No geochemical interaction between the injected CO₂ and the subsurface formations, beyond the dissolution of some gaseous CO₂ into the formation fluids is expected to occur at Project Minerva. As previously discussed in Section 2.8.2.2 (Macro-Scale Simulation), the Core Lab study confirmed the Frio Formation minerals remain largely unaffected by the CO₂ injection at reservoir conditions. Any interactions are highly unlikely to affect CO₂ injection operations or CO₂ storage integrity.

Although small-scale, localized mineral reactions may occur, these interactions are highly unlikely to affect CO₂ injection operations or CO₂ storage integrity. All well materials will be selected to be corrosion resistant throughout the life of the project (i.e., casing), or



45031 & 45032

replaceable (i.e., production tubing). Please see Appendix IX, CO₂ Stream Compatibility- Chrome Casing Specs.

Well materials will be selected to be corrosion resistant throughout the life of the project (i.e., casing), or replaceable (i.e., production tubing). Nippon Steel Corporation conducted a material selection analysis based on the provided CO₂ stream composition and well conditions. Super Duplex Stainless Steel (SM25CRW) is recommended as the best corrosive resistant option for expected conditions. Appendix IX Materials of Construction, Chrome Casing Specs, shows an overview of the study set up, analysis and results of the material section analysis for Project Minerva. The well material selections will be discussed in detail in Section 5 (Injection Well Construction).



45031 & 45032

8 TESTING AND MONITORING

8.1 PROJECT PLAN

The Testing and Monitoring Plan is provided as Attachment D of this Narrative. The Testing and Monitoring Plan Report satisfies the requirements of LAC 43:XVII §3607.C.2.n and §3625.A.

The plan covers in detail the overall strategy and approach for testing and monitoring, carbon dioxide stream analysis, continuous recording of operational parameters, corrosion monitoring, above Confining Zone monitoring, external mechanical integrity testing, pressure fall off testing, carbon dioxide plume and pressure front tracking, and sampling/analytical procedures.

A Quality Assurance and Surveillance Plan (QASP) is submitted as an appendix to the Testing and Monitoring Plan, and includes additional information related to project management, data generation and acquisition, assessment and oversight and data validation and usability.

8.2 GSDT SUBMISSION

The Testing and Monitoring Plan (Attachment D) has been submitted via the *Project Plan Submission* module in GSDT. The plan and supporting materials were uploaded within the *Testing and Monitoring* tab of the module.



45031 & 45032

9 INJECTION WELL PLUGGING PLAN

9.1 PROJECT PLAN

The Injection Well Plugging Plan is provided as Attachment E of this Narrative. The Injection Well Plugging Plan satisfies the requirements of LAC 43:XVII §3607.C.2.o and §3631.A.3.

The plan covers in detail the proposed tests and measurements to determine the bottom-hole reservoir pressure; planned external mechanical integrity tests; information on the proposed plugs; methods used for volume calculations; required notifications, permits and inspections; plugging procedures; and contingency procedures/measures.

9.2 GSDT SUBMISSION

The Injection Well Plugging Plan (Attachment E) has been submitted via the *Project Plan Submission* module in GSDT. The plan and supporting materials were uploaded within the *Injection Well Plugging* tab of the module.



45031 & 45032

10 POST INJECTION SITE CARE AND SITE CLOSURE

10.1 PROJECT PLAN

The Post-Injection Site Care (PISC) and Site Closure Plan is provided as Attachment F of this Narrative. The Post Injection Site Care and Site Closure Plan satisfies the requirements of LAC 43:XVII §3607.C.2.p and §3633.A.1.

10.2 GSDT SUBMISSION

The Post-Injection Site Care (PISC) and Site Closure Plan (Attachment F) has been submitted via the *Project Plan Submission* module in GSDT. The plan and supporting materials were uploaded within the *PISC and Site Closure* tab of the module.



45031 & 45032

11 EMERGENCY AND REMEDIAL RESPONSE PLAN

11.1 PROJECT PLAN

The Emergency and Remedial Response Plan (ERRP) is provided as Attachment G of this Narrative. The Emergency and Remedial Response Plan Report satisfies the requirements of LAC 43:XVII §3607.C.2.r and §3623.A.1.

The plan covers in detail the local resources and infrastructure, potential risk scenarios, response personnel and equipment, emergency communications plan, plan review, staff training, and exercise procedures.

11.2 GSDT SUBMISSION

The Emergency and Remedial Response Plan (Attachment G) has been submitted via the *Project Plan Submission* module in GSDT. The plan and supporting materials were uploaded within the *Emergency and Remedial Response* tab of the module.

12 REFERENCES

Archie, G. E. (1942, December). The Electrical Resistivity Log as an Aid in Determining Some Reservoir Characteristics. *Trans*, 146(1), 54-62. doi:10.2118/942054-G

Baker Jr, E. T. (1978). *Stratigraphic and Hydrogeologic Framework of Part of the Coastal Plain of Texas*. Austin: USGS, Texas Water Development Board.

Baker Jr, E. T. (1986). *Hydrology of the Jasper Aquifer in the Southeast Texas Coastal Plain*. Texas Water Development Board. Austin: U.S. Geological Survey.

Baria, L. R., Stoudt, D. L., Harris, P. M., & Crevello, P. D. (1982). Upper Jurassic Reefs of Smackover Formation, United States Gulf Coast. *AAPG Bulletin*, 66(10), 1449-1482. doi:10.1306/03B5A96C-16D1-11D7-8645000102C1865D

Beckman, J. D., & Williamson, A. K. (1990). *Salt-Dome Locations in the Gulf Coastal Plain, South-Central United States*. Austin: US Geological Survey.

Bethke, C. M., Altaner, S. P., Harrison, W. J., & Upson, C. (1988). Supercomputer Analysis of Sedimentary Basins. *Science*, 239(4837), 261-267. doi:10.1126/science.239.4837.261

Byerlee, J. (1978). Friction of Rocks. In Byerlee, J.D., Wyss, M. (eds) *Rock Friction and Earthquake Prediction. Contributions to Current Research in Geophysics (CCRG)*, vol 6. Birkhäuser, Basel.

Chowdhury, A. H., & Turco, M. J. (2006). Chapter 2. Geology of the Gulf Coast Aquifer, Texas. In T. W. Board, *Aquifers of the Gulf Coast of Texas* (pp. 23-50). Austin: Texas Water Development Board.

Clark, J. E. (1981). Groundwater Flow in Deep Saline Aquifers.

Clark, J. E., Papadeas, P. W., Sparks, D. K., & McGowen, R. R. (1991). *DuPont Borehole Closure Test Well Demonstration, Orange County, Texas*. Beaumont: E I du Pont de Nemours & Co., Inc.

Coleman, J., & Galloway, W. E. (1990). Petroleum geology of the Vicksburg Formation, Texas. *Gulf Coast Association of Geological Societies and Gulf Coast Section of Society of Economics, Paleontologists, and Mineralogist (SEPM)* (pp. 17-19). Lafayette, Louisiana: AAPG Bulletin.

Collier, A. L., & Sargent, B. P. (2018). *Water Use in Louisiana, 2015*. Louisiana Department of Transportation and Development. Baton Rouge: U.S. Geological Survey.

Core Laboratories. (1987, June 3). Petrographic Study of Selected Sidewall Core Samples from a Beaumont Disposal Well for DuPont Chemicals, Inc. Beaumont, Texas, United States of America: Litton Core Lab.

Core Laboratories. (1987, June 1). Special Core Analysis Study for E.I. duPont De Nemours & Company, Inc., Waste Disposal Tests. Beaumont, Texas, United States of America: Western Atlas International.

Davis, S. D., Pennington, W. D., & Carlson, S. M. (1989). A Compendium of Earthquake Activity in Texas. *Geological Circular* 89-3, 1-219.

Delaney, P. J. (1963). Stratigraphy of the Vicksburg Equivalent of Louisiana: ABSTRACT. *AAPG Bulletin*, 47(2), 355. doi:10.1306/BC7439B5-16BE-11D7-8645000102C1865D

DEQ of Louisiana. (2009). *Appendix 4 to the 2009 Triennial Summary Report: Evangeline Aquifer Summary, 2007*. QEG of Louisiana; Aquifer Sampling and Assessment Program.

DEQ of Louisiana. (2017). *Appendix 10 to the 2018 Triennial Summary Report*. DEG of Louisiana; Aquifer Sampling and Assessment Program.

Dewhurst, D. N., Cartwright, J. A., & Lonergan, L. (1999). The Development of Polygonal Fault Systems by Syneresis of Collodial Sediments. *Marine and Petroleum Geology*, 16, 793-810.

Diamond, L. W., & Akinfiev, N. N. (2003). *Solubility of CO₂ in water from - 1.5 to 100 C and from 0.1 to 100 MPa: evaluation of literature data and thermodynamic modelling*. University of Bern, Baltzerstrasse 1-3, Bern CH-3012, Switzerland, Institute of Geological Sciences.

DOE. (1978). Final Environmental Impact Statement: Strategic Petroleum Reserve Texoma Group Salt Dome. *U.S. Department of Energy, 1 of 5*. Retrieved from <https://www.energy.gov/sites/prod/files/2015/06/f23/EIS-0029-FEIS-volume1.pdf>

Doughty, C., Freifeld, B., & Trautz, R. (2015). Site Characterization for CO₂ Geologic Storage and Vice Versa: The Frio Brine Pilot, Texas, USA as a Case Study. *Lawrence Berkeley National Laboratory*.

Downey, M. W. (1984). Evaluating Seals for Hydrocarbon Accumulations. *AAPG*, 1752-1763.

Eaton, B. A. (1969). Fracture gradient prediction and its application in oilfield operations. *Journal of Petroleum Technology Transactions*, Vol. 246.

Ellsworth, W. L. (2013, July). Injection-Induced Earthquakes. *Science*, 341. doi:DOI: 10.1126/science.1225942

Engelder, J. T. (1974). Coefficients of friction for sandstone sliding on quartz gouge. In *Advances in rock Mech. Proc. Third Congress Int. Soc. Rock Mech., Denver, Part A* (p. 499).

EPA. (2023, August 18). *EPA FLIGHT*. Retrieved from EPA Greenhouse Gas Reporting Program (GHGRP): <https://ghgdata.epa.gov/ghgp/>

FEMA. (2024, May 13). *Earthquake Hazard Maps*. Retrieved from FEMA; Earthquake Risk: <https://www.fema.gov/emergency-managers/risk-management/earthquake/hazard-maps>

Foote, R. Q. (1984). *Summary report on the regional geology, petroleum potential, environmental consideration for development, and estimates of undiscovered recoverable O&G resources of the US Gulf of Mexico Continental Margin in the area of proposed O&G Lease Sales 81 and 84*. U.S. Geological Survey and U.S. Minerals Management Service. doi:10.3133/ofr84339

Frohlich, C., Potter, E., Hayward, C., & Stump, B. (2010). Dallas-Fort Worth Earthquakes Coincident with Activity Associated with Natural Gas Production. *The Leading Edge*, 270-275. doi:10.1190/1.3353720

Galloway. (1985). Depositional Framework of the Lower Miocene (Fleming) Episode, Northwest Gulf Coast Basin. *AAPG Bulletin*, 69(9), 1421. doi:10.1306/AD462CDB-16F7-11D7-8645000102C1865D

Galloway, W. E., Henry, C. D., & Smith, G. E. (1982). *Depositional Framework, Hydrostratigraphy, and Uranium Mineralization of the Oakville Sandstone (Miocene), Texas Coastal Plain*. Report of Investigations No. 113. doi:10.23867/RI0113D

Galloway, W. E., Hobday, D. K., & Magara, K. (1982). Frio Formation of Texas Gulf Coastal Plain: Depositional Systems, Structural Framework, and Hydrocarbon Distribution. *AAPG Bulletin*, 66(6), 649-688. doi:10.1306/03B5A2F5-16D1-11D7-8645000102C1865D

Ghanbari, S., Al-Zaabi, Y., Pickup, G. E., Mackay, E., Gozalpour, F., & Todd, A. C. (2006). Simulation of CO₂ Storage in Saline Aquifers. *Trans IChemE, Part A, Chemical Engineering Research and Design*, 84(A9), 764-775.

Gray, G. R., Darley, H., & Rogers, W. F. (1980). *Composition and Properties of Oil Well Drilling Fluids*. Houston, London, Paris, Tokyo: Gulf Publishing Company.

Gregory, J. L. (1966). Lower Oligocene Delta in Subsurface of Southeastern Texas: ABSTRACT. *AAPG Bulletin*, 50(10), 2323. doi:10.1306/5D25B745-16C1-11D7-8645000102C1865D

Griffith, J. M. (2003). *Hydrogeologic Framework of Southeastern Louisiana*. Louisiana Department of Transportation and Development. Baton Rouge: U.S. Geologic Survey.

Harder, A. H. (1960). *The Geology and Ground-Water Resources of Calcasieu Parish Louisiana*. United States Department of Interior. Washington, D.C.: U.S. Geological Survey.

Haskell, N., Nissen, S., & Hughes, M. (1999). Delineation of geologic drilling hazards using 3-D seismic attributes. *The Leading Edge*, 18(3), 373-382.

Hiland, P. (2010). *Memorandum: SAFETY/RISK ASSESSMENT RESULTS FOR GENERIC ISSUE 199, "IMPLICATIONS OF UPDATED PROBABILISTIC SEISMIC HAZARD ESTIMATES IN CENTRAL AND EASTERN UNITED STATES ON EXISTING PLANTS".*

Houser, B. B., & Ryan, G. S. (1983). Mineral Resource Potential Map of the Four Notch Roadless Area, Sam Houston National Forest, Walker County, Texas. *Miscellaneous Field Studies Map MF-1549*. Reston, Virginia, United States: USGS.

Hovorka, S. D., Collins, D., Bensen, S., Myer, L., Byrer, C., & Cohen, K. (2005). Update on the Frio Brine Plot: Eight months after injection. *FOURTH ANNUAL CONFERENCE ON CARBON CAPTURE AND SEQUESTRATION DOE/NETL*.

Hovorka, S., Tutton, P., & Trevino, R. H. (2018). *Feasibility study of CO2 storage in saline formations in the region of the planned Lake Charles Methanol Plant*. Austin: Gulf Coast Carbon Center Bureau of Economic Geology.

Intera. (2020). *The Delineation of the Burkeville Confining Unit and the Base of the Chicot Aquifer to Support the Development of the Gulf 2023 Groundwater Model*. Harris-Galveston-Fort Bend: Intera Incorporated. Retrieved from https://hgsubsidence.org/wp-content/uploads/2021/06/Final_HGSD_FBSD_Burkeville_Report_final.pdf

Intera, Frontera-Exploration, Hamlin, S., & Baker, E. (2012). *Final Report: Updating the Hydrogeologic Framework for the Northern Portion of the Gulf Coast Aquifer*. Austin: TWDB. Retrieved from https://texashistory.unt.edu/ark:/67531/metapth542209/m2/1/high_res_d/txcs-0715.pdf

Jackson, M. P., & Galloway, W. E. (1984). *Structural and Depositional Styles of Gulf Coast Tertiary Continental Margins: Application to Hydrocarbon Exploration*. Tulsa: AAPG Education Program.

Johnston, O., & Greene, C. J. (1979). *Investigation of Artificial Penetrations in the Vicinity of Subsurface Disposal Wells*. Texas Department of Water Resources.

Jolley, S. J., Dijk, H., Lamens, J. H., Fisher, Q. J., Manzocchi, T., Eikmans, H., & Huang, Y. (2007). Faulting and fault sealing in production simulation models: Brent Province, northern North Sea. *Petroleum Geoscience*, 13, 321-340.

Jones, P. H., Turcan Jr, A. N., & Skibitzke, H. E. (1954). Geology and Ground-Water Resources of Southwestern Louisiana. *Geological Bulletin No. 30*, 285.

Juanes, R., Spiteri, E. J., Orr Jr, F. M., & Blunt, M. J. (2006). Impact of relative permeability hysteresis on geological CO2 storage. *WATER RESOURCES RESEARCH*, 42(W12418). doi:10.1029/2005WR004806

Jung, H. S., & Wheeler, M. F. (2017). An Integrated Case Study of the Frio CO2 Sequestration Pilot Test for Safe and Effective Carbon Storage Including Compositional Flow and Geomechanics. *Society of Petroleum Engineers, SPE*.

Kharaka, Y. K., Hovorka, S., Cole, D. R., & Gunter, W. D. (2006). Gas-water-rock interactions in Frio Formation following CO₂ injection: Implications for the storage of greenhouse gases in sedimentary basins. *Geology*. doi:10.1130/G22357.1

Knipe, R. J. (1989). Faulting processes and fault seal. In R. M. Larsen, H. Brekke, B. T. Larsen, & E. Talleraas, *Structural and Tectonic Modelling and its Application to Petroleum Geology* (pp. 325-342). Leeds: Department of Earth Sciences, The University of Leeds.

Knipe, R. J. (1997). Juxtaposition and Seal Diagrams to Help Analyze Fault Seals in Hydrocarbon Reservoirs. *AAPG Bulletin*, 81(2), 187-195.

Kreitler, C. W., Collins, E. W., Davidson Jr., E. D., Dix, O. R., Donaldson, G. A., Dutton, S. P., . . . Wuerch, H. V. (1981). *Geology and Geohydrology of the East Texas Basin*. Austin: US Department of Energy.

Krevor, S. C., Pini, R., Zuo, L., & Benson, S. M. (2012). Relative permeability and trapping of CO₂ and water in sandstone rocks at reservoir conditions. *WATER RESOURCES RESEARCH*, 48. doi:10.1029/2011WR010859

Kumar, A., Ozah, R., Noh, M., Pope, G. A., Bryant, S., Sepehrnoori, K., & Lake, L. W. (2005). Reservoir Simulation of CO₂ Storage in Deep Saline Aquifers. *Society of Petroleum Engineers; SPE*, 336-348.

Leeds, D. J., & Associates. (1989). *Consultants in Engineering Seismology, Geology, Geophysics*. Beaumont: Leeds and Associates.

Lindaman, M. A. (2023). *Hydrogeologic Framework of Southwestern Louisiana*. Louisiana Department of Transportation and . Reston: U.S. Geological Survey.

Loucks, R. G., Dodge, M. M., & Galloway, W. E. (1986). *Controls on Porosity and Permeability of Hydrocarbon Reservoirs in Lower Tertiary Sandstones along the Texas Gulf Coast*. The University of Texas at Austin, Bureau of Economic Geology. doi:10.23867/RI0149D

Louisiana Geological Survey. (2000). Folio Series No. 8: Stratigraphic Charts of Louisiana 2000. *Folio Series No. 8: Stratigraphic Charts of Louisiana 2000*.

Lovelace, J. K., Fontenot, J. W., & Frederick, C. P. (2004). *Withdrawals, Water Levels, and Specific Conductance in the Chicot Aquifer System in Southwestern Louisiana*. U.S. Department of the Interior. Reston: U.S. Geological Survey.

Lundstern, J.-E., & Zoback, M. D. (2020, April 23). *Multiscale variations of the crustal stress field throughout North America*. Retrieved from Nature Communications, 11:195: <https://doi.org/10.1038/s41467-020-15841-5>

Mancini, E. A., Mink, R. M., Bearden, B. L., & Wilkerson, R. P. (1985). Norphlet Formation (Upper Jurassic) of Southwestern and Offshore Alabama: Environments of Deposition



45031 & 45032

and Petroleum Geology. *AAPG Bulletin*, 69(6), 881-898. doi:10.1306/AD462B14-16F7-11D7-8645000102C1865D

Mason, C. C. (1963). *Availability of Ground Water from the Goliad Sand in the Alice Area, Texas*. Texas Water Commission: USGS.

Milner, L. R., & Fish, C. (2009). *Geological Characterization of the Chicot/Atchafalaya Aquifer Region: Southwest Louisiana*. Louisiana Geological Survey: Water Resource Series No. 4.

National Ocean and Atmospheric Administration. (1985). *NOAA Ocean Exploration: National Centers for Environmental Information*. Retrieved from Gulf of Mexico Atlas: <https://www.ncei.noaa.gov/maps/gulf-data-atlas/atlas.htm>

Nicholson, A. (2012). *Empirical analysis of fault seal capacity for CO2 sequestration, Lower Miocene, Texas Gulf Coast*. GCCC Digital Publication Series #12-29.

Nicol, A., Seback, H., McNamara, D., & Field, B. (2016). *Fault Permeability*. IEA Environmental Projects Ltd. (IEAGHG).

Nyman, D. J. (1984). *The Occurrence of High Concentrations of Chloride in the Chicot Aquifer System of Southwestern Louisiana*. State of Louisiana, Department of Transportation of Development Office of Public Works: Water Resources. USGS.

ODNR. (2012). Preliminary Report on the Northstar 1 Class II Injection WELL and the Seismic Events in the Youngstown, Ohio, Area. *Ohio Department of Natural Resources*.

Parkhurst, D. L., & Appelo, C. A. (2024, August). *Description of Input and Examples for PHREEQC, version 3--A Computer Program for Speciation, Batch-Reaction, One-Dimensional Transport, and Inverse Geochemical Calculations*. Retrieved from USGS; Water Resources: <https://water.usgs.gov/water-resources/software/PHREEQC/documentation/phreeqc3-html/phreeqc3-2.htm>

Peng, D.-Y., & Robinson, D. B. (1976, February). A New Two-Constant Equation of State. *Industrial & Engineering Chemistry Fundamentals*, 15(1). doi:10.1021/i160057a011

Petroleum Experts Limited. (2019, November). REVEAL User Manual: IPM - Specialised Reservoir Numerical Simulator. Edinburgh, Scotland: 1990-2019 Petroleum Experts Limited.

Porter, W. M., & Newsom, S. W. (1987). *Shale Porosity and Permeability*.

Purpera, D. G. (2020). *Louisiana's Management of Water Resources*. Baton Rouge: Louisiana Legislative Auditor.

Rainwater, E. H. (1968). Geological History and Oil and Gas Potential of Central Gulf Coast: ABSTRACT. *AAPG Bulletin*, 52(9), 1826. doi:10.1306/5D25C4DF-16C1-11D7-8645000102C1865D

Ramos, G., Katahara, K., Keck, R., & Batzle, M. (1994). In-situ stress predictions and measurements in an unconsolidated sandstone formation, the Lower Frio, East Texas. *ARCO Exploration and Production Technolog*, 361-368.

Salem, H. S., & Chilingarian, G. V. (1999). The cementation factor of Archie's equation for shaly sandstone reservoirs. *Journal of Petroleum Science and Engineering*, 83-93.

Schlumberger. (1989). *Log Interpretation Principles/Applications*. Schlumberger Educational Services.

Secor Jr, D. T. (1965). Role of Fluid Pressure in Jointing. *American Journal of Science*, 633-646.

Shirley, P., & Myles, P. (2019). *Quality Guidelines for Energy Systems Studies: CO2 Impurity Design Parameters*. National Energy Technology Laboratory (NETL-PUB-22529).

Smith, D. A. (1966). Theoretical Considerations of Sealing and Non-Sealing Faults. *AAPG Bulletin*, 50, 363-374.

Smith, D. A. (1980, February). Sealing and Nonsealing Faults in Louisiana Gulf Coast Salt Basin. *AAPG Bulletin*, 64(2), 145-172.

Smoot, C. W. (1988). *Louisiana hydrologic atlas map no. 3: Altitude of the base of freshwater in Louisiana*. Baton Rouge: USGS. doi:10.3133/wri864314

Stolper, K. (1994). *Calculate a More Accurate Water Saturation by Visually Estimating "m"*. Houston Geological Society Bulletin.

Swanson, S. M., & Karlsen, A. W. (2009). PS USGS Assessment of Undiscovered Oil and Gas Resources for the Oligocene Frio and Anahuac Formations, Onshore Gulf of Mexico Basin, USA. *AAPG Annual Convention*. San Antonio, Texas: AAPG.

Swanson, S. M., Karlsen, A. W., & J, V. B. (2013). *Geologic assessment of undiscovered oil and gas resources—Oligocene Frio and Anahuac Formations, United States Gulf of Mexico coastal plain and State waters*. U.S. Geological Survey. doi:10.3133/ofr20131257.

Teeple, A. P., Becher, K. D., Walton-Day, K., Humberson, D. G., & Gallegos, T. J. (2022). Development and Description of a Composite Hydrogeologic Framework for Inclusion in a Geoenvironmental Assessment of Undiscovered Uranium Resources in Pliocene-to Pleistocene-Age Geologic Units of the Texas Coastal Plain. *Minerals*, 420. doi:10.3390/min12040420

The Dow Company. (2020, May 12). Well Test Interpretation for The Dow Company Injection Well No. 3 - 2020 Falloff. Jefferson County, Texas, United States of America.

Todd, R. G., & Mitchum, R. M. (1977). "Seismic Stratigraphy and Global Changes of Sea Level, Part 8: Identification of Upper Triassic, Jurassic, and Lower Cretaceous Seismic Sequences in Gulf of Mexico and Offshore West Africa". In C. E. Payton, *Seismic*



45031 & 45032

Stratigraphy — Applications to Hydrocarbon Exploration (Vol. 26). AAPG. doi:10.1306/M26490C10

Trevino, R. H., & Meckel, T. A. (2017). Geological CO₂ Sequestration Atlas of Miocene Strata, Offshore Texas State Waters. *Bureau of Economic Geology*.

U.S. Energy Information Administration (EIA). (2020, October 5). Retrieved from The Economic Impact of the Oil and Natural Gas Industry in Louisiana: https://www.eia.gov/state/seds/sep_prod/pdf/P4.pdf

USGS. (2018). *2018 Long-term National Seismic Hazard Map*. Retrieved from USGS: <https://www.usgs.gov/media/images/2018-long-term-national-seismic-hazard-map>

USGS. (2024, May 7). *Earthquake Hazards Program*. Retrieved from USGS: <https://earthquake.usgs.gov/earthquakes/map/?extent=7.88515,-147.74414&extent=59.933,-42.27539>

USGS. (2024, May 13). *Modified Mercalli Intensity Scale by Earthquake Hazards Program*. Retrieved from USGS; Earthquake Hazards Program Images: <https://www.usgs.gov/media/images/modified-mercalli-intensity-scale>

USGS. (2024). *USGS Earthquake Hazards Program: Interactive U.S. Fault Map*. Retrieved from U.S. Quaternary Faults: <https://usgs.maps.arcgis.com/apps/webappviewer/index.html?id=5a6038b3a1684561a9b0aadf88412fcf>

Vail, P. R., Mitchum, R. M., & Thompson III, S. (1977). Seismic Stratigraphy and Global Changes of Sea Level, Part 4: Global Cycles of Relative Changes of Sea Level. In C. E. Payton, *Seismic Stratigraphy — Applications to Hydrocarbon Exploration* (Vol. 26). AAPG. doi:10.1306/M26490

Walsh, R., Zoback, M., Lele, S., Pais, D., Weingarten, M., & Tyrrell, T. (2016-2018). *FSP 2.0: A program for probabilistic estimation of fault slip potential resulting from fluid injection*. Retrieved from Bureau of Economic Geology: <https://www.beg.utexas.edu/texnet-cisr/fsp>

Warner. (1988). Abandoned Oil and Gas Industry Wells and Their Environmental Implications. *The Portland Marriott, Portland, Oregon* (pp. 69-89). Rolla: American Petroleum Institute.

Warner, D. L., & Syed, T. (1986). *Confining Layer Study: Supplemental Report - Chapter 9*. Chicago: Engineering Enterprises, Inc.

Wesselman, J. B., & Aronow, S. (1971). *Ground-Water Resources of Chambers and Jefferson Counties, Texas*. Austin, Texas: Texas Water Development Board.

White, V. E., & Griffith, J. M. (2020). *Potentiometric surfaces, 2011–12, and water-level differences between 1995 and 2011–12, in wells of the “200-foot,” “500-foot,” and*



45031 & 45032

"700-foot" sands of the Lake Charles area, southwestern Louisiana. Reston: U.S. Geological Survey.

Williamson, A. K., Grubb, H. F., & Weiss, J. S. (1990). *Ground-water flow in the Gulf Coast Aquifer Systems, South Central United States -- A Preliminary Analysis*. Austin: U.S. Geological Survey.

Woessner, W. W., & Poeter, E. P. (2020). 4.2 Hydraulic Head. In W. W. Woessner, & E. P. Poeter, *Hydrogeologic Properties of Earth Materials and Principles of Groundwater Flow* (p. 205). Guelph, Ontario: The Groundwater Project.

Yale, D. P., Nabor, G. W., Russell, J. A., Pham, D., & Yousef, M. (1993). Application of Variable Formation Compressibility for Improved Reservoir Analysis. *SPE Annual Technical Conference and Exhibition* (pp. 435-450). Houston: SPE International.

Young, S. C., Ewing, T., Hamlin, S., Baker, E., & Lupton, D. (2012). *Final Report: Updating the Hydrogeologic Framework for the Northern Portion of the Gulf Coast Aquifer*. Austin: Texas Water Development Board.

Young, S. C., Knox, P. R., Budge, T., Kelley, V., Deeds, N., Galloway, W. E., & Baker, E. T. (2006). Chapter 6. Stratigraphic, Lithology, and Hydraulic Properties of the Chicot and Evangeline Aquifers in the LSWP Study Area, Central Texas Coast. In T. W. Board, *Aquifers of the Gulf Coast of Texas* (pp. 129-138). Austin: Texas Water Development Board.

Zeidouni, M., Pooladi-Darvish, M., & Keith, D. (2009). Sensitivity Analysis of Salt Precipitation and CO₂-Brine Displacement Saline Aquifers. *Society of Petroleum Engineers, SPE 126690*, 2-16.

Zheng, X., Zhuang, S., & Espinoza, N. D. (2019). Uniaxial Strain Unloading Compressibility of Frio Sand: Measurements and Implications on Reservoir Pressure Management for CO₂ Storage. Conference: *American Rock Mechanics Association*. New York City: American Rock Mechanics Association.

Zimmerman, R. W. (1991). *Compressibility of Sandstones*. Berkley: Elsevier.

Zoback, M. L., & Zoback, M. (1980). State of Stress in the Conterminous United States. *Journal of Geophysical Research*, 85(B11), 6113-6156.



APPENDICES

45031 & 45032

- Appendix 1 Environmental Justice
- Appendix 2 IT Analysis and Response
- Appendix 3 Drilling Plans
- Appendix 4 Operation Plans
- Appendix 5 Stimulation Program
- Appendix 6 Coring Plans
- Appendix 7 PermaSet